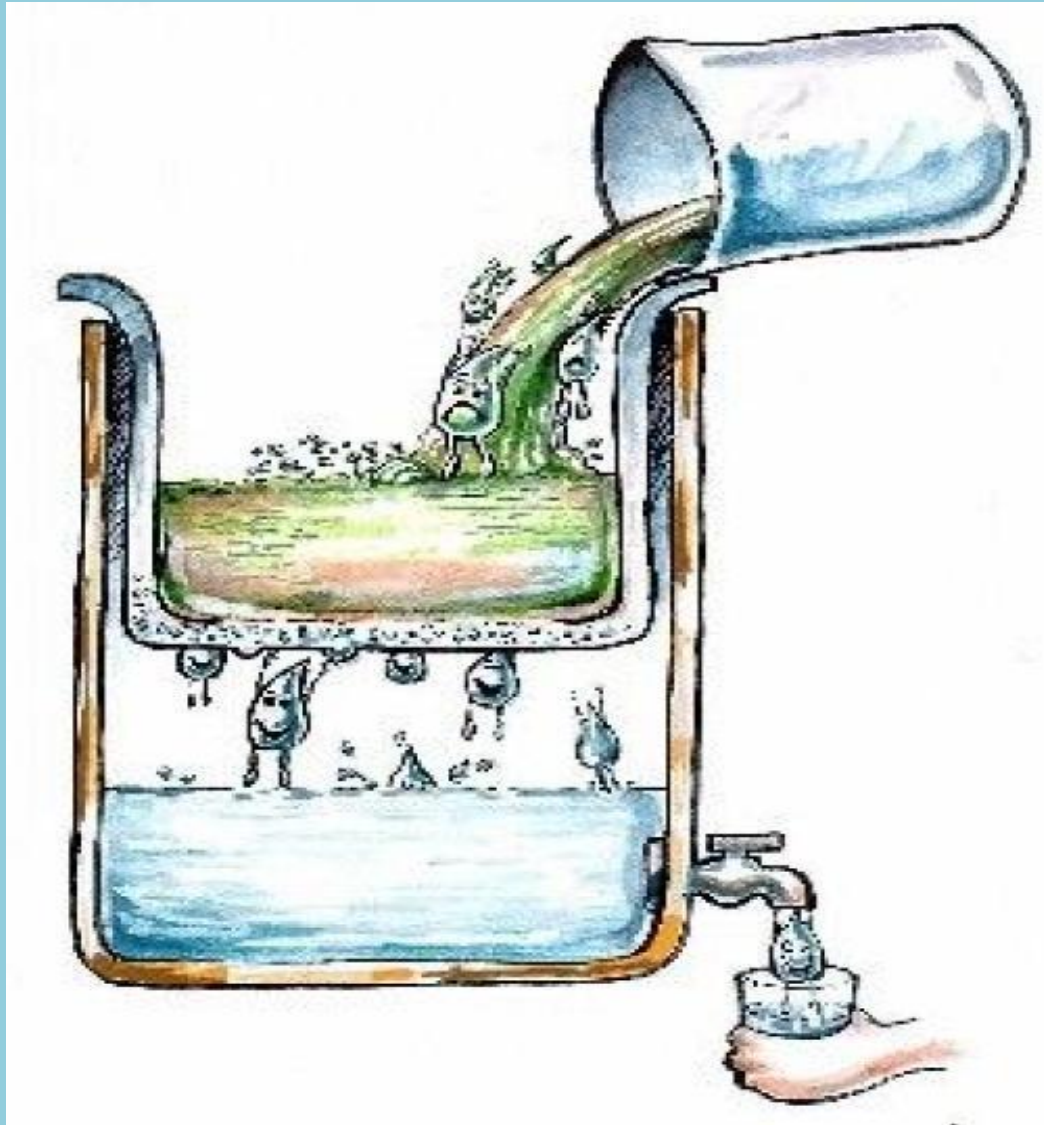


High Speed Sterilization of Water Using Cellulose Grafted Membranes with Metallic Nanoparticles.



By: Terica Raquel Sinclair

Supervisor: Dr. Manuel Arruebo Gordo

High Speed Sterilization of Water using Cellulose Grafted Membranes with Metallic Nanoparticles.

Terica Raquel Sinclair

Thesis submitted to the faculty of Chemical Engineering at the University of Zaragoza, Spain in partial fulfilment of the requirements for the degree of

Master of Science

In

Membrane Engineering with focus on Nanoscience

Dr. Manuel Arruebo Gordo, Supervisor

Dr. Reyes Mallada, EM3E Coordinator (Spain)

June 17, 2013

Zaragoza, Spain

© Terica Raquel Sinclair.



**European Master
ERASMUS MUNDUS MASTER IN
MEMBRANE ENGINEERING**

The EM3E Master is an Education Programme supported by the European Commission, the European Membrane Society (EMS), the European Membrane House (EMH), and a large international network of industrial companies, research centres and universities. www.em3e.eu.

The EM3E education programme has been funded with support from the European Commission. This publication reflects the views only of the author, and the Commission cannot be held responsible for any use which may be made of the information contained therein. Translation of this phrase in all EU languages (http://ec.europa.eu/dgs/education_culture/publ/graphics/beneficiaries_all.pdf).

ACKNOWLEDGEMENT

I would like to express my deepest gratitude to my advisor, Associate Professor Dr. Manuel Arruebo Gordo for his guidance and support throughout my Master's program of study and this project. No matter what kind of problem was discussed, his advice and encouragement always provided new perspectives. Einstein said it best knowledge is not knowing facts but training the brain to think. The expertise that he shared with me remains a tremendous source for the professional growth to me. I am very thankful for everything he has done for me. Also I would like to voice my appreciation to Mr. Maciej Zieba for giving technical suggestions, and generously providing me the use of many lab facilities, his time, his friendship, encouragement, suggestions, motivations, daily input, and the sharing of his expertise. All of his extraordinary help are greatly appreciated. Other people from whom I benefited in this research including, within and outside of the group to them also I am greatly appreciative. I have enjoyed doing research and discussing experimental details with them. Without their help, many things could have been much more difficult to achieve. I am also grateful to Dr. Victor Sebastian Cabeza and Dr. Nuria Navascues Garcia for their help with transmission electron microscopy, and Carlos Cuestas Ayllón as well for scanning electron microscopy. Their patience in accommodating my samples is greatly appreciated. Sara Orleans Bernad for ATR-FTIR, Dr. Silvia Irusta Alderete for XPS, Dr. Reyes Mallada for DLS and being a wonderful coordinator and everyone else who helped to make this project a success. I would also like to thank all my friends namely Umay, Shackera, Hakan and DJ for all their encouragement as well as my mother and the rest of my family for their continued support over the two years of this master without them it really would not have been possible complete this task. It is an inestimable pleasure to extend my gratitude to the EM3E program for giving me the opportunity to achieve yet another unforgettable and fulfilling goal in my academic journey. And last but most certainly not least I would like to thank God as without him nothing is ever possible.

TABLE OF CONTENT

Acknowledgements	
List of Tables	
List of Figures	
List of Abbreviations and symbols	
Abstract	
Chapter 1: Introduction	1
1.1 Small Scale Filter systems – A pressing need	1
1.1.1. Water filters	2
1.2 Emergence of nanotechnology in antimicrobial actions and protections from infectious diseases	4
1.3 Antimicrobial nano-materials	5
1.3.1 Silver, silver compounds and silver nanoparticles	6
Chapter 2: Literature Review and Background	6
2.1 Nanostructured Materials	6
2.1.1 Synthesis of Metallic nanoparticles	8
2.1.2 Optical properties of noble metallic nanoparticles	10
2.1.3 Shape control of geometrically-defined nano particles	12
2.1.4 Soft-template assisted growth of FCC metallic nanoparticles (Chemical reduction method “Polyol method”)	14
2.1.5 Biological applications of metallic nanoparticles	16
2.1.6 General Applications of metallic nanoparticles in Biological Area	16
2.1.7 Population Growth of Bacteria	17
2.1.8 Growth Rate and Generation Time	19
2.1.8.1 Calculation of Generation Time	19
2.1.9 Bactericidal Effects of Metallic Nanoparticles	20

2.2 Challenges and motivations of current study.....	21
2.3 Research goal and objectives.....	23
2.3.1 Research goal and approach.....	23
2.3.2 Objectives.	24
2.3.3 Thesis Organization.	25
2.4 Marketability and feasibility of high speed filters for sterilization.....	26
Chapter 3: Experimental and Methods.....	28
3.1 Materials Selection	
3.2 Synthesis of nanoparticles	
3.2.1 Synthesis of nano-wires	
3.2.2 Synthesis of nano-spheres	
3.3 Fabrication and characterization methods	
3.3.1 Chemical structure characterization	
3.3.2 Materials characterization	
3.4 Modification of cellulose filters	
3.4.1 Functionalization of cellulose fibres and attachment of metallic particles	
3.4.1.1 Thiol Modification of Cellulose filters using mercaptoacetic acid.	
3.4.1.2 Amine modification of cellulose filters using:	
• APTES.	
• PEI	
3.5 Characterization of thiolated and aminated cellulose filters.	
3.6 Assembly of modified cellulose and metallic nanoparticles filters	
3.6.1 Assembly of modified filters	
• Thiol modified filters	
• Amine (APTES and PEI) modified filters	

3.6.2	In situ preparation of metal-cellulose filter	
3.7	Release Testing of metal-cellulose membrane filter	
3.8	Characterization of metal-cellulose filter	
3.9	Bacterial Testing	
Chapter 4: Results		29
4.1	Characterization of silver nanoparticles	29
4.2	Characterizations of thiol and amine modified cellulose filters	35
4.3	Characterization of the metal cellulose filters	40
4.3.1	Material characterization	40
4.3.2	Release testing	48
4.4	Bacterial Testing	51
4.4.1	Bacterial growth testing	51
4.4.2	Bacterial viability testing	52
Chapter 5: General Discussion and future direction		57
5.1	Antimicrobial effects of Ag-cellulose filters	57
Chapter 6: Conclusion		60
6.1	Conclusion/Summary	60

References

Appendices

Appendix A- Chapter 3 Experimental and methods in detail.

Appendix B- Supplementary information, graphs, data, figures and all miscellaneous items omitted from the main report.

Appendix C- Pictures of some equipment used for characterization and experimental procedures.

LIST OF FIGURES

Figure 1- Various antimicrobial mechanisms of nanoparticles.

Figure 2 - a) Individual Lego pieces transformed into an apple computer fashioned by apple engineers representative of nano particles with well-defined shape. b) Silver nano particles of different shapes and sizes.

Figure 3 - Plasmon absorption spectrum of some representative shaped gold- and silver-nanoparticles within the visible region.

Figure 4 – (I) Reduction of silver salt precursor; (II) silver clusters formation; (III) nucleus formation, in the form of single crystal, multi-twinned decahedral or quasi-spherical; and (IV) nanoparticles growth into nano-cubes, nano-rods or nano-spheres. Light surface represents the {111} and dark gray surface represents {100} facets. Light gray lines represent twinned boundary and dark grey interior planes represent twinned planes.

Figure 5 -A typical configuration utilized in nano- biomaterials applied to medical or biological problems.

Figure 6 - A typical bacterial growth curve. Four distinct phases can be recognized, lag phase, exponential phase, stationary phase, and death phase respectively.

Figure 7 - Antimicrobial agents are a) incorporated into the fibre; b) applied on the fibres surface; c) chemically bound onto the fibres.

Figure 8 - Modes of antimicrobial action.

Figure 9 - Images of E. coli bacteria found in water

Figure 10 - Schematic Illustration of the preparation procedure of the Thiolated cellulose bound with nanoparticles.

Figure 11 - Synthesized silver nano-wires dispersed ethanol and nano-spheres dispersed in water.

Figure 12 - UV-vis absorption spectrum of silver nanoparticles, with absorption peak at 400-nm, and FWHM around 80-nm.

Figure 13 – TEM images of a) Silver nano-wires b) Silver nano-spheres.

Figure 14 - SEM image of Silver nano wires.

Figure 15 - Particle size distribution obtained by DLS (Sample February 7, 2013).

Figure 16 - Particle size distribution obtained by IMAQ (Sample February 7, 2013).

Figure 17 - TEM images a) Particle size distribution b) Large agglomerates.

Figure 18 - ATR FT-IR spectra of a) Unmodified cellulose fibres and b) Thiolated cellulose fibres (using esterified mercaptoacetic acid).

Figure 19 - ATR FT-IR spectra of a) Unmodified cellulose fibres and b) Aminated cellulose fibres (using APTES)

Figure 20 - ATR FT-IR spectra of a) Unmodified cellulose fibres and b) Aminated cellulose fibres (using PEI).

Figure 21 - Graph showing the positive shift in binding energy of the thiol modified cellulose relative to the Ag NPs.

Figure 22 - Graph showing the positive shift in binding energy of the thiol modified cellulose relative to the Ag NPs.

Figure 23 - Shift in binding energies of amine groups and nitrogen on amine modified filters.

Figure 24 - The photo images of a) APTES b) PEI and c) Thiol modified cellulose filter after the attachment of Ag NPs.

Figure 25 - SEM images of un-modified cellulose filters a) Top view b) cross section.

Figure 26 - SEM images of thiol -modified cellulose filters with Ag NPs a) Top view b) cross section.

Figure 27 - Schematic representation of cutting during sample preparation for HR(S)-TEM.

Figure 28 - HR(S)-TEM images of immobilized nanoparticles on the surface of Ag-cellulose filters at different levels.

Figure 29 - EDX spectra of Ag-cellulose filter.

Figure 30 - a) UV-vis graphs of release test performed on filters with non-covalent bonding at different pH and b) UV-vis graphs of release test performed on thiol-modified filters at different pH.

Figure 31- Pictures of filters with different functionalities a) Before release testing and b) After release Testing.

Figure 32 - Picture of bacteria in liquid solution (PBS) showing the decrease in turbidity with the addition of silver nanoparticles.

Figure 33 - Corresponding graph of log reductions/antimicrobial activity, from table 8.

Figure 34 - Corresponding graph of log reductions/antimicrobial activity, from table 9.

Figure 35 - Agar plate images of different concentrations (10^4 and 10^5) of E. coli after being passed through the filters 50 times a) Thiol Filter b) APTES Filter c) PEI filter and d) Control.

Figure 36 - SEM images of bacterial cells on thiol-modified filters after 50 passes of PBS containing E. coli on a) top surface and b) reverse surface (underneath).

LIST OF TABLES

Table 1 - Antimicrobial nanomaterials.

Table 2 - Parameter of commercial cellulose filters from Prat Dumas, France.

Table 3 - Data sheet of some microbial contaminants found in drinking water.

Table 4 - Amount of sulphur present in amine-modified cellulose filters.

Table 5 - Amount of sulphur present in thiol-modified cellulose filters.

Table 6 - Assignment of Binding Energies of Main XPS Regions for thiol-modified Ag-cellulose assembly.

Table 7 - a) Assignment of Binding Energies of Main XPS Regions for amine-modified Ag-cellulose assembly. b) Binding energy of nitrogen and amine group on amine modified cellulose.

Table 8 - Colony Forming Units per mL formed on agar plates for filters with different functionalities (over-night).

Table 9 - Colony Forming Units per mL formed on agar plates for filters with different functionalities (immediately (after several passes)).

LIST OF SYMBOLS AND ABBREVIATIONS

λ	Wavelength
G	Generation Time
LSPR	localized surface plasmon resonance
SPR	surface plasmon resonance
FCC	Face centred cube
FWHM	Full width at half maximum
AgNO ₃	Silver nitrate
AgNW's	Silver nano wires
APTES	3-Aminopropyl triethoxysilane
PEI	Polyethylenimine
PVP	Polyvinyl Pyrrolidone
EG	Ethylene glycol
Uv-Vis	Ultra violet visible spectroscopy
TEM	Transmission electron microscope
HR-TEM	High resolution Transmission electron microscope
SEM	Scanning electron microscope
DLS	Dynamic Light Scattering
ATR FT-IR	Attenuated total reflection Fourier-transform infrared spectroscopy
ICP-AES	Inductively coupled plasma atomic emission spectroscopy
EDXS	Energy-dispersive X-ray spectroscopy
XPS	X-ray <u>photoelectron spectroscopy</u>
PBS	Phosphate Buffered Saline

TSB	Tryptic Soy Broth
E. coli	Escherichia coli
CFU	Colony- forming Units
HSAB	Hard soft acid and base

RESUMEN

La eliminación de bacterias y otros microorganismos del agua es un proceso extremadamente importante no sólo en el agua de boca y de consumo sino también en sus distintas aplicaciones a nivel industrial donde el ensuciamiento por material biológica puede ser perjudicial. En este proyecto se describe un filtro de acetato de celulosa funcionalizado con nanopartículas de plata para la rápida esterilización de aguas contaminadas. Con el objetivo de analizar el poder biocida de la plata se analizaron tanto nanohilos como nanopartículas de plata, así como su combinación. Dichos materiales fueron caracterizados mediante microscopía electrónica (de barrido y de transmisión) para caracterizar su morfología, así como mediante dispersión dinámica de la luz (DLS) para conocer su distribución de tamaño de partícula como suspensión y finalmente mediante espectroscopia UVVIS para analizar los distintos espectros de extinción. Las fibras de celulosa de filtros comerciales fueron funcionalizadas mediante grupos amino o tiol para conseguir un enlace fuerte entre las nano-partículas/hilos de plata y dicha fibras celulósicas. Los filtros decorados con las correspondientes nanoestructuras fueron analizados mediante una batería de técnicas analíticas e instrumentales incluyendo SEM, HR(S)-TEM, ICP, XPS, FTIR, EDX, y con el objeto de demostrar el enlace estable formado entre las fibras funcionalizadas y los correspondientes nanomateriales basados en plata. Dichos filtros fueron sometidos a un gran esfuerzo mecánico mediante ultrasonidos para demostrar que las nanoestructuras no se desprendían de las fibras del filtro y para corroborar la fortaleza del enlace covalente formado además de para evitar una potencial liberación incontrolada de los nanomateriales desde el filtro. Dichos filtros mostraron una supresión bacteriana de hasta el 99.9% utilizando agua contaminada con *E. coli* como bacteria modelo de contaminación fecal. Así, se demuestra que los filtros desarrollados en esta investigación muestran un gran poder biocida con un bajo coste y durabilidad para el tratamiento de aguas contaminadas.

ABSTRACT

The removal of bacteria and other organisms from water is an extremely important process, not only for drinking and sanitation but also industrially as bio-fouling is a commonplace and serious problem. This project presents a cellulose membrane filter grafted with silver nanoparticles for the high speed sterilization of water. In order to study the antimicrobial effects of silver nanoparticles, silver nano wires and nano spheres were synthesized, dispersed in water and characterized by Scanning Electron Microscopy (SEM) and Transmission Electron Microscopy (TEM) to reveal their formation and corresponding morphologies, dynamic light scattering (DLS) particle size analyser for particle size distribution, RadWag for concentration and finally Ultraviolet visible (UV-vis) scanning spectrophotometry to detect the distinct spectrum of the silver nanoparticles produced. These nanoparticles were then covalently bonded to commercially available cellulose filters, and functionalized by either thiol or amine groups. Followed by characterization by HR(S)-TEM, FE-SEM, energy-dispersive X-ray spectroscopy (EDXS), inductively coupled plasma atomic emission spectroscopy (ICP-AES), Attenuated total reflection Fourier-transform infrared (ATR FT-IR) to reveal that the cellulose membranes were effectively modified by the thiol or amine groups and highly loaded with well dispersed nanoparticles. As well as X-ray photoelectron spectroscopy (XPS) analysis was used showed that the nanoparticles were immobilized in the membrane by a stable covalent bond with the respective functional groups. The resulting cellulose-metal membranes were subjected to mechanical release testing, thus proving their robustness and suppression to release of the nanoparticles from their cellulose backbone. The metal cellulose filters showed high antimicrobial activity in excess of 99.9% growth inhibition against E. coli a member of the total coliform group. Thus we anticipate our filters with their high antibacterial property and durability can be produced in a cost effective manner and if developed is capable of producing affordable, clean and safe drinking water.

CHAPTER 1

INTRODUCTION

1.1 Small Scale Filter systems – Current state of the art.

According to the World Health Organization, over one billion people do not have access to clean water. 780 million people worldwide lack access to clean water and 2.5 billion lack adequate sanitation [1]. Bacterial contaminations of water is a major cause of life threatening disease outbreaks, such as cholera or gastroenteritis especially after natural disasters and in poverty stricken countries. There is a pressing and urgent need for small-scale filter systems that can purify water of bacteria and other harmful microorganisms. They must also be cheap, safe, portable and easy to use.

Silver has been used for centuries to preserve potable water. Even in trace quantities, silver is a potent antibacterial and antifungal agent. Silver is now being packaged in nanoparticles – very small materials ten thousandth of the width of a human hair. They are composed of hundreds to thousands of silver atoms, either pure or with some type of coating. Due to the fact that they are so small, they expose a large surface to the contaminants, and are thus very effective at killing microorganisms [2]. There are many consumer products including socks, shirts and countertops – contain silver nanoparticles, Samsung™ has created and marketed a product line called Silver Nano, which includes silver nanoparticles on the surfaces of household appliances like washing machines and refrigerators to take advantage of their antimicrobial properties. The products are promoted as having anti-odour or bacteria killing properties amongst others [3].

However, studies have shown that silver nanoparticles in garments can detach in the washing machine and travel to the sewage treatment plant where they may kill beneficial water-treating bacteria. They also end up in rivers and lakes where they impact naturally occurring bacteria [4]. Other studies have said that once in the river silver forms silver sulphide which is an insoluble salt, however, laboratory studies with the less toxic silver compounds, such as silver sulphide and silver chloride, reveal that accumulation of silver does not necessarily lead to adverse effects. At concentrations normally encountered in the environment, food-chain bio-magnification of silver in aquatic systems is unlikely [3]. Thus, new applications using silver in

any form should verify how much of it is leaching and should be in accordance with the legislation which varies from country to country.

For applications such as water treatment, it is possible to capture nanoparticles of silver inside a porous material to prevent their release in the treated water. This researcher proposes a strategy using cellulose grafted fibres with silver nanoparticles for high speed water sterilization. A simple and inexpensive filtering system which could provide safe drinking water for millions of people who are in short supply of clean water, especially following natural disasters and other emergencies.

Bringing potable water to all populations is a daunting problem. The cholera outbreak in Haiti after the 2010 earthquake is a recent example of how tainted drinking water can create a public health crisis or an epidemic. Many died because human faecal material polluted the drinking water sources [1]. These filters could also be of importance industrially as they are not working on a size exclusion basis like conventional filters, but however, inactivating bacteria as it passes through and thus will not be easily fouled. Not only will this extend the life time of the filter but it will also decrease overhead costs, as maintenance will also be reduced and there will be shorter down time especially in continuous processes. With simple and innovative ideas such as this, problems such as these can be averted.

1.1.1 Water Filters

A water filter removes impurities from water by means of a fine physical barrier, a chemical process or a biological process. Filters cleanse water to different extents for purposes like irrigation, drinking water, aquariums, and swimming pools. During the 19th and 20th centuries, water filters for domestic water production were generally divided into slow sand filters and rapid sand filters (also called mechanical filters and American filters). While there were many small-scale water filtration systems prior to 1800, Paisley, Scotland is generally acknowledged as the first city to receive filtered water for an entire town [5]. Filters use sieving, adsorption, ion exchanges and other processes. Unlike a sieve or screen, a filter can remove particles much smaller than the holes through which the water passes. There are many

types of filters for water treatment, for example, water treatment filters, point-of-use-filters and portable water filters to name a few.

Point-of-use filters for home use include granular-activated carbon filters (GAC) used for carbon filtering, metallic alloy filters, micro-porous ceramic filters, carbon block resin (CBR), block resin (CBR), microfiltration and ultrafiltration membranes. Some filters use more than one filtration method. An example of this is a multi-barrier system. Jug filters can be used for small quantities of drinking water; Brita® a popular filter brand is sold worldwide and is well known for purifying drinking water. Some kettles have built-in filters, primarily to reduce limescale build-up. Point-of-use microfiltration devices can be directly installed at water outlets (faucets, showers) in order to protect users against *Legionella* spp., *Pseudomonas* spp., Nontuberculous mycobacteria, *Escherichia coli* and other potentially harmful water pathogens by providing a barrier to them and/or minimizing patient exposure [6].

Portable water filters are water filters are used by hikers, aid organizations during humanitarian emergencies, and the military. These filters are usually small, portable and lightweight (1-2 pounds/0.5-1.0 kg or less), and usually filter water by working a mechanical hand pump, although some use a siphon drip system to force water through while others are built into water bottles. Dirty water is pumped via a screen-filtered flexible silicon tube through a specialized filter, ending up in a container. These filters work to remove bacteria, protozoa and microbial cysts that can cause disease. Filters may have fine meshes that must be replaced or cleaned, and ceramic water filters must have their outside abraded when they have become clogged with impurities. These water filters should not be confused with devices or tablets that are water purifiers, some of which remove or kill viruses such as hepatitis A and rotavirus [6].

The filters proposed by this project are for general use and can be used as a point of use filter or a portable water filter in the case of natural disasters or other needs like stated above. They are flexible and scalable and hence depending on the end use the product can be adjusted to meet the required demand for the end use performances.

1.2 Emergence of nanotechnology in antimicrobial actions and protections from infectious diseases.

Novel metallic nanoparticles (NPs) have been of significant scientific interest because of their unique properties at the nano-scale. They have a wide range of applicability, from optical, or catalytic, to electrical, magnetic and use in antimicrobial devices. Due to the variety of applicability of metallic nanoparticles they have been introduced to a host of diverse substrates (metal oxides, carbon materials and polymers) with various shapes (e.g., particles, film and fabric) In particular, much effort has been devoted to the deposition of metal nanoparticles to polymeric fabric substrates, i.e., metal/ fabric nano-hybrids, due to their strong antimicrobial activity [7].

Most if not all metal and metal oxide NPs produce reactive oxygen species (ROS) under UV light and find their increasing uses in antimicrobial formulations and dressings [8]. In particular, nano-sized silver, zinc, and their compounds have been reported to be effective in inactivating various microorganisms. The high reactivity of titanium and zinc dioxide has also been extensively utilized in the bactericidal substances that are used in filters and coatings on catheters [9]. Recently a wide range of antimicrobial agents have been effectively administered using various NPs [10].

The term “antimicrobial” refers to a broad range of technologies that provide a varying degree of protection for materials against microorganisms. Antimicrobials are quite different in their chemical nature, impact on the environment, mode of action, handling characteristics, durability cost, regulatory compliance and how they interact with microorganisms [11]. An antimicrobial is an agent that kills microorganisms or inhibits their growth [12]. Antimicrobial agents are different from disinfectants. Disinfectants are substances that are applied to non-living objects to destroy microorganisms that are living on the objects. Disinfection does not necessarily kill all microorganisms, especially resistant bacterial spores; it is less effective than sterilisation, which is an extreme physical and/or chemical process that kills all types of life [13]. Disinfectants, such as chlorides and peroxides which are typically used for water purification, work by destroying the cell wall of microbes or interfering with the metabolism. The actual mechanism by which antimicrobial substances such as silver nanoparticles, control microbial growth is extremely

varied and depends on the type of agent used. Generally, antimicrobial agents prevent cell production, damage cell walls or cell permeability, denature proteins, block enzymes and make cell survival impossible [14].

1.3 Antimicrobial nano-materials.

Antibacterial NPs consist of metals and metal oxides, naturally occurring antibacterial substances, carbon-based nano-materials, and surfactant-based nano-emulsions [15]. High surface area to volume ratios and unique chemico-physical properties of various nano-materials are believed to contribute to effective antimicrobial activities [16]. A recent study, in 2009 also demonstrated that naturally occurring bacteria do not develop antimicrobial resistance to metal NPs [9]. Antimicrobial mechanisms of nanomaterials include: 1) photocatalytic production of reactive oxygen species (ROS) that damage cellular and viral components, 2) compromising the bacterial cell wall/membrane, 3) interruption of energy transduction, and 4) inhibition of enzyme activity and DNA synthesis [15, 16, and 9], these mechanisms are shown in the Figure below.

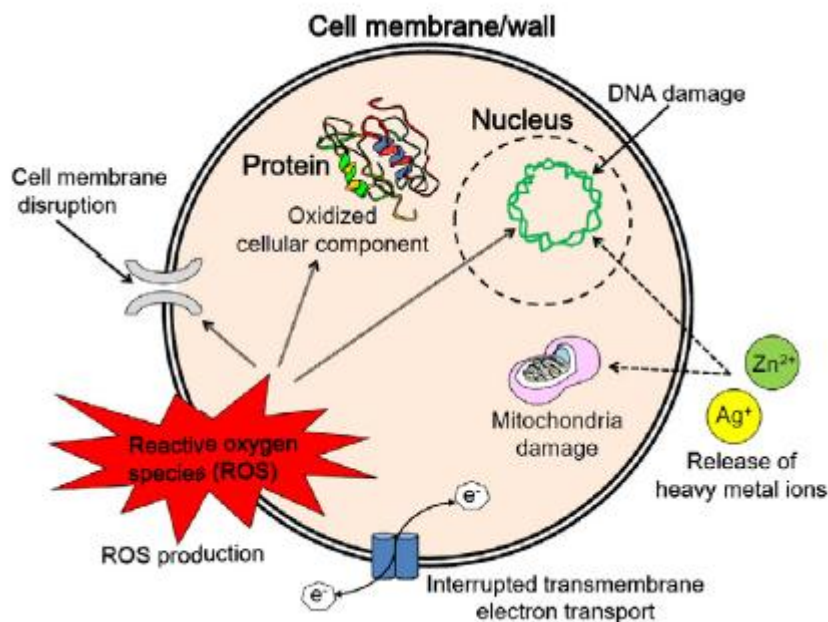


Figure 1 various antimicrobial mechanisms of nanoparticles [17].

Table 1 also summarizes nano-materials with their antimicrobial mechanisms, and potential clinical and industrial uses.

Table 1 Antimicrobial nano-materials [17]

Antimicrobial nanomaterials.		
Nanomaterial	Antimicrobial mechanism	Clinical and industrial applications
Ag NPs	Release of Ag ⁺ ions; disruption of cell membrane and electron transport; DNA damage	Dressing for surgical wound and diabetic foot; coatings for medical devices; portable water filters; antibacterial agent; antifungal agent
ZnO NPs	Intracellular accumulation of NPs; cell membrane damage; H ₂ O ₂ production; release of Zn ²⁺ ions	Antibacterial creams; lotions and ointment; surface coating of medical device; mouthwash
TiO ₂ NPs	Production of ROS; cell membrane and wall damage	Antibacterial agent; food sterilizing agent; air purifiers; water treatment systems
Au NPs	Interaction with cell membranes; strong electrostatic attraction	Photothermal therapy with near infrared light; adjuvant treatment after serious infections antibacterial agent; antifungal agent
Chitosan	Increased permeability and rupture of membrane; chelation of trace metals; enzyme inactivation	Drinking water disinfectants; bacteria immobilizer; microbicide in biomedical products
Fullerenes	Destruction of cell membrane integrity; enhancing activity of infiltrating neutrophil	Potential disinfection applications
CNTs	Cell membrane damage by ROS; oxidation of cell membrane proteins and lipids	Antibacterial agent; biofouling-resistant membranes; water filter; surface-coating
NO-releasing NPs	NO release and production of ROS	Infected wound and diabetic foot treatment
Nanoemulsion	Membrane disruption; disruption of the spore coat	Antimicrobial inhaler; anti-biofilm agent; nasal application; vaccine delivery agents

Abbreviations: Ag NPs, silver nanoparticles; ZnO NPs, zinc oxide nanoparticles; TiO₂ NPs, titanium oxide nanoparticles; Au NPs, gold nanoparticles; CNT, carbon nanotubes, NO, nitric oxide.

1.3.1 Silver, Silver compounds and Silver nanoparticle.

The antibacterial property of silver has been noticed or observed since ancient times. Silver has been used for burn wound treatment, dental work, catheters, and bacterial infection control, in the forms of metallic silver, silver nitrate, and silver sulfadiazine [18]. Using silver to treat bacterial infections became unpopular only after penicillin was introduced in the 1940s and became the primary defence medication [19]. The recent emergence of antibiotics-resistant bacteria and the limited effectiveness of antibiotics revived the clinical use of silver (e.g., wound dressings) [20]. Among the many different types of metallic and metal oxide NPs, Ag NPs have proven to be the most effective against bacteria, viruses, and other eukaryotic microorganisms [21, 22]. Ag NPs attack the respiratory chain and cell division that finally lead to cell death, while concomitantly releasing silver ions that enhance bactericidal activity [23]. The antimicrobial activity of Ag NPs is inversely dependent on size [24, 25] and also the shape [27]. Diverse applications of Ag NPs include wound dressings, coating for medical devices and surgical masks, impregnated textile fabrics, nano-gels, and nano-lotions amongst other uses that can also be seen in Table 1 above. There are many advantages to using silver and its compounds

however, it is not without disadvantages. Prolonged exposure to soluble silver-containing compounds may produce an irreversible pigmentation in the skin (argyria) and the eyes (argyrosis), in addition to other toxic effects, including organ damages (e.g., liver and kidney), irritation (e.g., eyes, skin, respiratory, and intestinal tract), and changes in blood cell counts [28]. On the contrary, metallic silver appears to pose a minimal risk to health and Ag NPs are suggested to be non-toxic in some studies [29, 30], but some studies reported concentration-dependent adverse effects of Ag NPs on the mitochondrial activity [31, 32]. The advent of Ag NPs as promising antimicrobial nano-materials, therefore, requires clear and full elucidations of their potential toxicity before use of any kind such as the one proposed in this project.

CHAPTER 2

LITERATURE REVIEW AND BACKGROUND

2.1 Nanostructured Materials.

Nanostructured materials have been the focus of intense research in recent decades due to their unique size-dependent physical and chemical properties [33-36]. Inorganic nanostructures at 1-100 nm exhibit properties that are different from their bulk counterparts; [33-35] they can be defect-free and can exhibit unusual or much improved mechanical, optical, and electrical properties. Since the particle size can be tailored readily with excellent to moderate control over size uniformity, the resulting novel properties of these materials have been exploited for various optical and electrical applications, including nano-electronics, photonic crystals [37], and sensors based on surface enhanced Raman scattering [38 – 40] and near-field microscopy [41]. In addition, since a big proportion of biological problems deals with dimensions of micron and sub-micron, nanostructured materials can easily fit into these areas, and consequently play important roles. Topics in molecular recognition, biomolecule-nano-crystal conjugates as fluorescence label for biological cells, and DNA-mediated groupings of nano-crystals are widespread, intriguing people from both biological and engineering backgrounds. However, little yet is known about the biological systems response to the existence of these nanostructured materials. Some recent publications in the literature reported encouraging results of bactericidal properties of nanostructured materials. Hamouda *et. al.* [42] found a broad-spectrum sporicidal activity of

nano-emulsions, which were stable, easily dispersed non-irritant, and nontoxic in comparison with conventional agents. Klabunde *et. al.* [43] reported that nano-sized magnesium oxide (MgO), adsorbed with halogen (Cl₂, Br₂), and was effective against Gram-positive and Gram-negative bacterial cells as well as spores. Silver has been known to be a disinfectant for several centuries and has been widely used in the treatment of clinical diseases, including new-born eye prophylaxis and topical burn wounds [44-46]. For this research we chose to focus on *Escherichia coli* (*E. coli*), a gram negative bacterium that is a common contaminant found in water. The distinctive feature of gram-negative bacteria is the presence of a double membrane surrounding each bacterial cell. Although all bacteria have an inner cell membrane, gram-negative bacteria have a unique outer membrane. This outer membrane excludes certain drugs and antibiotics from penetrating the cell, partially accounting for why gram-negative bacteria are generally more resistant to antibiotics than are gram-positive bacteria [47]. There are many types of *E. coli*, and most of them are harmless. But some can cause bloody diarrhoea. These are called enterohemorrhagic *E. coli* (EHEC). One common type is called *E. coli* O157:H7. In some people, this type of *E. coli* may also cause severe anaemia or kidney failure, which can lead to death. Other strains of *E. coli* can cause urinary tract infections or other infections [48].

In this study, the antimicrobial properties of silver nanoparticles are of specific interest. Silver nanoparticles serve as a potent antimicrobial agent, acting against an exceptionally broad spectrum of bacteria while exhibiting low toxicity to mammalian cells [3]. Since silver therapy is of significant clinical benefit in the control of bacterial infections, various forms of new agents medical, biological and pharmaceutical preparations [49-52] containing the silver ions, such as creams, solutions, electrodes, ligatures, biological skin and catheters, have been developed over the past decades. Therefore, not surprisingly, the antimicrobial properties of the silver ions have been extensively investigated [53, 54], and many of the findings are well accepted universally.

2.1.1 Synthesis of Metallic nanoparticles.

Nano structure can be fabricated using a classical top-down approach [55]. This involves taking a starting material and carving it down to the desired nanostructure into well-defined shapes and quality, akin to carving a statue from a block of marble. This approach is utilized in semiconductor industries for transistor fabrication that is down to submicron-scales in

dimensions. The starting block of material is first covered with a thin layer of polymer, known as photoresist. Next, a protective mask having the desired design pattern is placed over the starting block of material before exposing the coated block of material to light radiation. Subsequently, the light radiation within the exposed region alters the solubility of the resist. Depending on the choice of the resist, it can either become soluble (positive resist) or become insoluble (negative resist) in a developing fluid following the light exposure. The desired pattern is then achieved by etching away the exposed region of the block of material. Finally, the remaining protective resist is removed to reveal the patterned device. The precision and the quality of the product are determined by the wavelength of the radiation. The top down approach is usually employed in the fabrication of thin films rather than the synthesis of nanoparticles. The top down process is a subtractive one for producing nanostructures from bulk materials and usually use high energies and are most costly as they require the use of laser and other expensive and expert required knowledge. Examples of the top down fabrication process include milling, laser ablation, arch discharge, lithography etc.

On the opposite end, a bottom-up approach requires the availability of distinctive blocks for the construction of a complex hierarchical structure, which is analogous to LegoTM bricks constructions (Figure2). This necessitates the ability to synthesize nanostructured building blocks with different compositions, sizes and shapes, which indeed have been widely explored in the past years with diverse elemental compositions across the periodic table [56, 57]. Nanowires, nano-cubes, nano-triangles, nano-spheres, nano-plates, nano-belts, nano-plates, nano-stars and nano-rods are some examples of nanostructured materials that represent basic building blocks in the field of nanotechnology (Figure 2). In comparison to zero-dimensional structures like nano-dots or nanoparticles, one-dimensional nanowires and nanotubes possess additional degrees of freedoms for assembly leading to anisotropic properties [58].

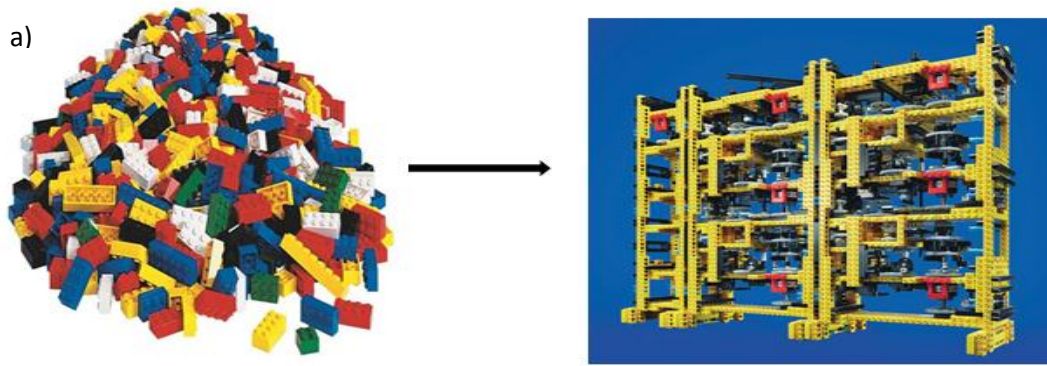


Figure 2 a) Individual Lego pieces transformed into an apple computer fashioned by apple engineers representative of nano particles with well-defined shape [60].

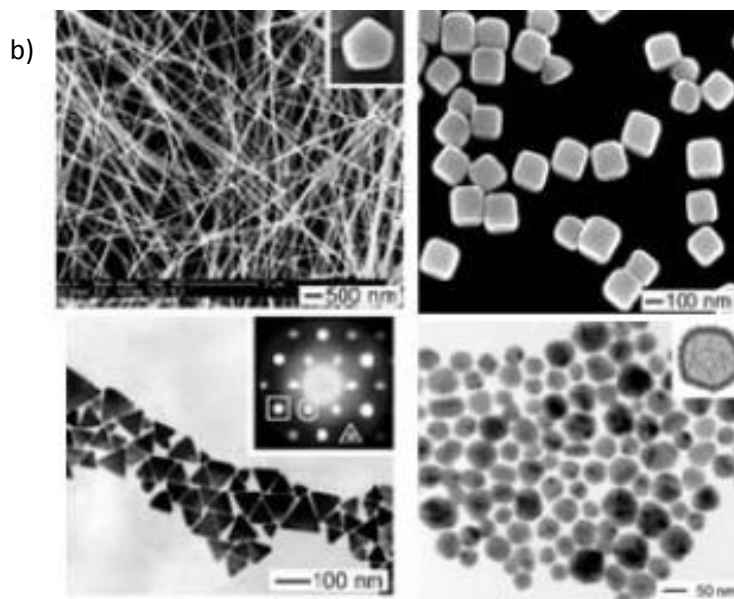


Figure 2 b) Silver nano particles of different shapes and sizes [61, 62].

Another challenge associated with a bottom-up approach is the ability to rationally assemble them precisely over a large area. Such knowledge is critical in designing rational and useful systems, which is the main focus of this and any research. Functionality, in addition to well-defined assembly, lies on measurable properties which may be unique (novel) or simply synergistic of the particular make-up of the assembled structure [59].

2.1.2 Optical properties of noble metallic nanoparticles.

In addition to their facile synthesis, metallic silver and gold in the nano-scale are a particularly interesting class of plasmonic materials. Since the electrons of silver nanostructures are weakly

bound, when exposed to electric field they oscillate from and beyond the neutral state resulting in charge distribution [63]. In nanoparticle case, such oscillation is confined and is also known as localized surface plasmon resonance, LSPR (Figure 3a). This is in contrast to a bulk film of silver or gold, where the oscillating electron could propagate anywhere along the infinitely spacious planar surface, and therefore is not localized and simply called surface plasmon resonance (SPR).

LSPR has a characteristic resonance frequency which, at that particular frequency, strongly absorbs the wavelength of light. The wavelength absorption occurs in the visible or near infrared range of light and it is distinctive to its shape, dimensions, inter-particle distance, and for—non-isotropic nanoparticles—orientation, as supported by numerous theoretical models (Figure 3b) [64]. The characteristic plasmon absorption at a certain wavelength of visible light is evident in coloured stained glass (burgundy, red, purple, etc.), which indeed contains finely divided colloidal gold or gold nanoparticles.

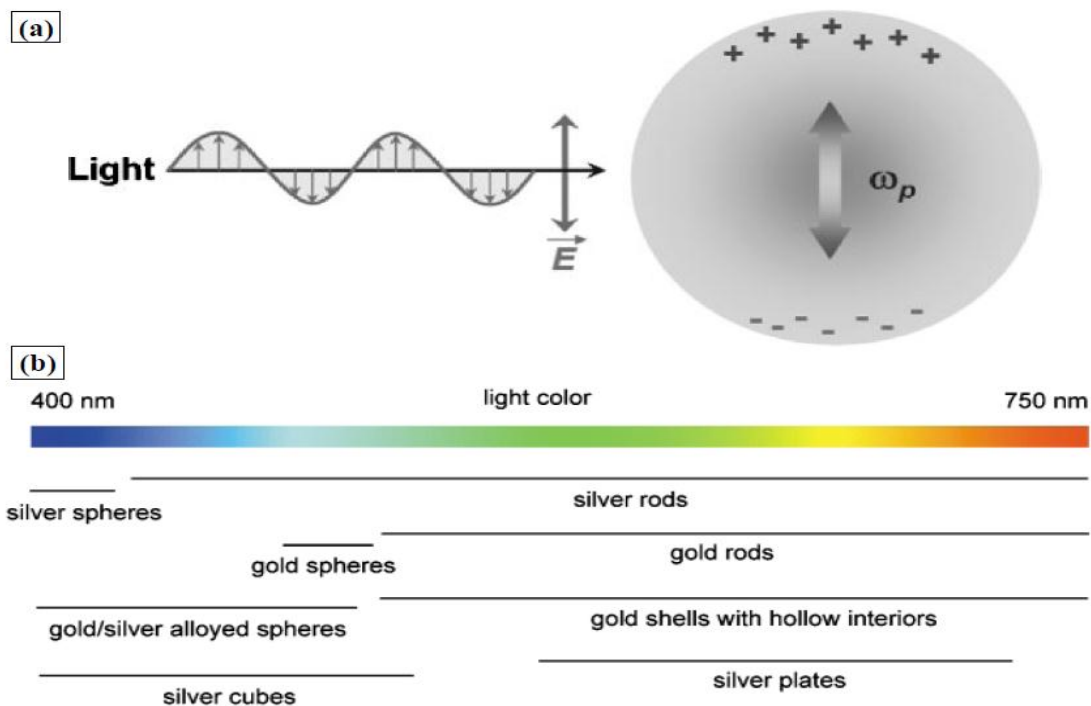


Figure 3 a) Plasmon oscillation at a characteristic plasmon frequency, ω_p , within a spherical metallic nanoparticle in the presence of exciting laser [63]. (b) Plasmon absorption spectrum of some representative shaped gold- and silver-nanoparticles within the visible region [65].

2.1.3 Shape control of geometrically-defined nano particles.

Few of the methods that have been proven successful to synthesize geometrically-defined nanoparticles include [66]: (I) sol-gel process, (II) chemical precipitation, (III) hydrothermal or solvothermal synthesis, (IV) pyrolysis, (V) vapour deposition, and (VI) soft-template assisted growth.

- I. Sol-gel process is a solution technique where the chemical precursor (metal oxides or metal alkoxides) is dissolved in a solvent which undergo hydrolysis condensation— inorganic polymerization—upon heating forming oxo (M-O-M) or hydroxo (M-OH-M) bridges, depending on whether metal oxide or metal alkoxide was used as the precursor. Such transformation is referred to as sol-to-gel transformation because the sol evolves into a gel-like biphasic system due to the formation of the oxo and hydroxo bridges that result in the formation of either a discrete or continuous particles. Metal oxide nanoparticles are typically synthesized in this manner (e.g. TiO_2 , SiO_2 , SnO_2 , ZnO) [67].
- II. Control over the kinetics of nucleation and particle growth in a homogeneous solution can lead to the precipitation of mono-disperse nanoparticles. Since nucleation occurs spontaneously when the solution reaches a critical super-saturation of the salt precursor, the mono-disperse nanoparticles can be achieved via controlled release of the salt precursor. Some factors that are essential to this process are precursor concentration, pH, and temperature (e.g. $\gamma\text{-Fe}_2\text{O}_3$) [68]. Various shapes of $\text{Cu}(\text{OH})_2$ nanostructures (nanowires, rectangles, seedlike, beltlike, and sheetlike) were grown in solution when the NaOH concentration is changed with respect to the $\text{Cu}(\text{NO}_3)_2$ salt precursor. $\text{Cu}(\text{OH})_2$ can then be transformed into CuO by subsequent heat treatment for half an hour at 80 °C [69]. Some inorganic substances dissolve in water at elevated temperature and pressures and subsequently recrystallize from the fluid and transforming the shape, size, and crystal structure. This process is called hydrothermal if water is used as the solvent [70], but it is called solvothermal process if other solvents are used instead. Non-spherical nanoparticles have also been obtained from this method (e.g. nano-rods, nanowires, and nanotubes of TiO_2) [71].

- III. Pyrolysis is a process where a chemical precursor is decomposed into a solid compound that is accompanied by evaporation of the unwanted waste under a given thermal process. A controlled thermal process is necessary to yield a product that is mono-dispersed in shape and compositions that is best achieved when the reaction is done in solution where the reaction rate is greatly reduced. Protecting agents in the form of polymer is sometimes used as well. Some examples include CoWO_4 , $\alpha\text{-Al}_2\text{O}_3$, GaN, and ZnO [72].
- IV. As the name implies, in a vapour deposition process the precursor is first vaporized and deposited via absorption onto the appropriate catalysts to grow into a well-defined structure. This method has been utilized to grow carbon nanotube forests with high aspect-ratio [73], but also applicable to other types of materials e.g. In_2O_3 , BN, LaB_6 , MgB_2 [74]. Structures other than one-dimensional column have been reported as well (e.g. ZnO nano-tetrapods) [75].
- V. A surfactant is usually represented by a molecule having a hydrophobic tail and a hydrophilic head. At a certain minimum concentration in a solvent medium, they form aggregate (or micelle). If the solvent is hydrophilic, e.g., water, the hydrophobic tail is oriented inside the aggregate to avoid contact with water and the hydrophilic head is oriented outside the aggregate to contact with the surrounding water. In the opposite case, if the solvent is hydrophobic, e.g., hexane, the hydrophobic tail is oriented outside the aggregate to contact with hexane and the hydrophilic head is oriented inside the aggregate to avoid contact with the surrounding hexane. This is known as reverse micelle. The geometry and size of reverse micelles is determined by their chemical compositions and chemical structures, which can be predicted by calculating the packing factor. These micelles can therefore function as soft-template for the reduction of metallic salt precursor in solution [76]. Gold and silver nanoparticles derivatives (e.g. nano-rods, nano-plates, nano-spheres) have been synthesized in this manner [77].

2.1.4 Soft-template assisted growth of FCC metallic nanoparticles (Chemical reduction method “Polyol method”).

The synthesis of geometrically-defined nanoparticles has particularly been successful for fcc metals (Pd, Pt, Au, Ag) in grams quantity, where polyvinyl pyrrolidone (PVP) functions as the soft-template [78]. This technique involves metallic salt precursor, ethylene glycol reducing agent (EG), and PVP capping agent that are heated to elevated temperature [79]. Within the early phase of the reaction, the metal ions precursor is reduced into elemental metal and subsequently forms elemental metal clusters (Figure 4). Below the critical nucleation size the silver cluster redissolves into solution, but passed the critical nucleation size the cluster continues to grow. Further growth occurs *via* Oswald ripening, where smaller clusters are consumed by larger clusters. The small clusters lower its surface energy by being incorporated onto larger clusters. To lower the surface energy silver nuclei incorporate twin-boundary defects. Change in defect structure is un-favoured as the nuclei grow because it will require additional driving force, therefore the shape of the nuclei from which a crystal grows determine its final shape. In a typical polyol reduction of metallic salt three types of nuclei are formed in the Boltzmann-like distribution that is comprised of single-crystal, multiply-twinned decahedron, quasi-spherical multi-twinned crystal seeds. The five-fold twinned decahedron is the most abundant because its free energy is the lowest [78].

The ability to selectively enrich a particular nucleus at the start of a polyol reaction means that subsequent nano-crystal growth will result in metallic nanoparticles with a certain geometrical shape. This is determined by the rate of reduction and the silver nitrate (AgNO_3) precursor to PVP capping agent ratio. Controlled growth subsequently take place due to specific adsorption of PVP onto the {100} facet, which confines the growth in the direction of the exposed facet. In the polyol synthesis of silver salt precursor for example, silver nano-cube, silver nanowire, and silver nano-sphere can be grown from singly-crystal seed, 5-twinned decahedral seed or multi-twinned quasi-spherical seed, respectively (Figure 4).

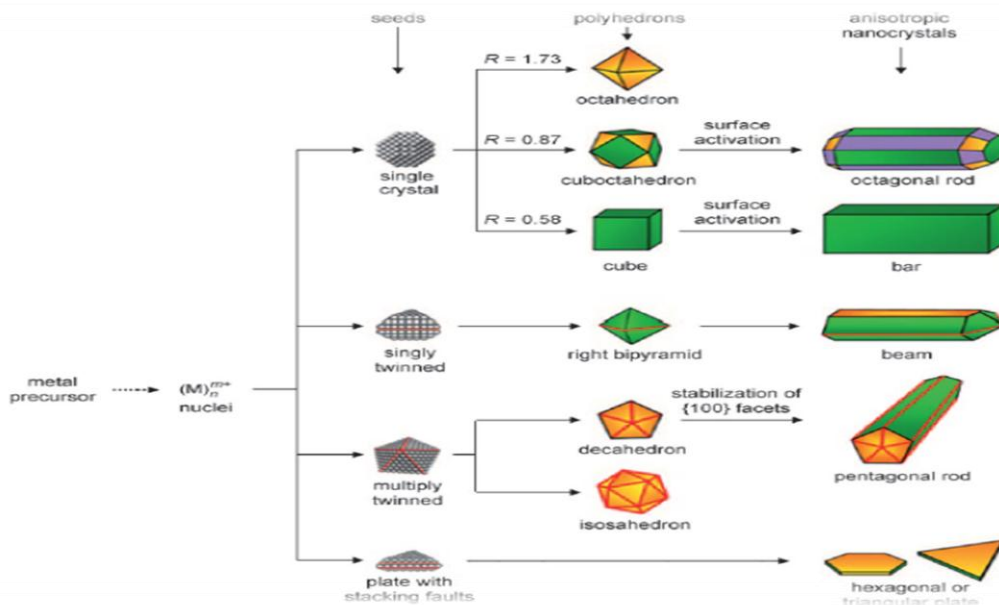


Figure 4 The evolution of fcc crystal formation which begins with the reduction of metal salt precursor into silver clusters formation, and followed by nucleus formation, in the form of single crystal, singly-twinned, multi-twinned, and plate with stacking-fault. The various crystalline facets, {100}, {111}, and {110} are represented by green, orange, and purple colours, respectively. The red lines represent twin planes. R is the ratio between the growth rates along the $\langle 100 \rangle$ and $\langle 111 \rangle$ directions [78].

2.1.5 Biological applications of metallic nanoparticles.

Living organisms are built of cells that are typically around $10 \mu\text{m}$ in size. However, the cell parts are much smaller and are in the sub-micron size domain. Even smaller are the proteins with a typical size of just 5 nm, which is comparable with the dimensions of smallest man-made nanoparticles [80]. This simple size comparison suggests that nanoparticles may be used as very small probes that would allow us to detect at the cellular stage without introducing too much interference [81]. Understanding of biological processes on the nano-scale level is a strong driving force behind development of nanotechnology. In this section some of the fundamental ideas of biological applications of metallic nanoparticles will be explored, an overview of current developments in anti-microbial research area will be demonstrated.

2.1.6 General Applications of metallic nanoparticles in Biological Area.

As mentioned above, nanoparticles exist in the same size domain as proteins which make them suitable for bio-tagging or -labelling. Some of the applications of nanoparticles in biological and medicine fields:

- Fluorescent biological labels [82,83];

- Drug and gene delivery [84,85];
- Bio detection of pathogens [86];
- Detection of proteins [87];
- Probing of DNA structure [88];
- Tissue engineering [89,90];
- Tumour destruction via heating [91];
- Separation and purification of biological molecules and cells [92] ;
- MRI contrast enhancement [93], and more.

However, size is just one of many characteristics of nanoparticles that it is rarely sufficient if one is to use nanoparticles as biological tags. In order to interact with biological target, a biological or molecular coating or layer acting as a bioinorganic interface should be attached to the nanoparticles. Examples of biological coatings may include antibodies, biopolymers like collagen [94], or monolayers of small molecules that make the nanoparticles biocompatible [95]. In addition, as optical detection techniques are wide spread in biological research, nanoparticles should be able to either couple with fluorescent materials or change their optical properties during the application.

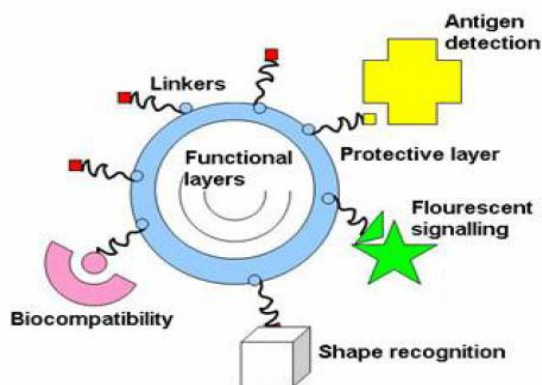


Figure 5 Typical configurations utilised in nano-bio materials applied to medical or biological problems [95].

From the view point of multi-functional, several functional groups can be attached on the nanoparticle's surface as depicted in Figure 5 above, and thus enabling the nanoparticle in detecting, transporting, and even destroying the biological molecules, which are of interest. However, it is important to point out that the more surface functionality the better the chances of being recognized by the immune system. Nanoparticle usually forms the core of the system; it

can be used as a convenient surface for molecular assembly, and may be composed of inorganic or polymeric materials. It can also be in the form of nano-vehicle surrounded by a membrane or a layer. The size and size distribution might be important in some cases, for example if penetration through a pore structure of a cellular membrane is required. The core itself might have several layers and be multifunctional. For example, by combining magnetic and luminescent layers, one can both detect and manipulate the particles. The core particle is often protected by several monolayers of inert material. Organic molecules that are adsorbed or chemisorbed on the surface of the particle are also used for this purpose. The same layer might act as a biocompatible material. More often, an additional layer of linker molecules is required to proceed with further functionalization. The linear linker molecule has reactive groups at both ends. One group is aimed at attaching the linker to the nanoparticle surface and the other is used to bind various moieties like antibodies, fluorophores, etc., depending on the function required by the application [95].

2.1.7 Population Growth of Bacteria.

Growth is an orderly increase in the quantity of cellular constituents. It depends upon the ability of the cell to form new protoplasm from nutrient available in the environment. In most bacteria, growth involves increase in cell mass and number of ribosomes, duplication of the bacterial chromosome, synthesis of new cell wall and plasma membrane, partitioning of the two chromosomes, septum formation, and cell division [96].

Under favourable conditions, a growing bacterial population doubles at regular intervals. Growth is by geometric progression: 1, 2, 4, 8, etc. or $2^0, 2^1, 2^2, 2^3 \dots 2^n$ (where n is the number of generations). This is called exponential growth. In reality, exponential growth is only part of the bacterial life cycle, and not representative of the normal pattern of growth of bacteria in nature.

When a fresh medium is inoculated with a given number of cells, and the population growth is monitored over a period of time, plotting the data will yield a typical bacterial growth curve (Figure 6). The bacterial growth curve is naturally divided to four parts, as duplication rate is taken into consideration [96].

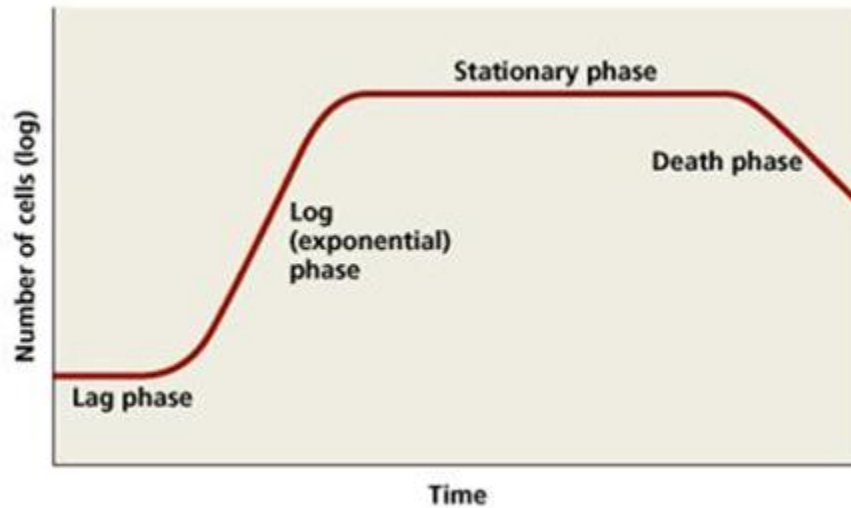


Figure 6 A typical bacterial growth curve. Four distinct phases can be recognized, lag phase, exponential phase, stationary phase and death phase respectively [61].

1.1 Lag Phase. Immediately after inoculation of the cells into fresh medium, the population remains temporarily unchanged. Although there is no apparent cell division occurring, the cells may be growing in volume or mass, synthesizing enzymes, proteins, RNA, and increasing in metabolic activity. The length of the lag phase is apparently dependent on a wide variety of factors including the size of the inoculums; time necessary to recover from physical damage or shock in the transfer; time required for synthesis of essential coenzymes or division factors; and time for synthesis of new enzymes that are necessary to metabolize the substrates present in the medium.

1.2 Exponential (log) Phase. The exponential phase of growth is a pattern of balanced growth wherein all the cells are dividing regularly by binary fission, and are growing by geometric progression. The cells divide at a constant rate depending upon the composition of the growth medium and the conditions of incubation. The rate of exponential growth of a bacterial culture is expressed as generation time, also the doubling time of the bacterial population. Generation time (G) is defined as the time (t) per generation ($n =$ number of generations). Hence, $G=t/n$ is the equation from which calculations of generation time (in the next section) derive.

1.3 Stationary Phase. Exponential growth cannot be continued forever in a batch culture (e.g. a closed system such as a test tube or flask). Population growth is limited by one of three factors: 1. exhaustion of available nutrients; 2. accumulation of inhibitory metabolites or end products; 3. exhaustion of space, in this case called a lack of "biological space". During the stationary phase, if viable cells are being counted, it cannot be determined whether some cells are dying and an equal number of cells are dividing, or the population of cells has simply stopped growing and dividing.

1.4 Death Phase. If incubation continues after the population reaches stationary phase, a death phase follows, in which the viable cell population declines. However, this decline cannot be observed by turbidimetric measurements. During the death phase, the number of viable cells decreases geometrically (exponentially), essentially the reverse of growth during the log phase [96].

2.1.8 Growth Rate and Generation Time.

Bacterial growth rate and generation time are two of the most important aspects in regard of bacterial growth. The determination of bacterial growth rate will give us a general sense of how the bacterial cells response to their environment. As mentioned above, bacterial growth rate during the phase of exponential growth, under standard nutritional conditions (culture medium, temperature, pH), defines the bacterium's generation time. An alternative way of defining the bacterial generation time is that it is the time interval required for the cells (or population) to divide. Generation times for bacteria vary from about 12 minutes to 24 hours or more. Even for the same bacterium, the generation time may be quite different depend on the inoculation conditions, and on the initial bacterial concentration. For the bacteria that will be used in this research, *E. coli* the generation time in a laboratory is in the range of 20 to 30 minutes [97].

2.1.8.1 Calculation of Generation Time

When growing exponentially by binary fission, the increase in a bacterial population is by geometric fashion. If we start with one cell, when it divides, there are 2 cells in the first generation, 4 cells in the second generation, and 8 cells in the third generation, and so on. Therefore we can easily derive the equations for calculating the bacterial generation time, based on some simply mathematic transformations. Hence, by comparing the typical bacterial

generation time and the experimental data, it is not difficult to find out the bacteriological properties of nanoparticles added into the bacterial medium [97].

2.1.9 Bactericidal Effects of Metallic Nanoparticles.

People have known about the bactericidal properties of many metallic ions, as well as bulk metals for a long time. Enormous work has been dedicated to find out the fundamental physical and biological mechanisms for these metallic ions, and some satisfactory explanations have been derived. However, knowledge nowadays in biological and anti-pathogen properties of nanostructured materials is still limited, especial for the nanostructured metals in the anti-bacteria field. Some of the recent studies reported encouraging results of bactericidal properties of several nanostructured materials. Hamouda *et al.* [42] revealed the broad-spectrum sporicidal activity of certain nanoemulsions. These nanoemulsions were also found to be stable, easily dispersed, non-irritant, and nontoxic compared with other agents. Klabunde *et al.* [43] reported that when significantly adsorbed with halogen (Cl_2 , Br_2), magnesium oxide (MgO) was very effective against Gram-positive and Gram-negative bacterial cells as well as spores [98]. These studies only provided us a possible approach in bactericidal study using nanostructured materials.

To find a more direct fashion to discover the bactericidal properties of nanostructured materials, researchers turn their focus on some well-known bactericidal metals. As is well known, some elements by themselves are harmful to microorganisms, and silver is the most toxic one among them [99, 100]. Therefore, silver ions and silver-containing products are widely used in medical applications. For instances, silver compounds are used for treatment of serious burns, in bandages for trauma and diabetic wounds [101], and are used to coat the catheters and other medical devices to prevent the growth of bacterial biofilms [103]. Numerous studies have done to reveal the mechanisms of bactericidal property and even bacterial resistance of silver ions [53, 54] as was stated before there are however, a recent study also demonstrated that naturally occurring bacteria do not develop antimicrobial resistance to metal NPs [9]. And in regard of nanostructured silver, not until recently, Sondi *et al.* [103] reported the antimicrobial property of silver nanoparticles against *E. coli*, which is a gram-negative bacterium [104]; it was the first paper on the study of bactericidal property of nanostructured metal for this research we will use *E. coli* as it is one of the most common contaminants in water. Conclusively, the silver

nanoparticles used in their experiment to some extent possessed bactericidal effects, as the biological tests in agar plates showed that only few bacterial colonies were formed under the treatment of silver nanoparticles. And in the medium culture tests, notable difference between control sample and the samples mixed with silver nanoparticles had been found. However, from the efficiency point of view, their experiments were limited due to the non-ideal stability of the silver nanoparticles. The silver-containing samples were found not stable after the mixing of silver nanoparticles and bacterial culture.

The possible explanation is given to the surface charge attraction of bacterial cells and the silver nanoparticles. In addition, the dispersion of nanostructured materials, which is also called a colloid, is very sensitive to the liquid medium. Colloidal systems stability can be easily destroyed by changing the medium pH or even environmental temperature. As a consequence, since there is no biological benign stabilizer in their test, the colloidal stability cannot be sustained when mixed with bacterial medium. Silver nanoparticles soon agglomerated together and eventually precipitated down to the bottom of the testing tubes, and resulted in the reduction of bactericidal effects.

2.2 Challenges and motivations of current study.

Bottom-up assembly is a promising path towards the design and fabrication of functional materials because it allows control over compositions and, contrary to the top-down approach, which is not severely limited in spatial resolution. Furthermore, there are growing varieties of techniques discovered for the synthesis of well-defined inorganic building blocks that serve as the necessary starting components for a bottom-up assembly, which spans from a dry-state to solution-based techniques. Solution-based technique is often preferred because it does not require expensive setup and is more feasible for lab based research. For solution-based technique, one can choose between a template or non-template approach. In a template approach, the formed nanoparticles are usually stable and well-dispersible in various solvents. On the other hand, non-template approach leads to bare-nanoparticles that allow surface modifications; however, they may be prone to aggregations.

While much fundamental studies have been achieved in understanding the mechanisms of geometrically-specific nanoparticles growth and surface modifications, the next step will be to combine the nanoparticles covalently with a cellulose membrane and explore its anti-

microbial properties of the silver nanoparticles extensively. However in order to realize the full capabilities of these assemblies with performance exceeding current technology, the gap between fundamental and laboratory study and engineering needs to be bridged.

The general challenges associated with the bottom-up assembly of such nanostructures into functional micro/nano-materials can thus be summarized as follows:

- 1.1 Many nanoparticles that possess novel properties have only been synthesized in a low-yield.
- 1.2 They tend to aggregate due to their high-surface area per volume ratio.
- 1.3 It is difficult to obtain a uniform long-range assembly over a large area.
- 1.4 The level of difficulty is increased as the particle size decreases from the bulk to the micro or nano scale, thus making nano and or micro particles more difficult or even impossible to handle.
- 1.5 There is limited number of characterization techniques to understand their physical properties at the nano-scale. Conventional techniques are very often not applicable at the nano-scale.

The challenges for the assembly of the membrane though simple might be viewed as complex. Ensuring that the nanoparticles are covalently attached to the functional thiol or amine groups on the cellulose fibres is the most difficult task as if there is too much leeching of the particles into the water it may cause the toxicity to be too high and render the filter not passing the standard for human use. Thus it is necessary to have mechanical testing and correct functionalization (thiolation/amination) of the cellulose fibres in the membrane to avoid losing too many or any particles. The functionalization is also a crucial step as it is the step that determines the loading amounts of silver and whether or not the loaded silver nanoparticle will be able to oxidize to silver ions which are responsible for the biocidal activity. The manner in which the antimicrobial agents work is either by contact or by diffusion. So in the assembly it is important to allow the bacteria to have contact with the silver ions long enough of inhibit or inactivate the bacteria.

When working with bacteria all the parameters have to be monitored carefully, and time is of utmost importance which is the major challenge when working with live bacteria in order to

ensure good and accurate results. However, with proper time management and sterile (aesthetic) conditions almost all problems can be averted.

2.3 Research goal and objectives.

2.3.1 Research goal and approach.

This current work is aimed at presenting a study of the synthesis of metallic silver nanoparticles using a template approach. The resulting nanoparticles are characterized through various methods and will later be attached covalently to cellulose fibres in the hope of designing a nano structured filter for high speed water sterilization. The ultimate goal of this first phase of the project is to understand the fundamentals of the bottom up assembly of inorganic building blocks for the design of an engineered filter.

Silver nanoparticles as inorganic building blocks were chosen due to the facile and high yield synthesis as well as silver is a well know disinfectant for several centuries. Silver serves as a potent antibacterial agent, acting against an exceptionally broad spectrum of bacteria whilst, exhibiting low toxicity to mammalian cells as was mentioned earlier.

The second goal of this project is to make or assemble a water filter for high speed sterilization by covalently bonding the synthesized nanoparticles to cellulose fibres and investigating the antibacterial effects. Since antibacterial effects fall under two categories:

- Bactericidal
- Bacterial growth inhibitory

Bacterial growth and bacterial viability tests will be conducted to identify the bacterial effect of this cellulose grafted fibre filter.

Other methods based on a membrane approach works as a function of size exclusion of the bacteria which requires a high pressure drop and will intern lead to clogging [105]. The approach of this research however, combining the nanoparticles inactivates the bacteria as they pass through the membrane thus reducing the chance of fouling. The use of commercially available cellulose membranes may cause the price of the filters to be a tad more expensive, than if the fibres starting material came from cotton fibres which is less expensive, but both are

commercially and readily available and either one can be used as the backbone for the membrane filter. Not only are they cost effective they are mechanically and chemically robust. These considerations are extremely important for making filters of practical importance and are a challenge for many other technologies, including electro-spun nano-fibrous filters [106]. The pores between fibres in cotton are in the range of tens to hundreds of micrometres, much larger than the length scale of bacteria, which prevents the device from mechanically clogging during use [105], the same can be said for the commercially available cellulose membranes which are employed in his project ranging from 2-3 microns and can be extended to as much as 5 microns. The next components of the filter are the silver nanoparticles, wires and spheres. The wires will provide a secondary mesh and the spheres which have a higher rate of inactivating the bacteria are used to increase the effectiveness and efficiency of the filter. The wires possess strong binding points with the fibres of the cellulose membrane thus forming an interconnected network and when coupled with the spheres form an effective barrier. This leads to a gravity fed, bio-fouling resistant device that can inactivate bacteria at faster flow rates than conventional filters while consuming less energy or no energy at all. Recently a similar filter has been produced in India, with the hopes of providing microbially safe drinking water for all. This filter uses a nano-composite which exhibits sand-like properties and releases silver ions to purify water at a low cost without the use of any alternate form of energy [107].

2.3.2 Objectives.

The design, fabrication and characterization of these filters are being under taken in several steps in order of design complexity and are as follows:

1. Synthesis of metallic particles:
 - Nano wires (NW's)
 - Nano spheres
2. Assembly of cellulose grafted membrane filter by covalent attachment of the metallic nanoparticles by modifying the cellulose with thiol and amine functional groups, and then immersion in a colloidal solution of the nanoparticle. The resulting metal-cellulose filter is then subjected to rigorous mechanical testing before going to the third and final phase of this research.

2.2 Antibacterial tests, by bacterial medium growth tests and bacterial viability tests.

2.3 Evaluation and discussion.

2.3.3 Thesis Organization.

Chapter 1- This chapter provides the general overview of micro-nano structures fabrications, *i.e.*, top-down approach versus bottom-up approach. The properties, preparation and the various assembly techniques of the starting components for bottom-up assembly are also discussed here.

Chapter 2- Research goal and objectives of the current study are delineated in this chapter.

Chapter 3- Experimental procedures including nanoparticles synthesis, materials preparations, bacterial medium growth tests, and bacterial viability tests will be introduced as well as characterization methods are described in this chapter.

Chapter 4- Is devoted to the results upon the experiments carried out in chapter 3. From the different characterization techniques images will be provided for the nanoparticles. Extensive information, such as silver nanoparticle size distribution, full width at half maximum (FWHM) of surface plasmon peak in the UV-vis absorption spectrum, will also be characterized. Information about the degree of thiolation of the cellulose fibres and the covalent attachment of the nanoparticles will be provided and interpreted. In regard of the antibacterial tests, bacterial growth curves, colonies on agar plates, images will be presented, and analysed carefully.

Chapter 5- Is a discussion of the experimental results. General concerns on synthesizing silver nanoparticles, assembly of the membrane filter and the antibacterial effects of silver nanoparticles on *E. coli* bacterium. As well as the future direction of this work.

Chapter 6- The final chapter provides a summary of the entire project and makes a conclusion on all the work that has been completed.

2.4 Marketability and feasibility of high-speed filters for high-speed sterilization.

Sometimes the solution to an enormous problem is tiny. Silver nanoparticles may be the key to supplying clean, affordable drinking water worldwide. Many ideas have been coined but what sets this filter apart from the other filters is that it is not working on a size exclusion principle like conventional filters in the inactivation of bacteria and other harmful viruses, fungi and protozoa. The filter is made of a cellulose acetate backbone with silver nanowires providing a secondary mesh and embedded with silver nanoparticles of less than 10 nm. This is a gravity fed filter in which water passes through and the silver NPs are oxidized, releasing silver ions which are responsible for the antimicrobial property and in turn kills the harmful constituents of the water being treated. One may wonder is this safe? Although some nanoparticles leach into the water they are in low concentrations that will not pose a threat to health.

The filters are quite cheap to produce (cost estimation can be found in the appendices) and as such could be the solution to having clean drinking water at your fingertips whether you are in the comfort of your home, on outdoor excursions, a part of the armed forces, in case of a natural disaster or you live in a poverty stricken area with no access to clean water. This filter is a multifaceted filter that is scalable to meet the demands required by the intended users.

According to the World Health organization over one billion people do not have access to clean water [1]. This is definitely a cry for help as in these modern times its difficult to fathom why this is possible. The public drinking water supply has grown with an average annual rate of 9% and high investment in this field is expected. The World Bank has granted an investment of over 450 Billion US dollars for the next 10 years. For over one third of the world's population in many regions, especially Africa, South America and parts of Asia, the drinking water is a quality problem and supply shortage too. There are also such problems even in industrial countries. The highest growth rates (14% in 2011) are in sectors mineral and bottled water, this markets are expected to double from 2015 [106]. The bottled water sector is also generating lots of waste and increasing the carbon footprint of the world. With these Filters we can help to reduce this whilst providing clean water at cheaper rates and in much faster and larger quantities.

After the 2010 Earthquake in Haiti, many people died because of they consumed faecal contaminated water, with filters such as these many lives could have been saved. Not only are

the filters able to be small, portable and cheap they are safe. Natural disasters can happen anywhere without prejudice and so it is necessary for us to be prepared in case of an unfortunate occurrence. These filters could also be used by aid associations like the Red Cross or UNICEF to help victims have clean water and try to improve their sanitation facilities as best as is possible in times of crisis. Some 2.4 billion people, one-third of the world's population, will remain without access to improved sanitation in 2015, according to a joint WHO/UNICEF report. Faster progress on sanitation is needed and both organizations call for a final push to meet the Millennium Development Goal sanitation target [1]. Bacterial contaminations of water is a major cause of life threatening disease outbreaks, such as cholera or gastroenteritis especially after natural disasters and in poverty stricken countries. Soldiers who also go on these missions after disasters or in the event of war also need to rehydrate themselves and as such can use these filters to have access at all times to clean water even in remote location.

An excursion often takes people outside of their homes to locations and unpredictable situations. People on these excursions may require clean water and at times it may not be possible, but these small filters will provide the means necessary to convert the resources which are available into the resources you need. Also the recreational use of water can deliver important benefits to health and well-being yet; there may also be adverse health effects associated with recreational use if the water is polluted or unsafe. And thus there is a need to have a filter of this nature which can ensure that you are safe and will be able to enjoy your recreational activities.

There is also a need to purify waste water, worldwide 14% of all waste water in the year 2010 was purified. Bottom of this development are South America and Africa with less than 2% waste water purification. The most important influential factors are population development, increasing demand for foodstuff and thus demand for water, urbanization, germination, pesticides, nitrates and above all resistance to antibiotics in surface water in the industrialized countries [108]. With the population on the rise it is important to play our role in improving the quality of life and thus we can bridge the gap between engineering and laboratory science and real life applications. There is a need for these filters and if developed could have the potential to lower mortality from lack of clean water and infectious disease caused by poor sanitation.

The overall goal is to have sustainable access to safe drinking water; nanotechnology in my opinion can and should make a lasting impact on society with projects like these. Not only will it save and or improve lives it can also contribute to philanthropic works as well as the economy as if developed commercially it can also provide jobs for many. The principle of the filter also makes it commercially viable industrially as it should not be easily fouled as the bacteria is killed as it passes through the cellulose fibres and as such would reduce the maintenance cost, improve the operating hours as down time is reduced thus making the overall process more efficient and cost effective.

CHAPTER 3

EXPERIMENTAL AND METHODS

This chapter will be given in appendix A, and goes in detail should any reader of this project decides to reproduce any of the experimental procedures utilized in this work.

CHAPTER 4

RESULTS

4.1 Characterization of silver nanoparticles.

Silver nanoparticles were prepared by chemical reduction of metal salts which is the most commonly used method for the solution-phase synthesis of metal nanoparticles. The synthesis as described previously, in chapter 3 involves a soluble metal salt AgNO_3 as the silver precursor, a stabilizing agent which also has reducing power, PVP and a chemical reducing agent EG. Silver nano wires were synthesized by soft template assisted growth and silver nano spheres were synthesized by microwaves. Both wires and spheres were dispersed in deionized water, as a heterogeneous nucleation and stabilization medium and were used for the assembly of the Ag-cellulose filters (wires were also dispersed in ethanol for characterization purposes only). The particles were characterized carefully using the following techniques:

Ultra-Violet-visible absorption Spectroscopy (UV-vis).

UV-vis is one of the most widely used techniques of structural characterization of silver nanoparticles due to their characteristic localized surface plasmon resonance (LSPR). Optical spectra of the particles were obtained in the wave length range of 200-800 nm. Quartz cuvettes with an optical path length of 10 mm were used for the measurements. A pulse of wide-spectrum light, generated by a tungsten bulb, is passed through the sample and the resulting extinction (i.e. absorption and scattering) is collected and the blank sample is subtracted out. Theoretically, silver nanoparticles, possess optical spectrum with absorption peak, also known as the surface plasmon resonance (SPR) peak, lies ~400 nm. The full width at half maximum (FWHM), is typically around 50~90 nm depending on the polydispersity of the sample. Metallic nanoparticles show distinct absorption spectrum when suspended in aqueous suspension. Figure 11 below shows nano wires of silver dispersed in ethanol having a distinct greyish or silverfish colour and nano spheres having a dark brown colour, these colours were indicative of silver nanoparticles [16].

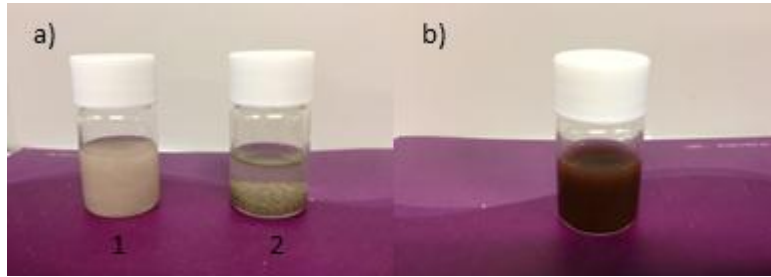


Figure 11 Dispersed silver nanoparticles a) Silver nano wires in 1. Ethanol and 2. Acetone (not well dispersed) and b) Silver nano spheres dispersed in water.

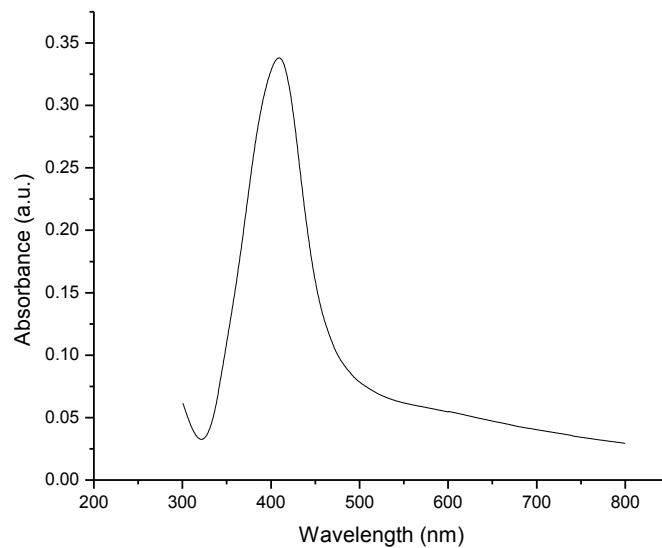


Figure 12 UV-vis absorption spectrum of silver nanoparticles, with absorption peak at 400-nm, and FWHM about 80-nm.

The spectrum shown in Figure 12 is distinct of silver nanoparticles of silver nano-spheres, where both peak (404.4 nm) and FWHM (73 nm) were in accordance with that of silver nanoparticles. The position and shape of the plasmon absorption is however, dependent on the particle size, shape and dielectric constant of the surrounding medium.

Transmission Electron Microscopy (TEM)

Transmission Electron Microscopy (TEM) investigations of the nanoparticles are a direct and effective approach to determine their particle size and morphology as well as dispersion uniformity at the nano-scale. During the operation of TEM, an electron beam is focused on a thin layer of dried nano particles which were stabilized in ethanol, which were deposited on a 200 mesh copper grid. Electrons pass through the particles at a slower rate than through the carbon grid due to the difference in atomic electron density and have an increased chance of scattering. Therefore, by collecting the number of electrons, the electron sensor is able to identify the high-density area from the overall background. Particles with high density will appear darker in the TEM negative films, and in our case, silver nanoparticles are the darkest ones and at times having lighter areas representative of excess polymer that has not been removed thoroughly during the purification process, the images are below in Figure 13.

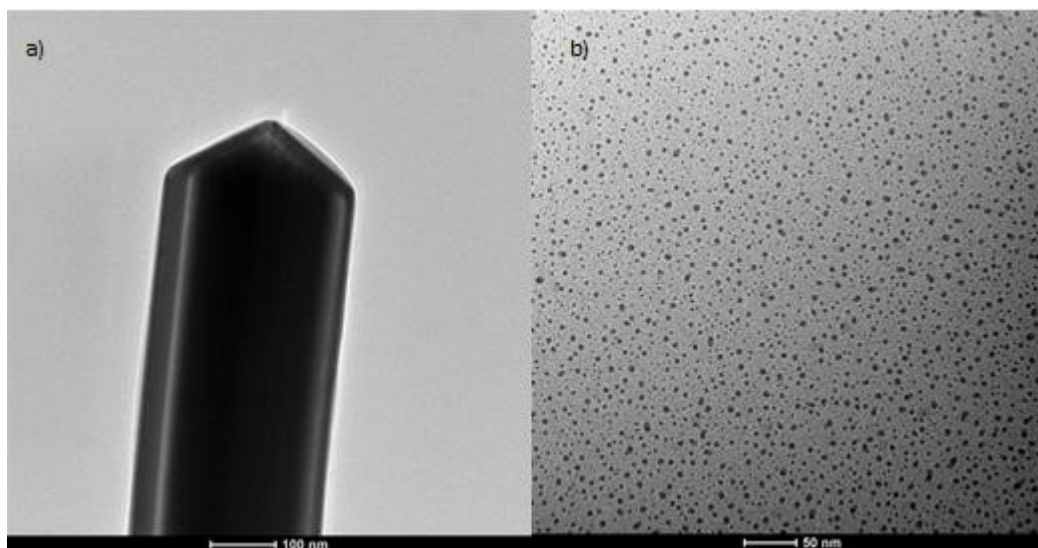


Figure 13 TEM images of a) Silver nanowire and b) Silver nano-spheres

In regard of the particle size distribution, most of the silver nanowires dimensions varied between few tenths of a nano-metre and a few hundred (50-150 nm) nano-meters in diameter and sometimes the length extended in the micrometric range (2-40 μm). The influence of particle size is considered as another issue in this research and will be discussed in detail later. The major objective here was to synthesize the nanoparticles and optimize the process ensuring it is

reproducible. The antimicrobial activity of Ag NPs is inversely dependent on their size [25]; this was the emphasis in the construction and assembly phase of the filter production.

Scanning Electron Microscopy (SEM)

Scanning Electron Microscopy (SEM) was the second technique used to obtain information about the particle size and morphology of the silver nanoparticles. The wires were dried in the oven at 90°C over night to be viewed by the environmental SEM. The Environmental SEM excels at High Resolution Imaging capable of resolution of 5 nm, excellent backscatter images. This SEM can image wet, dirty, oily or outgassing samples using the low vacuum or environmental mode. In this case a dry sample was used to observe the size and morphology of the silver nano-wires and produced the following image below (Figure 14).

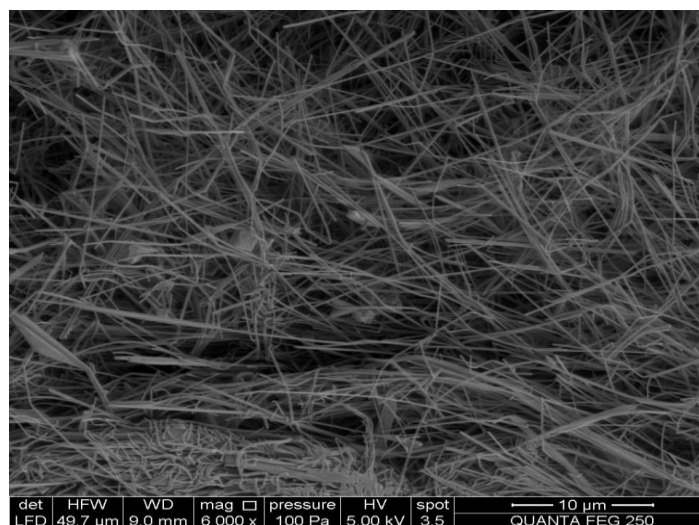


Figure 14 SEM image of silver nanowires

The SEM images acquired revealed that a sufficient amount of long wires with lengths in microns (2-40 μm) and diameters from a few tens to a few hundreds (50-150), as was the case with TEM previously. We were able to produce and replicate wires which were ready for use in the assembly of the metal-cellulose filter.

Dynamic Light Scattering (DLS)

From the colloidal dispersion of nanoparticles that were produced in order to attain their particle size distribution and zeta potential this characterization technique was employed. The technique

works on the basis of measuring the Brownian motion by collecting the scattered light from suspended particles to obtain diffusion rates to calculate their particle size. From Figure 15 below, it can be seen that the nanoparticles produced had a range of values with the majority being in the desired range of 1-10 nm which was the goal of our experiments. The DLS results showed that the hydrodynamic diameter of approximately 60% of the particles were between 0-25nm and had a mean diameter of 4.3 nm. Other graphs for other samples can be found in appendix B. A second method was also used to confirm the size of the nanoparticles produced, the size was determined statistically using National Instruments IMAQ vision builder software. From the TEM pictures obtained the size of the particles could be ascertained using IMAQ and was in accordance with the results from DLS (mean diameter, 4.3 nm). From these results the best samples, i.e. samples having nanoparticles 10 nm or less were used in the assembly of the filter membranes.

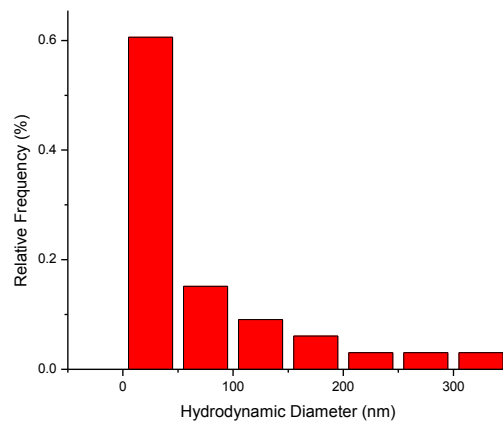


Figure 15 Particle size distribution obtained by DLS.

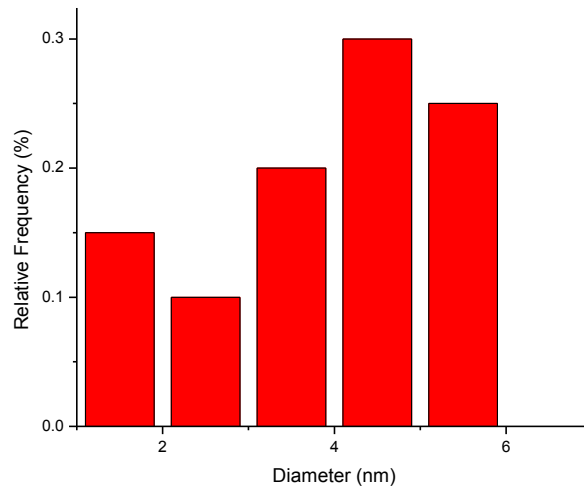


Figure 16 Particle size distribution obtained by IMAQ.

From DLS the distribution covers all the particles in the sample including the large agglomerates and hence why the diameters extend beyond 10 nm. The diameter given from DLS as well is the hydrodynamic diameter of the particle which is slightly larger than that of the actual particle because it includes the hydration sphere around the nanoparticles. The aggregations could have been caused Oswald ripening or during the preparation of the TEM holding grid. With IMAQ the first column from the DLS graph is broken down further and the results are shown in the Figures above. According to the TEM images below in Figure 17, there were a few large agglomerates however, a more uniform distribution was more dominant and corroborated with the results from IMAQ and DLS.

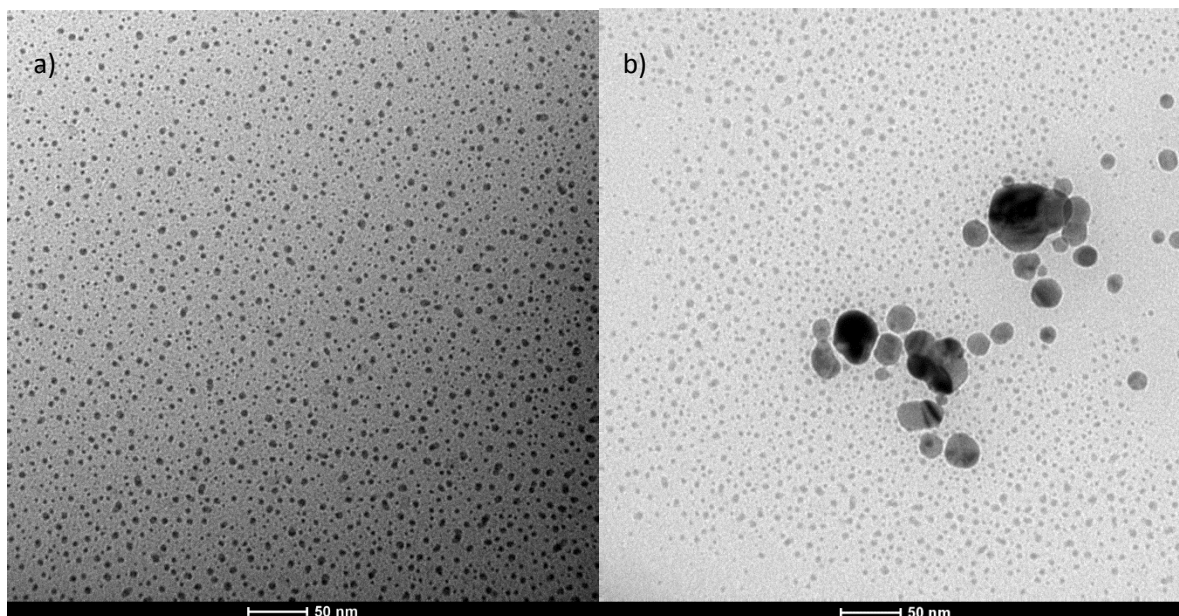


Figure 17 TEM images a) Particle size distribution b) Large agglomerates

4.2 Characterization of thiolated and amine-modified filters

Attenuated Total Reflection Fourier-transform Infrared spectroscopy (ATR FT-IR)

An Attenuated Total Reflection Fourier-transform infrared spectroscopy (ATR FT-IR) with a scan range from 4000 to 400 cm^{-1} was used to monitor the thiol and amine-modifications of the cellulose filters. These were the two functional groups selected to modify the surface of the cellulose fibres, a) Thiol and b) Amine groups.

As was mentioned previously the thiolated cellulose was prepared by first esterifying mercaptoacetic acid and then reacting it with the hydroxyl groups of the cellulose fibres. The thiol groups easily react with soft metal elements according to the Pearson's hard soft acid and base theory (HSAB) [154,155]. The theory defined a soft base as having a low electronegativity and large radii like those which can be found in compounds such as thiols, sulphides and phosphorous. These soft bases tend to have covalent bonds with soft acids, which are in turn described by the theory as having relatively high electronegativity and low charges (+1 or +2), and have a large radius as well like Au^+ , Ag^+ , Pd^{+2} , and Pt^{+2} [156].

Figure 18 shows the ATR FT-IR spectra of thiolated cellulose in comparison to un-thiolated cellulose. The ATR FT-IR spectrum of the thiol-modified spectrum is almost identical to that of the un-modified cellulose with the exception of a peak at approximately 1731 cm^{-1} . This peak is the carbonyl (C=O) peak corresponding to the ester formation between the acid and the hydroxyl groups of the cellulose as was stated previously. Similarly in amine-modified filters exhibited the similar characteristic peaks at $1630\text{-}1650\text{ cm}^{-1}$, denoting the esterification of the APTES or PEI with the hydroxyl groups and can be seen in Figures 19 and 20.

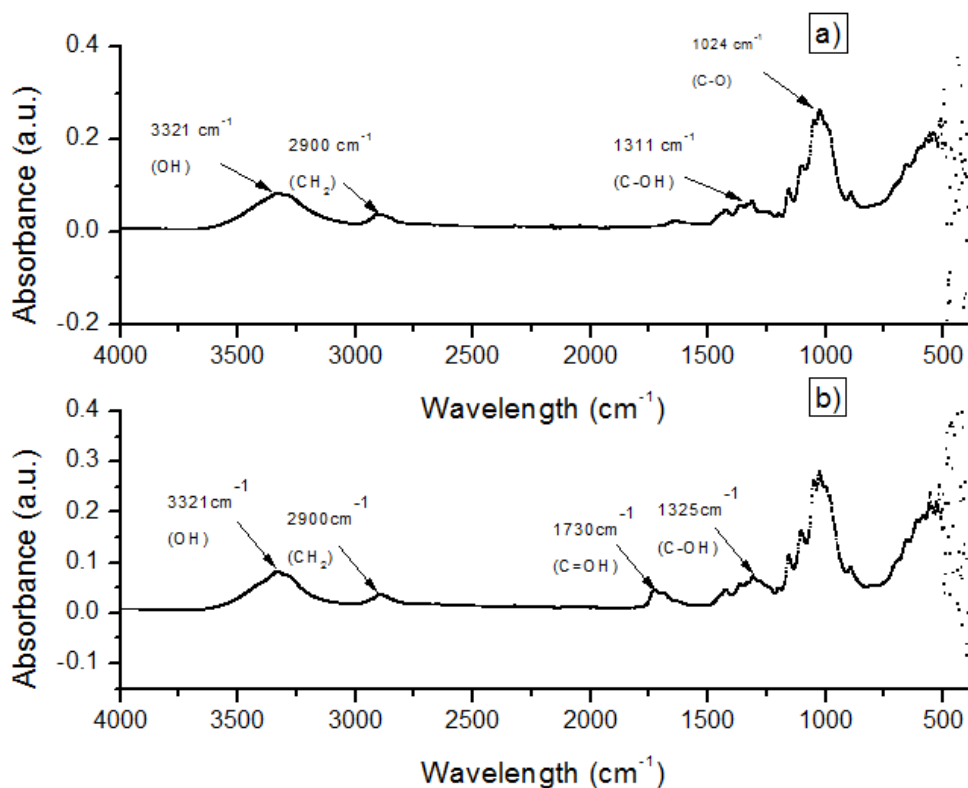


Figure 28 ATR FT-IR spectra of a) Unmodified cellulose fibres and b) Thiolated cellulose fibres using esterified mercaptoacetic acid.

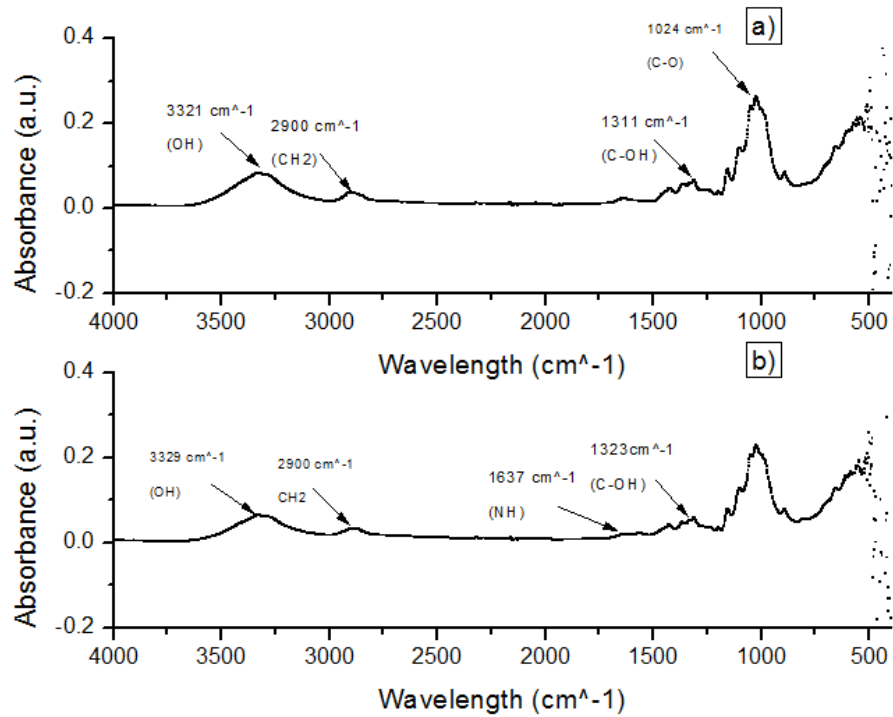


Figure 19 ATR FT-IR spectra of a) Unmodified cellulose fibres and b) Aminated cellulose fibres (using APTES)

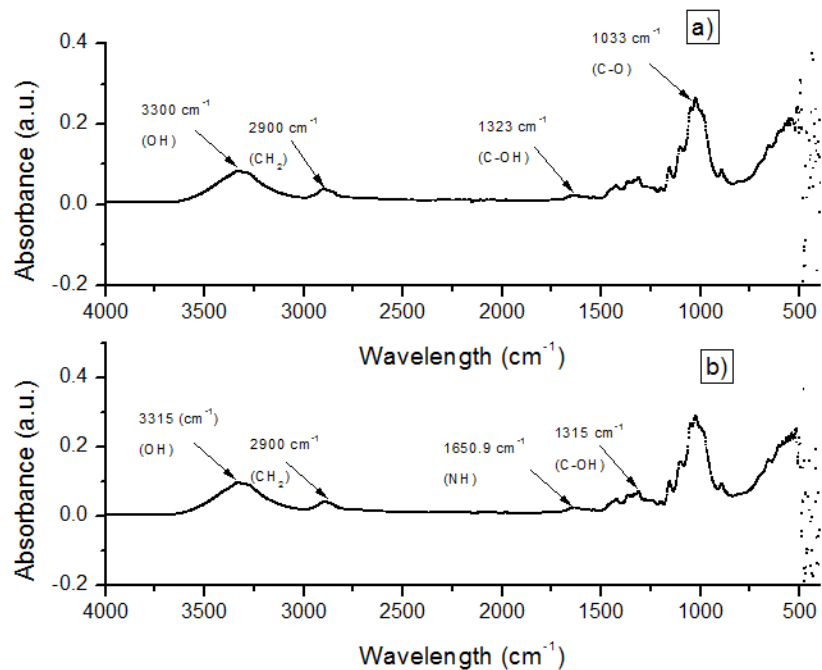


Figure 30 ATR FT-IR spectra of a) Unmodified cellulose fibres and b) Aminated cellulose fibres (using PEI)

The amination of the cellulose is recognized by the appearance of distinct peaks, one relative to the amine group corresponding to the NH anti-symmetric deformation located at approximately 1650.9 cm^{-1} PEI and 1632 cm^{-1} for APTES as compared to the thiol modified cellulose which had a distinct peak at 1730 cm^{-1} corresponding to the carbonyl group of the ester. All three modifications had the characteristic peaks of cellulose roughly between $1020\text{-}1030\text{ cm}^{-1}$ and depending on the functionalization had their specific peaks which were all in accordance with values found in literature [157].

XPS Analysis

The degree of thiolation was measured by determining the sulphur element content of the modified cellulose using XPS. The Table 5 below shows that approximately 2.11 wt. % was detected in the modified filters which indicated that a significant amount of hydroxyl groups per glucose unit in the cellulose fibre was successfully converted to thiol groups. For aminated paper it was approximately 5 wt. % of nitrogen was present as seen in Table 4.

Table 4 Amount of sulphur present in amine-modified cellulose filters

Aminated paper	Atomic %				N/C	Ag/C
	C 1s	O 1s	N 1s	Ag 3d		
Paper	62.89	26.25	10.86	-	0.17	-
Spheres	61.01	27.75	4.47	6.77	0.07	0.107
Wires	64.22	31.30	3.35	1.13	0.05	0.017
Wires and spheres	64.37	24.92	5.13	5.53	0.08	0.085
Wires then spheres	68.09	20.20	8.38	3.32	0.12	0.048

Table 5 Amount of sulphur present in thiol-modified cellulose filters.

Filter	Treat.	side	Atomic %				Ag/S	Ag/C
			C 1s	O 1s	S 2p	Ag 3d		
Blank 1			63.78	36.17	0.05	-		
Blank 2			63.67	36.27	0.06	-		
Spheres only	+S		61.68	37.22	1.50	-		
	+S+Ag	1	74.92	21.31	2.27	1.50	0.66	0.020
2		77.92	19.54	1.46	1.08	0.79	0.014	
Wires then spheres	+S		64.13	34.50	1.37	-	-	-
	+S+AgW	1	61.99	35.52	1.93	0.56	0.29	0.009
		2	62.79	35.19	1.73	0.29	0.16	0.004
	+S+AgW+SAg	1	71.22	19.97	4.28	4.53	1.05	0.063
		2	62.19	34.61	2.07	1.12	0.54	0.018
	+S+Ag	1	70.23	24.76	3.13	1.88	0.60	0.026
2		71.64	25.15	2.11	1.09	0.51	0.015	
Wires only	+S		64.83	33.90	1.27	-	-	
	+S+Ag	1	64.71	31.46	2.65	1.17	0.44	0.018
2		66.69	31.14	1.78	0.39	0.22	0.006	

Not only the total amount of silver present is important to obtain high antimicrobial efficiency but also the oxidation state of that silver is important together with the contact between bacteria and the Ag^+ -releasing material. From this perspective different addition mechanisms for the silver nanoparticles were examined as seen in the Tables above. The information attained from the different mechanisms was used to determine the order of addition of the nanoparticles. The Ag-cellulose filters were then assembled by first adding wires followed by the addition of the spheres following the procedure from chapter 3.

4.3 Characterization of the metal cellulose filters

4.3.1 Material Characterization

XPS Analysis

The bonding property between the silver nanoparticles and the modified cellulose filter was then characterized by XPS analysis. From the data in Table 6 below it can be seen that the Ag $3d_{5/2}$ binding energy of the Ag-cellulose positively shifted relative to the Ag NP and is shown in Figure 21.

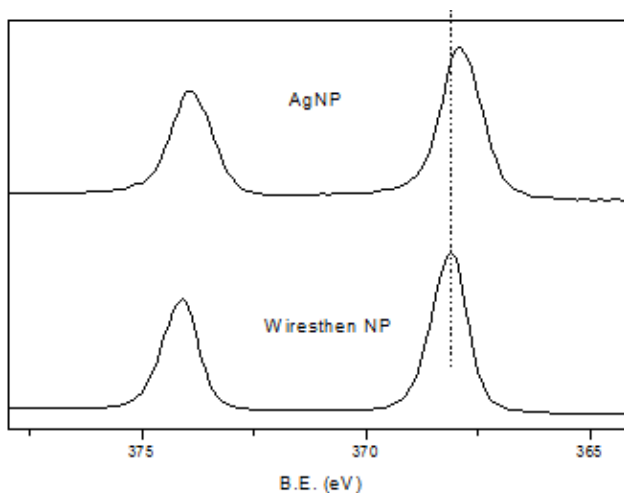


Figure 21 Graph showing the positive shift in binding energy of the thiol modified cellulose relative to the Ag NPs.

Ag 3d peak at higher BE values is attributed to the more oxidized surface Ag atoms bonding the thiol molecule through a S-bridge (Ag-S-R) [158]. It is known that a formation of metal sulphur covalent bond decreases the electron density of the metal, resulting in a shift of the binding

energy of the 3d orbital in metal and is shown in Table 6 [159]. Thus this shift observed in the silver in the metal-cellulose filters can be believed to be attributed to the decrease in the electron density of the nanoparticles by the covalent assembly of the Ag NPs and the thiol groups of the modified cellulose. Most transition metals cause a shift in the 3d orbital binding energy toward a higher energy by binding electron negative groups [156]. Thus these results confirmed that the Ag NPs were covalently immobilized to the cellulose filter by the metal-sulphur covalent bond.

Table 6 Assignment of Binding Energies of Main XPS Regions for thiol-modified Ag-cellulose assembly.

Filter	Treat.	side	B.E (eV)	
			5/2	3/2
Spheres only	+S+Ag	1	368.2	374.2
		2	368.1	374.1
Wires then spheres	+S+AgW	1	368.3	374.3
		2	368.3	374.3
	+S+AgW+SAg	1	368.4	374.1
		2	368.2	374.2
Wires and spheres	+S+Ag	1	368.4	374.4
		2	368.2	374.2
Wires only	+S+Ag	1	368.3	374.3
		2	368.3	374.2
AgNP			367.8	373.8

There was a similar positive shift in the binding energy of the amine-modified cellulose filters as well and is shown in the Table 7 and Figure 22 and 23.

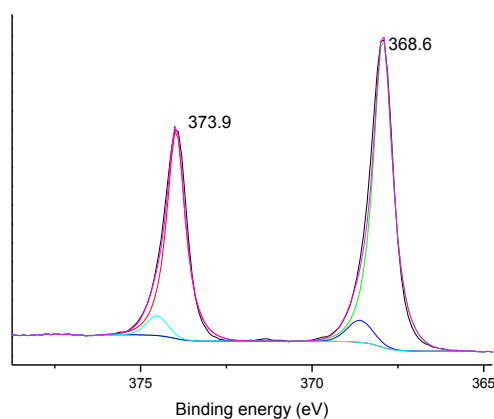


Figure 22 Graph showing positive shift in the binding energy in amine modified cellulose filters.

XPS also showed that the cellulose may act as a reducing agent through its hydroxyl groups. Due to fact that polyols act as reducing agents for silver. However, the reducing power is low and has been reported to be effective only at a high temperature [160,161]. The use of amino groups to modify cellulose surfaces also has the ability to immobilize Ag NPs. This is a good reason to use amine groups as our back-up for the modification of the cellulose fibres in the production of our water filters. Both sulphur and nitrogen when coupled with silver forms strong covalent bonds which are essential in the design and fabrication of these filters to avoid any accidental leaching of silver.

Table 7 a) Assignment of Binding Energies of Main XPS Regions for amine-modified Ag-cellulose assembly.

Aminated paper	B.E (eV)			
	5/2		3/2	
	Ag ⁰	Ag ⁺	Ag ⁰	Ag ⁺
Spheres	367.9	368.6	373.9	374.6
	91%	9%		
Wires	367.8	368.5	373.9	374.2
	81%	19%		
Wires and spheres	367.9	368.6	373.9	374.5
	92%	8%		
Wires then spheres	367.8	368.4	373.8	-
	90%	10%		
AgNP	367.8	-	373.8	-

Table 7 b) Showing Binding energies of nitrogen and amine groups present on modified cellulose fibres

	B.E (eV)*	
	-NH ₂	N ⁺
Aminated paper	399.3	400.8
	70%	30%
Aminated paper Spheres	399.6	401.2
	72%	28%
Aminated paper Wires	399.7	401.5
	72%	28%
Aminated paper Wires and spheres	399.8	401.3
	78%	22%
Aminated paper Wires then spheres	399.6	401.1
	80%	20%

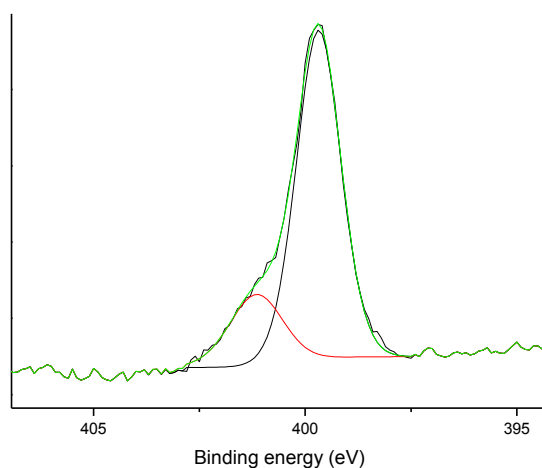


Figure 23 Shift in binding energies of amine groups and nitrogen on amine modified filters.

The silver ions present and shown in Table 7 a) are those interacting with the amine group [162]. Also by XPS it is demonstrated that more silver remains in its oxidation state when using thiol as linker that when we use amino groups.

SEM Analysis

The assembly of the filters were done by immersing the modified filters into dispersions of nanoparticles (first in wires and then in a dispersion of spheres). After the immersion process was completed and the filter rinsed and dried and later analysed. The filters experience a change in colour from white to a greyish colour when wires were added and then to a brownish colour when spherical nanoparticles were added. For each functionalization there were different hues of brown however, when wires were added it was more or less the same shade of grey. These results were greatly influenced by the plasmon resonance absorption of the immobilized Ag NPs on the cellulose fibres and can be seen in Figure 24.



Figure 24 The photo images of a) APTES b) PEI and c) Thiol -modified cellulose filter after the attachment of Ag NPs.

Once the assembly was completed the morphology of the surface and cross-section of the samples were analysed using SEM and produced the following images. From the SEM images obtained in Figure 25 for the un-modified cellulose it was clear that the modification did not destroy the integrity of the fibres and had no effect on the pore size for the Ag-cellulose. The wetting of the membrane may also have played a role in their efficiency this was demonstrated by using rhodamine (see appendix B for images) to observe the wettability of the membranes with each type of functionality. This experiment showed that the PEI-modified filters were most like the blank or un-modified filters in terms of wetting followed by the thiol-modified filter. APTES modified filters however, appeared to be slightly hydrophobic but after some time the liquid penetrated through the filter by capillary action. It is not clear why the interaction of the rhodamine differs drastically between the two amine modified cellulose filters. On the contrary

to make the thiol and APTES-modified filters more hydrophilic they simply had to be rinsed once or twice more after being functionalized. The speed of penetration was also evaluated under non-steady or quasi steady state at atmospheric pressure and again the thiol filters proved to be the fastest at allowing 50 mL of water to permeate in under 1minute. This time was at times faster than the un-modified filter and hence SEM analysis was carried out to ensure that the integrity had not been compromised (pin holes or defects , see appendix B). The SEM Analysis revealed that the integrity had not been tarnished. From Figure 26 the filters showed the attachment of nano-wires on the top forming a secondary mesh and spherical nanoparticles dispersed throughout the depth of the fibres of the filters which was the functionality we wanted to achieve.

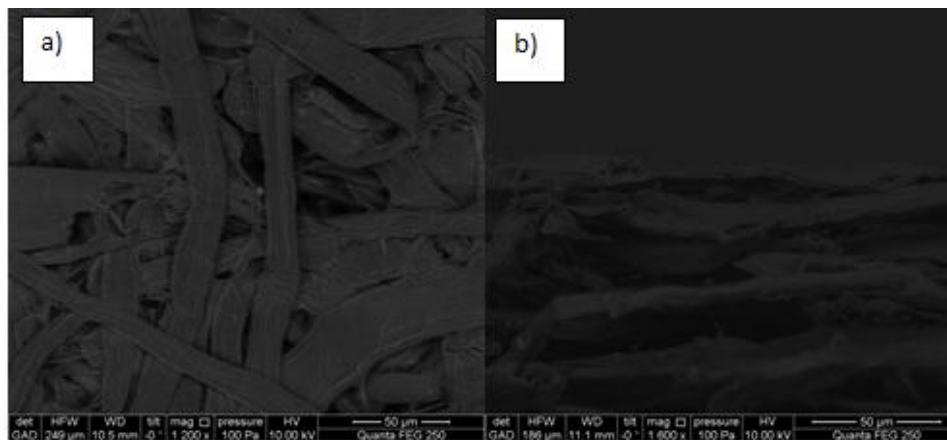


Figure 25 SEM images of un-modified cellulose filters a) Top view b) cross section.

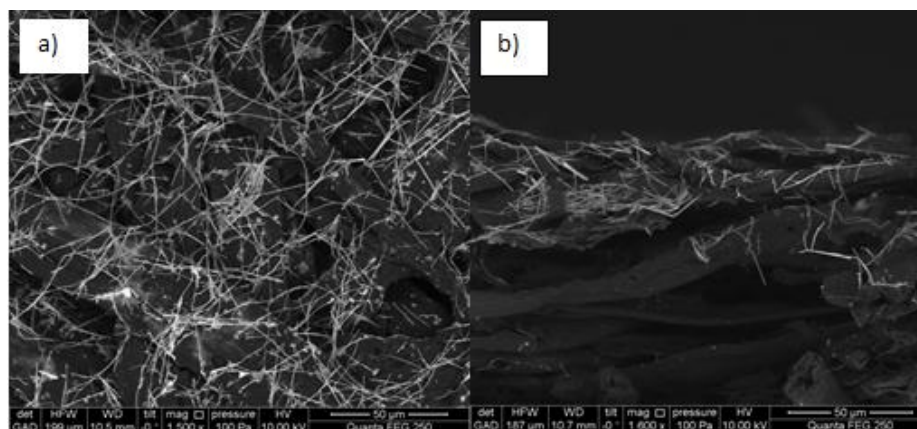


Figure 26 SEM images of thiol -modified Ag-cellulose filters with Ag NPs a) Top view b) cross section.

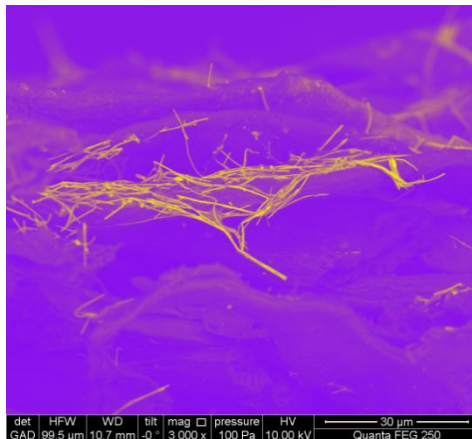


Figure 26 b) SEM Image of cross sectional view of thiol-modified Ag-cellulose.

HR(S)-TEM

HR(S)-TEM of the surface of the Ag-cellulose filters showed that the wires were position on the top of the filters whilst the spherical nanoparticles were dispersed throughout the filter. The filters samples for HR(S)-TEM was prepared by cutting three thin layers in order to investigate the positioning of both types of nanoparticles. Figure 27 depicts a schematic representation of how the layers were cut for analysis.

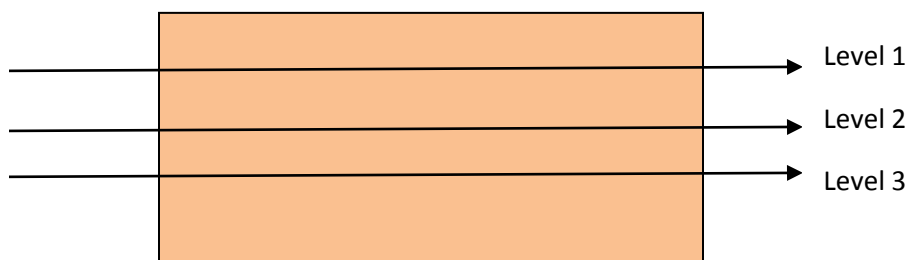


Figure 27 Schematic representation of cutting during sample preparation for HR(S)-TEM.

From the analysis of the different layers, wires were only found in level one whilst spherical particles were successfully positioned all throughout the filter deep within the interior of the cellulose fibres and not just at the surface as they were present in all levels analysed. The nanoparticles were positioned both at the interior and exterior of the cellulose fibres with the larger particles or agglomerates positioned at exterior. Thus providing evidence that the nanoparticles were immobilized by the covalent bonding between the thiol of the modified cellulose and the silver nanoparticles. Based on the images in Figure 28 HR(S)-TEM provided a better contrast between the silver nanoparticles (white dots) and the paper or epoxy resin (dark areas). Though it was possible to use HR-TEM to get images with a better resolution,

the paper was unstable and proved challenging to focus and was also at times easily burnt the images acquired but, revealed the expected results.

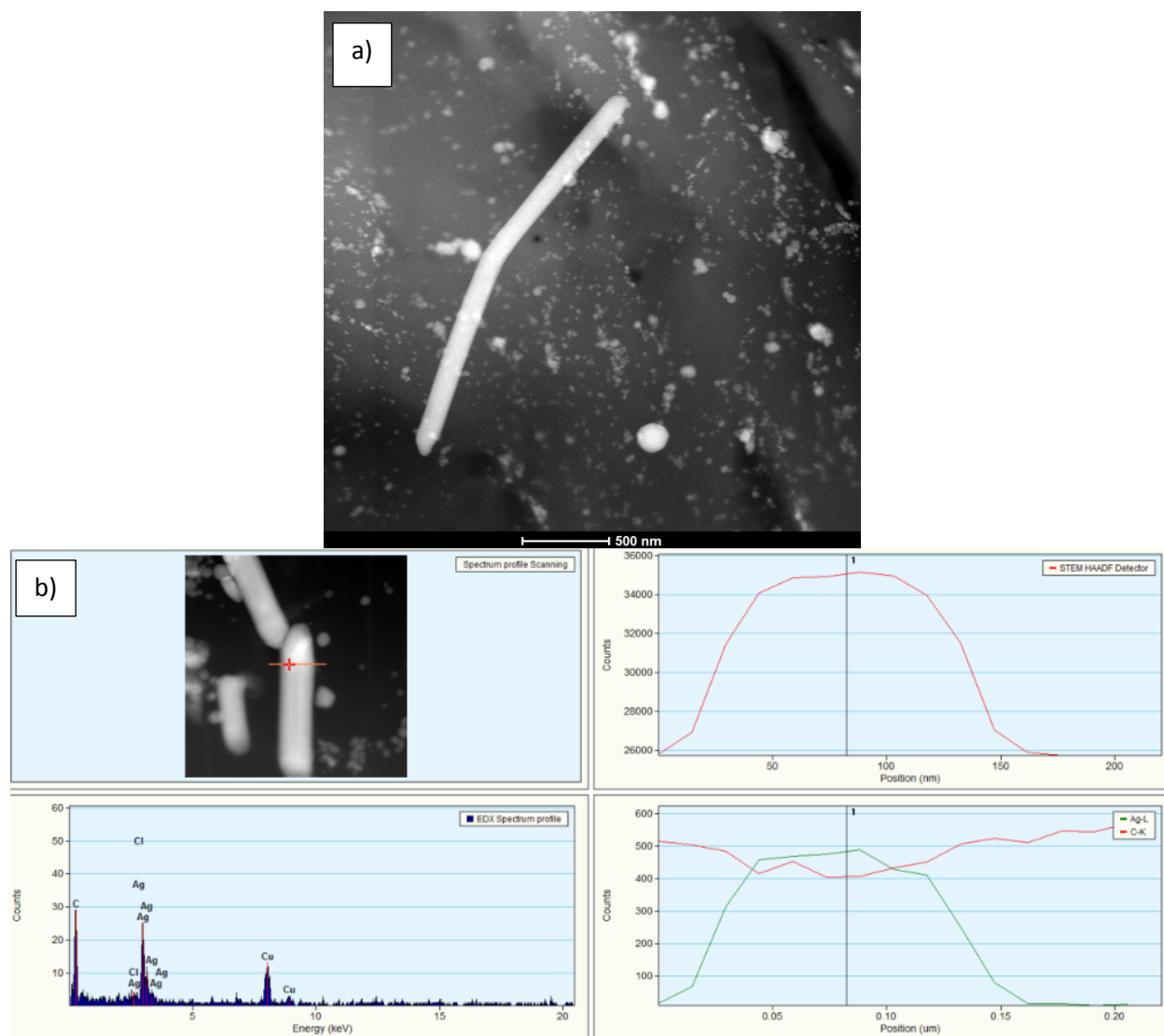


Figure 4 a) HR(S)-TEM image of thiol-modified paper with silver nanoparticles (Level 1) and b) EDX spectra.

EDX Analysis

In order to confirm that particles imaged in SEM and HR(S)-TEM were composed of silver the energy dispersive spectra was acquired. From the images ascertained by HR(S)-TEM and SEM which disclosed the morphology of the surface of the Ag-cellulose filters, it clearly showed that spherical and rod like (wire) particles were attached to the surface of the modified cellulose fibres. Due to time constrains only the thiolated fibres were imaged by HR(S)-TEM and EDX was performed on these samples. The results

confirmed that the particles were indeed silver based on the peaks from the Ag-cellulose filters and can be seen in the Figure 29 below. The other elements that were present in the EDX analysis like sulphur was from the thiol-modification or like chlorine which was from the epoxy, whilst carbon and oxygen came from the cellulose paper and the large contribution of copper was distinctive of the copper grip on which the same was placed for analysis.

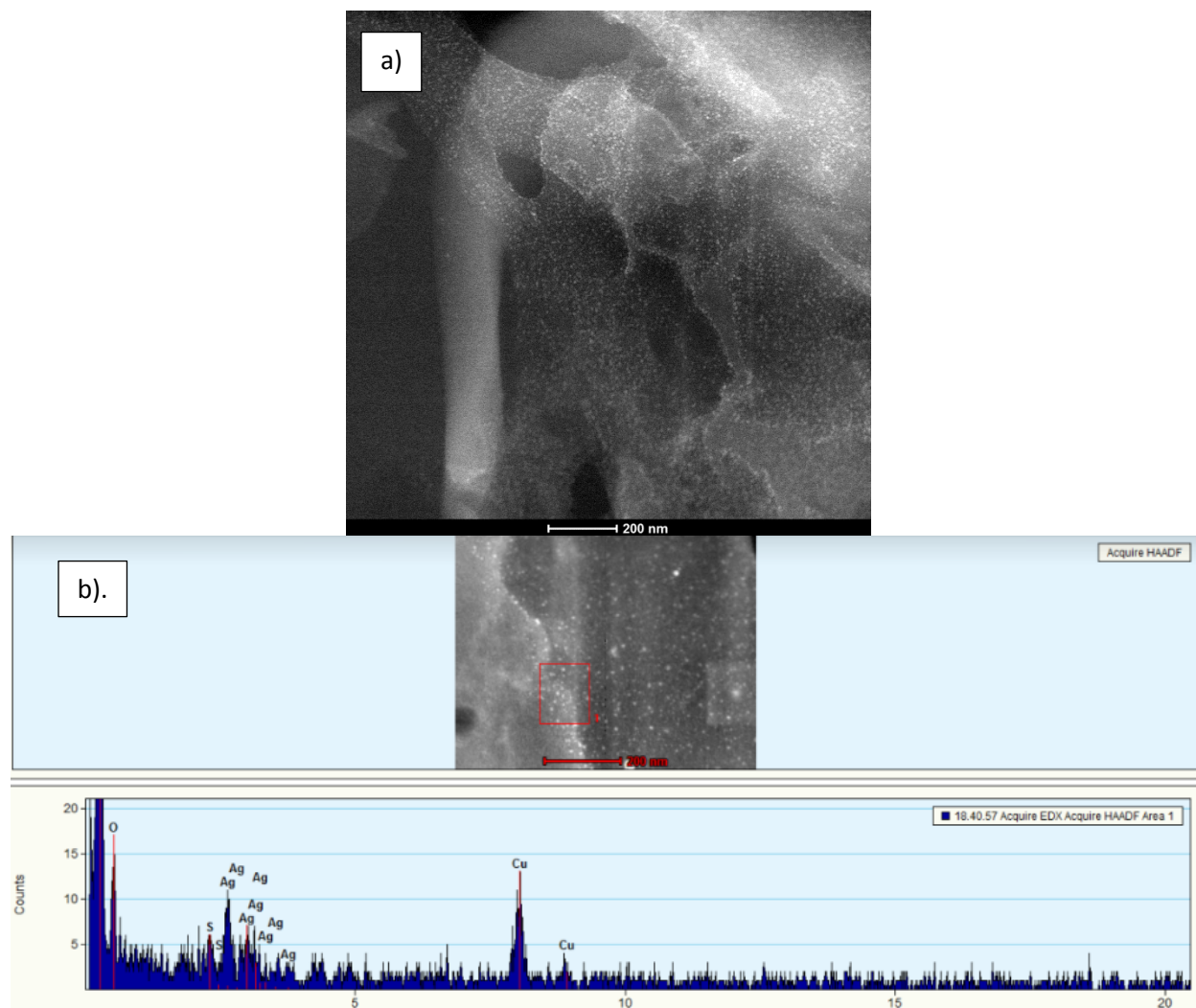


Figure 29 a) HR(S)-TEM image of thiol modified paper with silver nanoparticles b)EDX spectra of Ag-cellulose.

4.3.2 Release Testing

The binding durability between the Ag NPs and the cellulose fibres were also investigated by means of a release test. For comparison the release test was also conducted on filters with nanoparticles that were not covalently attached as controls. These filters were assembled by

using the in situ synthesis method described in chapter 3. The loading amounts were to be determined by ICP-AES however, this task was not completed and will be considered as future work as there were time limitations. Ultraviolet-visible spectrum was used to track the silver that was being released from the filters after washing in different pH environments and using ultrasonic bath for 20 minutes (increments of 5 minutes/cycle). Sonication was used in order to break the intermolecular interactions in the filters. It has numerous effects both chemically and physically as it uses sound energy to agitate particles inside the filter samples, cavitation effects as well as hot spots presence are indicative of the high energy applied when using sonication. The filters are exposed to high levels of stress whilst in the sonicator and hence the results gave evidence of the durability of the filters. From the release test the most durable filter was that of the thiol functionalized filters and hence the results are shown below in Figure 30, other results can be found in appendix B.

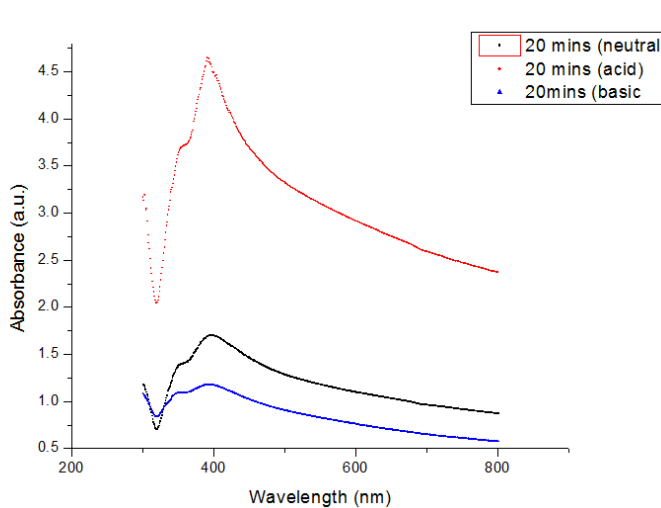


Figure 30 a) UV-vis graphs of release test performed on filters with non-covalent bonding at different pH.

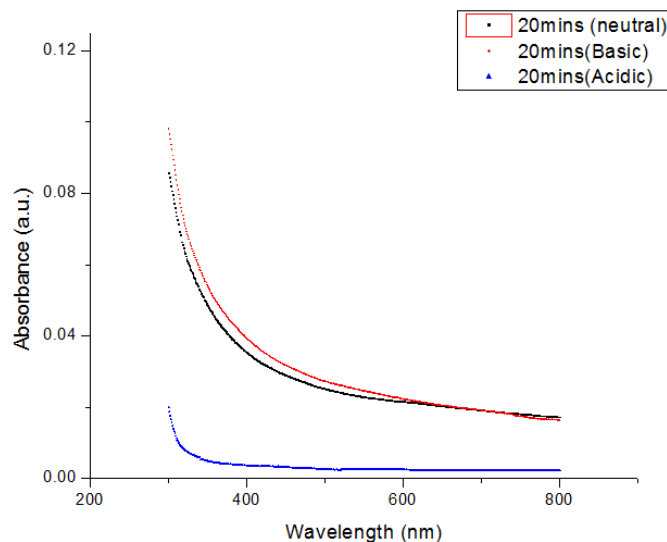


Figure 30 b) UV-vis graphs of release test performed on thiol-modified filters at different pH.

The results demonstrated that the durability of the Ag-cellulose with the covalent linkage was much higher than that with none covalent links which can also be seen in the pictures of the filters after washing below (Figure 31), it is clear that the nanoparticles are still attached as the filters still exhibit the brownish colour they acquired from the nanoparticles.

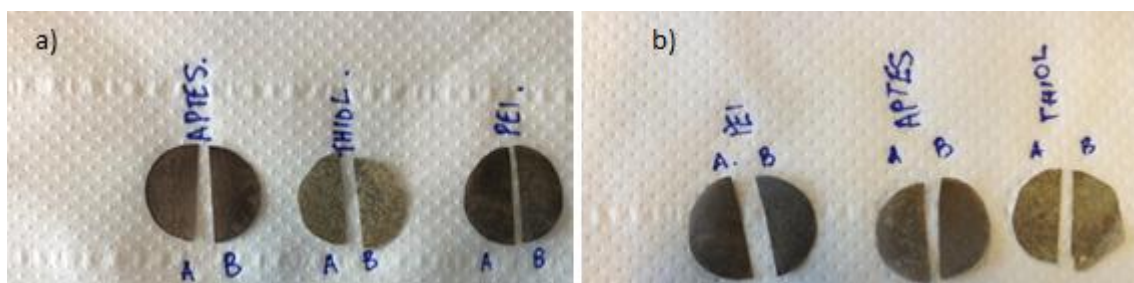


Figure 31 Pictures of filters with different functionalities a) Before release testing and b) After release Testing.

Under different pH conditions the breakaway of the Ag from the cellulose in the filters with covalent linkage was greater and indicated that the sulphur-silver, S-Ag and the nitrogen- silver N-Ag are maintained during various pH washing conditions. The different functionalities showed different behaviours in the different environments. PEI was the least durable of the 3 as under acidic conditions there was leaching of silver as the Plasmon resonance peaks were distinctive of silver at approximately 400nm and extremely low absorbance (maximum abs. 0.032). Under basic conditions the PEI filters had little or no leaching that could have been detected by the UV-

vis. With the APTES filters there was slight detection of silver nanoparticles in acid conditions and no noticeable detection when exposed to basic washing conditions (see Appendix B). The thiol functionalized filters proved to be the most durable of the filters as there was no significant detectable leaching of silver in either environments and it was also analysed under neutral conditions and the results remained the same. If the loading is sufficient and exhibit this type of binding durability, these filters could lead to a sustainable and technically efficient production of Ag-cellulose filter and could make an attractive method of sterilizing water for various uses in a host of conditions and for a wide range of users. The main result from this test is that this “smart-paper filter” is eco and human-friendly robust nano-hybrid.

4.4 Bacterial Testing

Bactericidal tests were conducted as described in previous section. For each set of tests, bacterial medium growth test and bacterial viability test, at least three parallel tests were conducted to obtain reliable results. Bacterial growth test will be done to analyse turbidity of the liquid solutions containing bacteria and bacterial viability test were conducted using standard agar plate tests by counting colonies.

Samples containing dispersions of silver nanoparticles as well as immobilized nanoparticles on cellulose filters possessed strong influence to bacterial viability and duplication ability on *E. coli*. The different functional groups although having the ability to inactivate bacteria to some extent, like in the case of PEI which has been reported to inactivate *E. coli* up to 16% [163], had no significant impact on the overall biocidal activity of the filters. Therefore we can conclude that the bacterial effects are as a result of the Ag NPs and or wires only.

4.4.1 Bacterial Growth

For the medium growth test, the number of bacteria was to be determined by recording the bacterial optical density. The measurements of the optical density of the bacterial cultures in liquid nutrient medium, with the measuring wavelength set at 600 nm, is a measurement used by microbiologists to determine the number of bacterial cells present in a liquid culture. Growth of bacteria could always be considered as four distinct phases, namely, lag phase, exponential phase, stationary phase, and death phase. However, the lag phase, stationary phase, and death phase were to some extent related to many environmental conditions, such as temperature,

nutrient concentration etc. Therefore, we wanted to examine the exponential phase as the phase of interest in this project as it provides most the information concerning the bacteria themselves. However, we were not able to conduct this test instead we tracked the turbidity over time. This gave us a general idea as to whether or not the silver nanoparticles have any significant effect on bacterial cells. From these results over a testing period of 6 hours (30 minute intervals) the turbidity decreased with time. Using different concentrations of silver also showed that with increased concentration the turbidity decreased. If incubation continues after the population reaches stationary phase, a death phase follows, in which the viable cell population declines. However, this decline cannot be observed by turbidimetric measurements. And hence bacterial viability tests were used to support these findings. In the hopes of proving our hypothesis, that the bacteria were killed or their growth was inhibited by the silver nanoparticles.

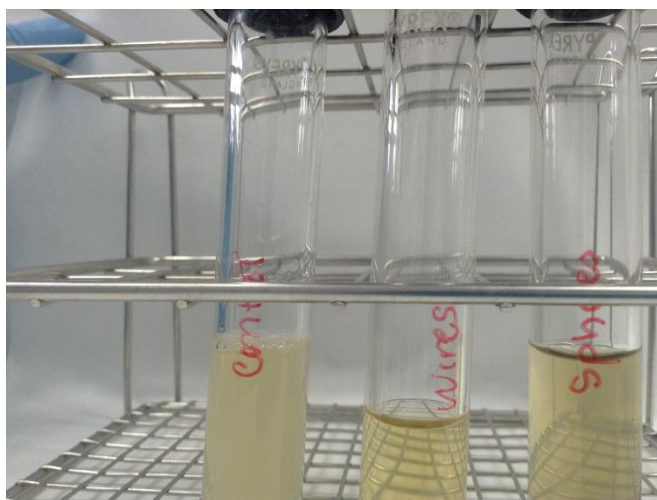


Figure 32 Picture of bacteria in liquid solution (PBS) showing the decrease in turbidity with the addition of silver nanoparticles.

4.4.2 Bacterial Viability Tests

Based on the data obtained from the bacterial growth tests, we were able to safely assume that the bacterial cell number dropped tremendously; although we were not certain if they had indeed died. Therefore, we were now interested in finding out whether the bacterial cells were really being killed by silver nanoparticles, or just their duplication ability had been limited. This required evidence from the bacterial viability after the treatment of silver nanoparticles and later filters loaded with silver nanoparticles in a covalent attachment. Two techniques were used to determine bacterial viability:

1. After several hours' (18-24h) of treatment with the Ag NPs only and filters loaded with Ag NPs, agar plate tests (Method 1: Bacteria in a liquid medium of PBS was put in contact with filters without passing the liquid through).

- 1.2 Immediate treatment by passing bacteria through the filters (multiple times) and immediately putting them to agar plates (Method 2: Bacteria in a liquid medium of PBS were passed through the filters).

For the *E. coli* bacteria, the medium growth tests were conducted before the bacterial viability test, so we made the assumption that a silver concentration of 4 mg/mL for both wires and spheres was high enough in killing most of the bacterial cells based on previous results. Therefore, we focused our attention on silver concentrations of 4 mg/mL for nanoparticles only viability tests. And hence filters were assembled using these concentrations of the nanoparticles as well. After 18-24 hours' inoculation with silver nanoparticles and filters 37 °C, 25 µL silver-containing bacterial suspensions were transferred to the agar plates using a micropipette after agitation. And for the filters they were first put an ultrasonic bath for 30 followed by which the same method was applied and 3, 25 µL drops of the suspension were placed on the agar plates. All of the agar plates were then stored in an oven (37 °C) overnight to allow the formation of bacterial colonies. The numbers of colonies were counted manually.

Method 1: Silver nanoparticles

The effect of the nanoparticles were then evaluated over 24 hours and there was no colony formed on the agar after; however, a very small number of colonies were found in other samples with the same bacterial and silver nanoparticle concentration which is not significant. Duplicates were used to verify the data. It should be clear that almost all the bacterial cells were killed under the influence of this concentration of the silver nanoparticles. Therefore it fair to conclude that only a small proportion of *E. coli* remained alive after counting the as-formed bacterial colonies.

Filters of different functionalities loaded with silver nanoparticles.

After 24 hours PEI and APTES functionalized filters exhibited 2 log reductions (99%) whilst filters functionalized with thiol groups showed a significant bacteriostatic reduction of 3 logs (99.9%). Duplicates were also used to verify the data presented in Table 8 and Figure 33. These results revealed that silver-cellulose filters had an excellent antimicrobial property. Coupled with

the strong binding durability which was revealed during the mechanical testing thus gives credibility to the fact that the nanoparticles are strongly immobilized due to the covalent bonds and we were able impart the antimicrobial activity of the NPs from these tests.

Table 8 Colony Forming Units per mL formed on agar plates for filters with different functionalities (over-night).

Filter	<i>E. Coli</i> CFU/mL
\bar{x} control	$6.4 * 10^8$
\bar{x} PEI	$10 * 10^6$
\bar{x} APTES	$1 * 10^6$
\bar{x} THIOL	$27.2 * 10^4$

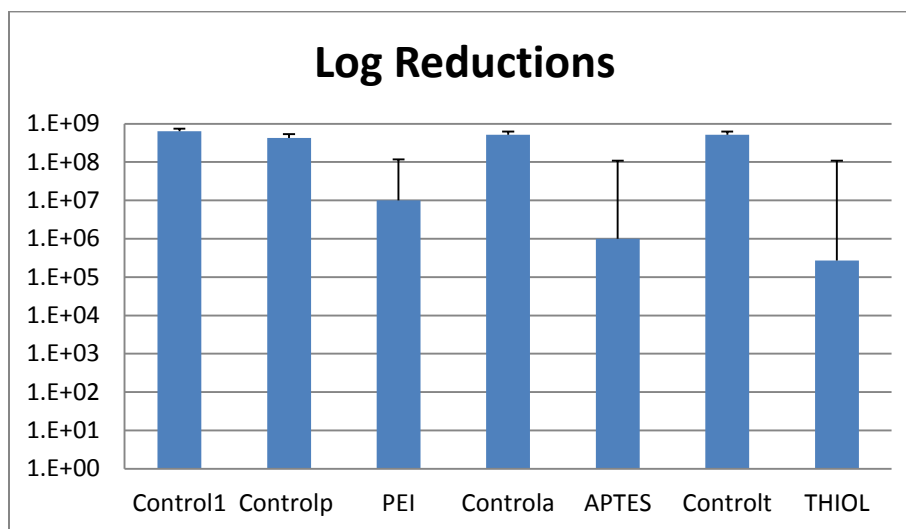


Figure 33 Corresponding graph of log reductions/antimicrobial activity, from Table 8.

Method 2: Immediate testing of filters of different functionalities

The main objective of this project was to produce filters for high speed sterilization. Thus time is of the essence in the hope of delivering clean water immediately and hence this parameter (time) needed to be evaluated in conjunction with the antimicrobial activity of the filters. From the previous results in Method 1 it was obvious that the filters possessed high antimicrobial power. Now it was time to evaluate the speed at which the antimicrobial activity could be disseminated. Bacteria in a liquid media were passed through the filters using a gravity fed device (can be seen in a picture in appendix C) after multiple passes (10, 20, 30 and 50) the resulting solutions were diluted and 25 μ L drops were again place on the agar plates, stored in an oven (37 $^{\circ}$ C) overnight

to allow the formation of bacterial colonies and the colonies counted. The best results were after 50 passes and again the thiol modified filters were the most effective as demonstrated in the Figure and Table below.

Table 9 Colony Forming Units per mL formed on agar plates for filters with different functionalities (immediately (after several passes)).

Filter	<i>E. coli</i> CFU/mL
\bar{x} control	1.96E+08
\bar{x} PEI	4.60E+06
\bar{x} APTES	4.40E+06
\bar{x} THIOL	2.40E+06

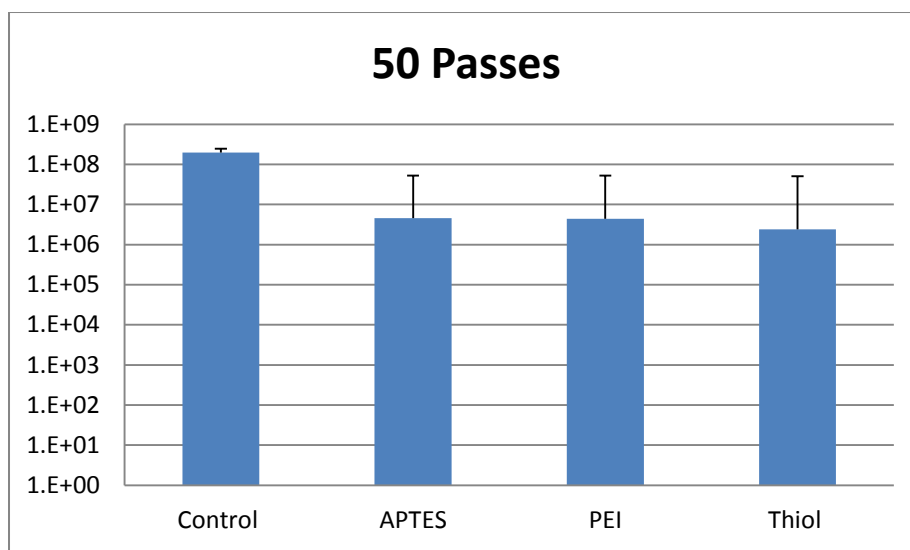


Figure 34 Corresponding graph of log reductions/antimicrobial activity, from Table 9.

There was a slight decrease in the log reduction; however it was still significant enough to demonstrate the efficiency of the filter in a short space of time thus validating the description high-speed sterilization. There was a 2 log reduction and this is equivalent to 99% reduction. The filters are approximately 200 μm thick and hence an attempt was made to determine the number of passed through the filter that yielded significant biocidal effects on the *E. coli* bacteria. After passing the liquid medium (PBS) containing bacteria through the filters 10, 20, 30 and 50 times and then putting the resulting residual liquid to agar plates and inoculating it for 24 hours, the colonies formed were counted and the results demonstrated that after 30 passes there was a 90% reduction and with 50 passes a 99% reduction. Thus leading to the conclusion that

after 50 passes over a 7-10 minute time span the filters (with all three functionalities) were effective and efficient, with the thiol-modified filter being the most effective.

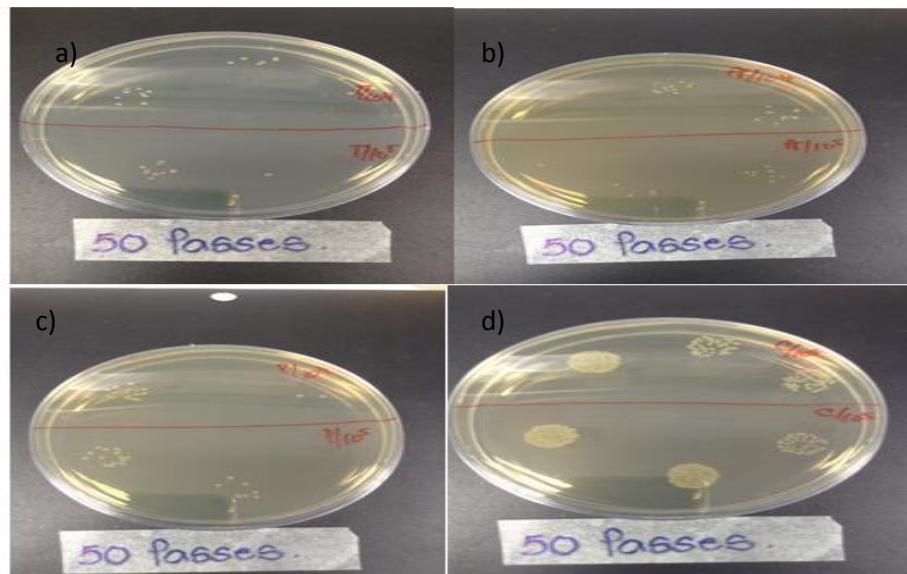


Figure 35 Agar plate images of different concentrations (10^4 and 10^5) of *E. coli* after being passed through the filters 50 times
a) Thiol Filter b) APTES Filter c) PEI filter and d) Control.

The thiol-modified filter was then analysed by SEM after 50 passes of PBS containing *E. coli*, the results demonstrated that there is flow of bacteria through the filter as there are bacteria on either side of the filter as shown in Figure 36. The bacteria were generally located in regions where there were little or no silver nanoparticles and or wires. However, the major objective was achieved to have the bacteria inactivated as they passed through the filter which reduces fouling whilst still being highly effective against bacterial activity.

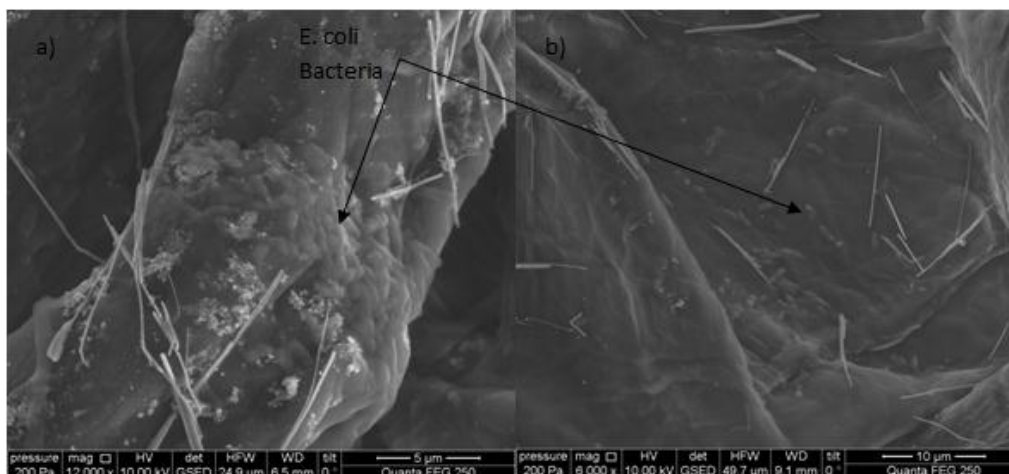


Figure 36 SEM images of bacterial cells on thiol-modified filters after 50 passes of PBS containing *E. coli* on a) top surface and b) reverse surface (underneath).

CHAPTER 5

GENERAL DISCUSSION AND FUTURE DIRECTION

5.1 Antimicrobial effects of Ag-cellulose filters.

We were able to develop robust filters based on covalent bonds between silver and cellulose substrates. The cellulose substrates had different functionalities from amine or thiol-modifications which were the key issue in their efficiency. From the ATR-FTIR and element analysis results we were able to confirm that the hydroxyl groups on the commercial cellulose filters used in the assembly were successfully modified by the different functional groups. SEM and HR(S)-TEM undoubtedly showed that the nanoparticles had been immobilized on the modified cellulose and XPS revealed that the immobilization was indeed attributed to the bonds between the silver and the groups. The release testing conducted on the filters also showed that covalent bonds in the Ag-cellulose filters were highly efficient and durable when compared to filters with non-covalent bonding and in different pH. More analysis is needed to quantify the amount of silver and we hope to have ICP-AES measurements in the future. The potential accidental release from the filters was only evaluated by tracking UV-vis was done to see whether or not silver was released and could be observed by its plasmon resonance after strong sonication performed on the Ag-cellulose filters. From the durability test the thiol functionalized filters were the most durable as they showed minimal leaching of silver when compared with APTES which was ranked second and followed by PEI in acidic, basic and neutral conditions. The initial loading of silver also needs to be quantified via ICP-AES, this is of great importance and is one of the primary objectives in the future work of this project. The ultimate goal of the filters was to be effective in inactivating bacteria namely those found in contaminated water like *E. coli*. The Ag-cellulose filters showed strong antimicrobial activity against *E. coli* with concentration 1×10^5 cells/mL achieved inactivation rates in excess of 99.9% reduction in bacterial viability. The functionality to the membrane surface by thiol and amine provided the covalent attachment which from a technical point of view lead to a very robust filter which makes them quite attractive for the environment as well as render them not only eco but also human friendly. They also possess a wide range of application ranging from point of use filters for sterilization of water after natural disaster, or for soldiers in remote locations without access

to clean water as well as biomedical technologies due to their excellent antimicrobial activity and the well demonstrated low toxicity to humans [3] which is enhanced by their durability. The filters also based on their design could also be of use industrially for pre-treatment as they do not foul very easily as is it is shown in the SEM image in chapter 4. However, future work is needed in order to provide some extra safety and precautionary measure for silver and bacterial sequestering and also to evaluate the life span of the filters in order evaluate how much contaminated water they can process before having to be replaced. This safety feature should ideally be nontoxic and eco-friendly. There should be a protection which mimics nature (e.g. clay with thiol groups) and will produce an insoluble salt should any accidental leaching occur to ensure that the filter remains eco-friendly.

The silver nanoparticles that were used in the assembly had different contents of silver obtained from ICP-OES; the spheres had 0.03 % whilst the wires had 5.22% (see Appendix B for nanoparticle parameters). At first glance it may appear that the wires are more biocidal but after normalization with the silver content it was shown that for the same concentration of wires and spheres there was a greater log reduction when using spheres and hence it demonstrated that the spheres were more toxic. Nanoparticle size appears to be the primary or dominant determinant of the nanoparticle's toxicity, with smaller particles such as the sphere with were on average 4.3 nm, they exhibit greater antimicrobial activity in comparison to larger particles such as the wires [163]. It was with this in mind that we chose the particular method of attachment where we used the wires as a secondary mesh and tried to evenly disperse the spheres throughout the filters to increase the antimicrobial effects. The biocidal activity of these filters is due to the Ag NPs as was described in the material selection there are a number of ways in which the Ag NPs work; they may destabilize the cellular membrane by incorporation and form permeable pits which disrupt the proton motive force. They may also dissolve slowly into silver ions and interfere with the transport and respiratory enzymes in the external membrane. Ions denature ribosomes and hinder ATP production which intern leads to death. And lastly they may form reactive species when a cells respiratory activity is coupled from the proton motive force and an insufficient number of terminal oxygen receptors are present. There may also be DNA damage which is not conclusive. Studies have linked the physiochemical properties if Ag NPs to their antimicrobial activity and proteomic response in the lab and environmental systems [163]. It is well known

how the nanoparticles work but in this project we assembled filters with different functionalities and from all indication and test the thiol functionalized filters proved to be the most durable and most efficient in inactivating bacteria. This let to evaluate the reasons for this as all three functionalities were durable and had high efficiencies. We hypothesized that agglomeration state of the nanoparticle played a role in this as well as the oxidation sate. From the TEM images it was obvious that with the thiol functionality there were more evenly dispersed nanoparticles distributed throughout the layers of the cellulose filters and this would increase the contact when in contact with bacteria and also Ag^+ release would speed up due to the larger surface exposed. The contact is a mode of the Ag NPs antimicrobial activity and hence with increased contact there would be higher degrees of inactivation. From XPS the amine modified filters showed that there was approximately 10% of Ag^+ and 90% of Ag^0 and as was previously mentioned it is the ions that are responsible for the antimicrobial activity. The binding energy corresponding to Ag^+ is approximately 368 eV in the $3d_{5/2}$ orbital and from Table 6 the thiol functionalized filters possessed the exact binding energy and we demonstrated that there were a higher percentage of ions than that found in the amine-modified Ag-cellulose filters and hence why they are the best in our case study. The filters are able to work efficiently with inactivating *E. coli* but in the future it may be extended to other pathogenic microbial organisms and to check the nominal cut off- of the filters. And finally develop a working prototype of a device containing these filters.

CHAPTER 6

CONCLUSION

6.1 Conclusion/Summary

We have developed an approach for designing durable Ag-cellulose membrane filters derived from silver-sulphur and silver-nitrogen interactions by covalent bonds. All of which are capable of inactivating high loads of *E. coli* bacteria often present as a common constituent of contaminated water. In the field of water purification there will always be a need to have membranes such as these that are not only able to separate but also destroy contaminants. The filters with their dual functionality also boast strong durability and are eco and human friendly. Our filters with thiol-modification have proven to be the best and can be used to maximize the efficiency of nanoparticle usage to reduce cost and increase performance in order to bring clean drinking water to millions all over the world who lack this basic commodity.

REFERENCES

1. Progress on Drinking Water and Sanitation 2012, by: The WHO/UNICEF (<http://www.unicef.org/media/files/JMPReport2012.pdf>).
2. P. Dibrov, J. Dzioba, K.K. Gosink, C.C. Häse, Chemiosmotic mechanism of antimicrobial activity of Ag⁺ in *Vibrio cholera*, *Antimicrob. Agents Chemother.* 46 (8) (2002) 2668–2670.
3. World Health Organization. “Burden of health care-associated infection worldwide (fact sheet).” http://www.who.int/gpsc/country_work/summary_20100430_en.pdf (accessed December 12, 2012). And Samsung's Silver Nano Washer Ads Reportedly Exaggerated, (<http://www.appliancemagazine.com/news.php?article=9434&zone=0&first=1>).
4. Cristina Buzea, Ivan. I. Pacheco Blandino and Kevin Robbie. Nano-materials and nanoparticles: Sources and toxicity. *Biointerphases* vol. 2, issue 4 (2007) pages MR17-MR1721.
5. Baker, Moses N. (1981). *The Quest for Pure Water: the History of Water Purification from the Earliest Records to the Twentieth Century*. 2nd Edition. Vol. 1. Denver: American Water Works Association, 64-80.
6. Wikipedia. http://en.wikipedia.org/wiki/Water_filter#Point-of-use_filters.
7. Sung Yong Park, Jae Woo Chung, Rodney D Priestley, Seung-Yeop Kwak, Cellulose assembly of metal nanoparticles on cellulose fabric and its antimicrobial activity, 2012, 2141-2151.
8. R.P. Allaker, G. Ren, Potential impact of nanotechnology on the control of infectious disease, *Trans. R. Soc. Trop. Med. Hyg.* 102 (1) (2008) 1–2.
9. M. Mühling, A. Bradford, J.W. Readman, P.J. Somerfield, R.D. Handy, An investigation into the effects of silver nanoparticles on antibiotic resistance of naturally occurring bacteria in an estuarine sediment, *Mar. Environ. Res.* 68 (2009) 278–283.
10. S.C. Abeylath, E. Turos, Drug delivery approaches to overcome bacterial resistance to β -lactam antibiotics, *Expert Opin. Drug Deliv.* 5 (9) (2008) 931–949.
11. White WC, Bellfield R, Ellis J, Vandeldaele IP. Controlling the spread of infections in hospital wards by the use of antimicrobials on medical textiles and surfaces. In: *medical and Healthcare textiles*, Woodhead Publishing Limited, 2010.
12. Antimicrobial agent “Definition from the Merriam-Webster Online Dictionary”. Accessed May 16, 2013.
13. www.cdc.gov/oralhealth/infectioncontrol/glossary.htm. Accessed January 12, 2013.
14. Vigo TL. Antimicrobial Polymers and Fibres: Retrospective and Prospective. In: *Bioactive fibres and Polymers*. American Chemical Society. 11, 175-200, 2001.
15. Q. Li, S. Mahendra, D.Y. Lyon, L. Brunet, M.V. Liga, D. Li, P.J. Alvarez, Antimicrobial nanomaterials for water disinfection and microbial control: potential applications and implications, *Water Res.* 42 (2008) 4591–4602.

16. E. Weir, A. Lawlor, A. Whelan, F. Regan, The use of nanoparticles in anti-microbial materials and their characterization, *Analyst* 133 (2008) 835–845.
17. Ae Jung Huh, Young Jik Kwon, “Nanoantibiotics”: A new paradigm for treating infectious diseases using nanomaterials in the antibiotics resistant era, *Journal of controlled release*, vol. 156, 2011, 128-145.
18. P. Dibrov, J. Dzioba, K.K. Gosink, C.C. Häse, Chemiosmotic mechanism of antimicrobial activity of Ag⁺ in *Vibrio cholera*, *Antimicrob. Agents Chem other.* 46 (8) (2002) 2668–2670.
19. I. Chora, The increasing use of silver-based products as antimicrobial agents: a useful development or a cause for concern? *J. Antimicrob. Chem other.* 59 (2007) 587–590.
20. G. Taubes, The bacteria fight back, *Science* 321 (2008) 356–361.
21. V.K. Sharma, R.A. Yngard, Y. Liu, Silver nanoparticles: green synthesis and their antimicrobial activities, *Adv. Colloid Interface Sci.* 145 (1–2) (2008) 83–96.
22. Y. Liu, L. He, A. Mustapha, H. Li, Z.Q. Hu, M. Lin, Antibacterial activities of zinc oxide nanoparticles against *Escherichia coli* O157:H7, *J. Appl. Microbiol.* 107 (2009) 1193–1201.
23. H.J. Klasen, Historical review of the use of silver in the treatment of burns. I. Early uses, *Burns* 26 (2000) 117–130.
24. F. Raimondi, G.G. Scherer, R. Kötz, A. Wokaun, Nanoparticles in energy technology: examples from electrochemistry and catalysis, *Angew. Chem. Int. Ed Engl.* 44 (2005) 2190–2209.
25. I. Sondi, B. Salopek-Sondi, Silver nanoparticles as antimicrobial agent: a case study on *E. coli* as a model for gram-negative bacteria, *J. Colloid Interface Sci.* 275 (2004) 177–182.
26. Henglein, A.; *J. Phys. Chem.*, 1993, 97(21), 5457-5471.
27. S. Pal, Y.K. Tak, J.M. Song, Dose the antibacterial activity of silver nanoparticles depend on the shape of the nanoparticle? A study of the gram-negative bacterium *Escherichia coli*, *Appl. Environ. Microbiol.* 27 (6) (2007) 1712–1720.
28. P.L. Drake, K.J. Hazelwood, Exposure-related health effects of silver and silver compounds: a review, *Ann. Occup. Hyg.* 49 (7) (2005) 575–585.
29. H.J. Johnston, G. Hutchison, F.M. Christensen, S. Peters, S. Hankin, V. Stone, A review of the in vivo and in vitro toxicity of silver and gold particulates: particle attributes and biological mechanisms responsible for the observed toxicity, *Crit. Rev. Toxicol.* 40 (4) (2010) 328–346.
30. G. Oberdörster, E. Oberdörster, J. Oberdörster, Nanotoxicology: an emerging discipline evolving from studies of ultrafine particles, *Environ. Health Perspect.* 113 (7) (2005) 823–939.
31. L. Braydich-Stolle, S. Hussain, J.J. Schlager, M.C. Hofmann, In vitro cytotoxicity of nanoparticles in mammalian germ line stem cells, *Toxicol. Sci.* 88 (2005) 412–419.

32. S.M. Hussain, K.L. Hess, J.M. Gearhart, K.T. Geiss, J.J. Schlager, In vitro toxicity of nanoparticles in BRL 3A rat liver cells, *Toxicol. In Vitro* 19 (2005) 975–983.
33. Henglein, A.; *J. Phys. Chem.*, 1993, 97(21), 5457-5471.
34. Mulvaney, P.; *Langmuir*, 1996, 12(3), 788-800.
35. U. Kreibig and M Volmer, *Optical Properties of Metal Clusters*, Springer Series in Material Science Vol. 25 (Springer-Verlag, Berlin, 1995).
36. C. F. Bohren and D. R. Huffman, *Absorption and Scattering of Light by Small Particles* John Wiley and Sons Inc. New York, (1998).
37. K. Sakoda, *Optical Properties of Photonic Crystals*, Springer Series in Optical Sciences Vol.80 Springer-Verlag, Berlin, (2001).
38. S. Nie and S. R. Emory; *Science*, (1997), 275, 1102-1106.
39. K. Kneipp et al.; *Phys. Rev. Lett.*, (1997), 78, 1667-1670.
40. H. Xu, E. J. Bjerneld, M. Ka, and L. Börjesson; *Phys. Rev. Lett.* (1999), 83, 4357-4360.
41. D.W. Pohl and D. Courjon, *Near Field Optics*; NATO ASI, Ser. E, Vol. 241 Kluwer, Dordrecht, 1993.
42. T. Hamouda, M. Hayes, Z. Cao, R. Tonda, K. Johnson, W. Craig, J. Brisker, J. Baker; *J. Infect. Dis.* (1999) 180, 1939-1949.
43. P.K. Stoimenov, R.L. Klinger, G.L. Marchin, K.J. Klabunde; *Langmuir*, (2002), 18, 6679-6686.
44. Monafo, W.W. and Freedman, B.; *Surg. Clin. North Am.* (1978) 67, 133-145.
45. Becker, R.O.; *Met.-based Drugs*, (1999), 6, 297-300.
46. Sampath, L.A., Chowdhury, N., Caraos, L. and Modak, S.M.; *J. Hosp. Infect.* (1995) 30, 201-210.
47. <http://www.anapsid.org/gramnegative.html>. Accessed January 10,2013
48. <http://www.webmd.com/a-to-z-guides/e-coli-infection-topic-overview>. Accessed January 10, 2013.
49. I. Brigger, C. Dubernet, P. Couvreur, *Adv. Drug Deliver. Rev.* (2002), 54, 631.
50. F. Forestier, P. Gerrier, C. Chaumard, A.-M. Quero, P. Couvreur, C. LabarreJ. *Antimicrob. Chemother.* 1992, 30,173.
51. L. Joguet, I. Sondi, E. Matijevi´c, *J. Colloid Interface Sci.* (2002), 251, 284.
52. M.L. Hans, A.M. Lowman, *Curr. Opin. Solid State Mater.* (2002), 6, 319.
53. R.M. Slawson, M.I. Van Dyke, H. Lee, J.T. Trevors, *Plasmid.* (1992), 27, 72.
54. G.J. Zhao, S.E. Stevens, *Biometals.* (1998), 11, 27.
55. Wilson, M.; Kannangara, K.; Smith, G. in Michelle Simmons, Burkhard Reguse in *Nanotechnology: basic science and emerging technologies*, Chapman & Hall/CRC, 2002.
56. Halford, B. *Chemical & Engineering News* (2005), August.
57. Burda, C.; Chen, X.; Narayanan, R.; El-Sayed, M. A. *Chemical Reviews* (2005) 105, 1025.

58. Salem, A. K.; Chen, M.; Hayden, J.; Leong, K.W.; Searson, P.C. *Nano Letters* (2004) 4, 1163.
59. Yang, P.; Kim, F. *Chem. Phys. Chem.* (2002) 3, 503.
60. Image is taken from: www.mooreed.com.au and www.stochastix.wordpress.com. Accessed December 2, 2012
61. Xiong, Y.; Wiley, B. J.; Xia, Y. *Angew and the Chemie, International Edition* (2007), 46, 7157
62. Wiley B.; Sun Y.; Mayers B.; Xia Y. *Chemistry (Weinheiman der Bergstrasse, Germany)* (2005), 11, 454.
63. Ko, H.; Singamaneni, S.; Tsukruk, V. V. *Small* (2008), 4, 1576.
64. Wiley, B. J.; Im, S. H.; Li, Z-Y.; McLellan, J.; Siekkinen, A.; Xia, Y. *J. Phys. Chem. B* (2006), 110, 15666.
65. Sun, Y.; Xia, Y. *Analyst* (2003) 128, 686.
66. Burda, C.; Chen, X.; Narayanan, R.; El-Sayed, M. A. *Chem. Rev.* (2005) 105, 1025.
67. (a) Teoh, L. G. *Current Nanoscience* (2009), 5, 113. (b) Silvestri, B.; Costantini, A.; Tescione, Luciani, G.; F.; Branda, F.; Pezzella, A. *Journal of Biomedical Materials Research, Part B: Applied Biomaterials* (2009), 89B, 369. (c) Hassanzadeh, A.; Moazzez, B.; Haghgooie, H.; Nasserri, M.; Golzan, M. M.; Sedghi, H. *Central European Journal of Chemistry* (2008), 6, 651. (d) Chen, Y. W.; Qiao, Q.; Liu, Y. C.; Yang, G. L. *Journal of Physical Chemistry C* (2009), 113, 7497.
68. Reyhani, A.; Mortazavi, S. Z.; Novinrooz, A. J. *Synthesis and Reactivity in Inorganic, Metal-Organic, and Nano-Metal Chemistry* (2009), 39, 31.
69. Singh, D. P.; Ojha, A. K.; Srivastava, O. N. *Journal of Physical Chemistry C* (2009), 113, 3409.
70. Zhang, Z.; Brown, S.; Goodall, J. B. M.; Weng, X.; Thompson, K.; Gong, K.; Kellici, S.; Clark, R. J. H.; Evans, J. R. G.; Darr, J. A. *Journal of Alloys and Compounds* (2009), 476, 451
71. Wang, R.; Ruan, C.; Kanayeva, D.; Lassiter, K.; Li, Y. *Nano Letters* (2008), 8, 2625.
72. (a) Thongtem, S.; Wannapop, S.; Thongtem, T. *Ceramics International* (2009), 35, 2087. (b) Chandradass, J.; Kim, K. H. *Materials and Manufacturing Processes* (2009), 24, 541. (c) Ogi, T.; Kaihatsu, Y.; Iskandar, F.; Tanabe, E.; Okuyama, K. *Advanced Powder Technology* (2009), 20, 29. (d) Islam, M. R.; Podder, J. *Crystal Research and Technology* (2009), 44, 286.
73. Wang, Y.; Wu, J.; Wei, F. *Carbon* (2003), 41, 2939.
74. Yin, W.; Cao, M.; Luo, S.; Hu, C.; Wei, B. *Crystal Growth & Design* (2009), 9, 2173, (b) Chen, Y.; Tong, Z.; Luo, L. *Chinese Journal of Chemical Engineering* (2008), 16, 485. (c) Zhang, H.; Zhang, Q.; Tang, J.; Qin, L.-C. *Journal of the American Chemical Society* (2005), 127, 2862. (d) Yang, Q.; Jian, S.; Ma, X.; Ji, Y. Yang, D. *Superconductor Science and Technology* (2004), 17, L31.

75. Yu, D.; Hu, L.; Qiao, S.; Zhang, H.; Len, S.-E. (Andy); Len, L. K.; Fu, Q.; Chen, X.; Sun, K. *Journal of Physics D: Applied Physics* (2009), 42, 055110.
76. Pileni, M.-P. *Nature* (2003), 2, 145.
77. Murphy, C. J.; Sau, T. K.; Gole, A. M.; Orendorff, C. J.; Gao, J.; Gou, L.; Hunyadi, S. E. Li, T. J. *Phys. Chem. B*, (2005), 109, 13857.
78. Xia, Y.; Xiong, Y.; Lim, B.; Skrabalak, S. E. *Angew. Chem. Int. Ed.* (2009), 48, 60.
79. Wiley, B.; Sun, Y.; Xia, Y. *Acc. Chem. Res.* (2007), 40, 1067.
80. Taton TA: Nanostructures as tailored biological probes. *Trends Biotechnol* (2002) 20:277-279.
81. Whitesides GM: The 'right' size in Nanobiotechnology. *Nature biotechnology* (2003), 21:1161-1165
82. Bruchez M, Moronne M, Gin P, Weiss S, Alivisatos AP: Semiconductor nano-crystals as fluorescent biological labels. *Science* (1998), 281:2013-2016
83. Wang S, Mamedova N, Kotov NA, Chen W, Studer J: Antigen/antibody immune-complex from Cd Te nanoparticle bio-conjugates. *Nano Letters* (2002), 2:817-822.
84. Mah C, Zolotukhin I, Fraites TJ, Dobson J, Batich C, Byrne BJ: Microsphere-mediated delivery of recombinant AAV vectors in vitro and in vivo. *Mol Therapy* (2000), 1:S239
85. Panatarotto D, Prtidos CD, Hoebeke J, Brown F, Kramer E, Briand JP, Muller S, Prato M, Bianco A: Immunization with peptide-functionalized carbon nanotubes enhances virus-specific neutralizing antibody responses. *Chemistry & Biology* (2003), 10:961-966.
86. Edelstein RL, Tamanaha CR, Sheehan PE, Miller MM, Baselt DR, Whitman LJ, Colton RJ: The BARC biosensor applied to the detection of biological warfare agents. *Biosensors Bioelectron* (2000), 14:805-813.
87. Nam JM, Thaxton CC, Mirkin CA: Nanoparticles-based bio-bar codes for the ultrasensitive detection of proteins. *Science* (2003), 301:1884-1886.
88. Mahtab R, Rogers JP, and Murphy CJ: Protein-sized quantum dot luminescence can distinguish between "straight", "bent", and "kinked" oligonucleotides. *J Am ChemSoc* 1995, 117:9099-9100
89. Ma J, Wong H, Kong LB, Peng KW: Biomimetic processing of nano-crystallite bioactive apatite coating on titanium. *Nanotechnology* (2003), 14:619-623.
90. de la Isla A, Brostow W, Bujard B, Estevez M, Rodriguez JR, Vargas S, Castano VM: Nanohybrid scratch resistant coating for teeth and bone viscoelasticity manifested in tribology. *Mat ResInnovat* (2003), 7:110-114
91. Yoshida J, Kobayashi T: Intracellular hyperthermia for cancer using magnetite cationic liposomes. *J MagnMagn Mater* (1999), 194:176-184.
92. Molday RS, MacKenzie D: Immuno specific ferromagnetic iron dextran reagents for the labeling and magnetic separation of cells. *J Immunol Methods* (1982), 52:353-367.

93. Weissleder R, Elizondo G, Wittenburg J, Rabito CA, Bengele HH, Josephson L: Ultra small superpara magnetic iron oxide: characterization of a new class of contrast agents for MR imaging. *Radiology* (1990), 175:489-493
94. Sinani VA, Koktysh DS, Yun BG, Matts RL, Pappas TC, Motamedi M, Thomas SN, Kotov NA: Collagen coating promotes biocompatibility of semiconductor nanoparticles in stratified LBL films. *Nano Letters* (2003), 3:1177-1182
95. Zhang Y, Kohler N, Zhang M: Surface modification of superpara magnetic magnetite nanoparticles and their intracellular uptake. *Biomaterials* (2002), 23:1553-1561.
96. Principles of Biotechnology, A.J. Nair, Laxmi Publication (2008) pg. 716
97. Dynamics of Microbial Growth, D.W. Tempest, University of Amsterdam
98. P.K. Stoimenov, R.L. Klinger, G.L. Marchin, K.J. Klabunde; *Langmuir* (2002), 18, 6679-6686.
99. Berger TJ, Spadaro JA, Bierman R, Chapin SE, Becker RO.; *Antimicrob Agents Chem other.* (1976), 10, 856-860.
100. Golubovich VN, Rabotnova IL.; *Microbiol.* (197) 4, 43, 948-950.
101. Becker, R.O.; *Met.-based Drugs* (1999) 6, 297-300.
102. Sampath, L.A., Chowdhury, N., Caraos, L. and Modak, S.M.; *J. Hosp. Infect.* (1995), 30, 201-210.
103. Ivan Sondi, and BrankaSalopek-sondi; *J. Colloid Interface Sci.* (2004) 275, 177-182.
104. Monafó, W.W. and Freedman, B.; *Surg. Clin. North Am.* (1978) 67, 133-145.
105. David T. Schoen, Alia P. Schoen, Liangbing Hu, Han Sun Kim, Sarah C. Heilshorn, and Yi Cui High Speed Water Sterilization Using One-Dimensional Nanostructures, American Chemical Society, *Nano Lett.* (2010) 10, 3628—3632.
106. Yuan, J. K.; Liu, X. G.; Akbulut, O.; Hu, J. Q.; Suib, S. L.; Kong, J.;Stellacci, F. *Nat. Nanotechnol.* (2008), 3, 332.
107. MohanUdhayaSankar, SahajaAigal, Shihabudheen M. Maliyekkal, Amrita Chaudhary, Anshup, Avula Anil Kumar, Kamalesh Chaudhari, and Thalappil Pradeep. Biopolymer-reinforced synthetic granular nano-composites for affordable point of use water purification, *PNAS*, (2013).
108. <http://www.hkc22.com/watermarketsworldwide.html>.
109. Gao Y, Cranston R. Recent Advances in Antimicrobial Treatments of Textiles. *Textile Research Journal.* (2008); 87:60-72.
110. New Multifunctional Textiles: Antimicrobial Treatments, International Workshop, Thesaloniki, Greece. Available at: http://texmail.ca/002/files/000MNu00ItFU0mF4XF0x/Anti-microbial_treatment.pdf. Accessed December 12, 2012.
111. Hashem M, Ibrahim NA, El-Sayed WA, El-Husseiny S, El-Enany E. Enhancing antimicrobial properties of dyed and finished cotton fabrics. *Carbohydrate Polymers.* (2009) 78, 502–510.

112. Vigo TL. Antimicrobial Polymers and Fibres: Retrospective and Prospective. In: Bioactive Fibres and Polymers. American Chemical Society (2001) 11, 175-200.
113. Stashak ST, Farstvedt E, Othis A. Update on Wound Dressings: Indication and Best Use. *Clinical Techniques in Equine Practice* (2004) 3,148-163.
114. Belyaev EY. Drug Synthesis Methods and Manufacturing Technology, New Medical Materials Based on Modified Polysaccharides (Review). *Pharmaceutical Chemistry Journal*. (2000) 34, 11, 607-612.
115. Heine E, Knops HG, Schaefer K, Vangeyte P, Moeller M. Antimicrobial Functionalization of Textile Materials. In: Multifunctional Barriers for Flexible Structure, Textile, Leather and Paper. Springer-Verlag, Berlin Heidelberg (2007).
116. Tankhiwale R , and BajpaiS. K., Graft copolymerization onto cellulose-based filter paper and its further development as silver nanoparticles loaded antibacterial food-packaging material. *CollodvSurf. Biointerfaces* (2009), 69(2), 164-168.
117. Carlson C., Hussain S. M. , Schrand A. M., Braydich-Stolle L. K., Hess K. L., Jones R. L., and Schalger J. J., Unique cellular interaction of silver nanoparticles: Size-Dependent Generation of Reactive Oxygen species. (2008), *Journal of Physical Chemistry B*, 112 (43), 13608-13619.
118. An Inventory of nanotechnology-based Consumer products currently on the market. http://www.nanotechproject.org/inventories/consumer/analysis_draft/. Accessed May 11, 2013
119. Quadros M.E., Marr L.C., *Environ. Sci. Technol.* (2011), 45(24), 10713-10719.
120. Richard JW, Spencer BA, McCoy LF, Carina E, Washington J, Edgar P, et al. Acticoat versus silverlon: the truth. *J Burns Surg Wound Care* (2002); 1:11–20.
121. El-Rafie MH, Mohamed AA, Shaheen THI, Hebeish A. Antimicrobial effect of silver nanoparticles produced by fungal process on cotton fabrics. *Carbohydrate Polymers*. (2010); 80:779-782.
122. Dastjerdi R, Montazer M, Shahsavan S. A new method to stabilize nanoparticles on textile surfaces. *Colloids and Surfaces, A:Physico chemical Engineering Aspects*. (2009); 345:202- 210.
123. TijanaRistić, Lidija Fras Zemljič, Monika Novak, MarjetkaKraljKunčič, Silva Sonjak, Nina Gunde Cimerman3 and SimonaStrnad , Antimicrobial efficiency of functionalized cellulose fibres as potential medical textiles (2011), *Formatex*.
124. Schindler WD, Hauser PJ. *Chemical Finishing of Textiles*. Wood head Publishing Ltd, Cambridge, 213, (2004).
125. Simoncic B, Tomsic B. Structures of Novel Antimicrobial Agents for Textiles – A Review. *Textiles Research Journal*, doi: 10.1177/0040517510363193, (2010).
126. Silver S, Le Phung T, Silver G. Silver as biocides in burn and wound dressings and bacterial resistance to silver compounds. *Journal of Industrial Microbiology and Biotechnology*. (2006); 33:627-634.

127. Levard, C.; Hotze, E. M.; Lowry, G. V.; Brown, G. E. *Environ. Sci. Technol.* (2012), 46 (13), 6900–6914.
128. Choi, O.; Hu, Z. Q. *Environ. Sci. Technol.* (2008), 42 (12), 4583–4588.
129. Choi, O.; Cleuenger, T. E.; Deng, B. L.; Surampalli, R. Y.; Ross, L.; Hu, Z. Q. *Water Res.* (2009), 43 (7), 1879–1886.
130. Xiu, Z. M.; Ma, J.; Alvarez, P. J. J. *Environ. Sci. Technol.* (2011), 45 (20), 9003–9008.
131. Yang, X. Y.; Gondikas, A. P.; Marinakos, S. M.; Auffan, M.; Liu, J.; Hsu-Kim, H.; Meyer, J. N. *Environ. Sci. Technol.* (2012), 46 (2), 1119–1127.
132. Morones, J. R.; Elechiguerra, J. L.; Camacho, A.; Holt, K.; Kouri, J. B.; Ramirez, J. T.; Yacaman, M. J. *Nanotechnology* (2005), 16 (10), 2346–2353.
133. Pal, S.; Tak, Y. K.; Song, J. M. *Appl. Environ. Microbiol.* (2007), 73 (6), 1712–1720.
134. El Badawy, A. M.; Silva, R. G.; Morris, B.; Scheckel, K. G.; Suidan, M. T.; Tolaymat, T. M. *Environ. Sci. Technol.* (2011), 45 (1), 283–7.
135. Sotiriou, G. A.; Pratsinis, S. E. *Environ. Sci. Technol.* (2010), 44 (14), 5649–5654.
136. Liu, J. Y.; Hurt, R. H. *Environ. Sci. Technol.* (2010), 44 (6), 2169–2175.
137. Liu, J. Y.; Sonshine, D. A.; Shervani, S.; Hurt, R. H. *ACS Nano* (2010), 4 (11), 6903–6913.
138. http://en.wikipedia.org/wiki/Escherichia_coli Accessed May 12, 2013.
139. <http://blog.budgetwater.com/water-treatment/2011/e-coli-and-coliform-in-your-water/> Accessed May 10 2013.
140. <http://water.epa.gov/drink/contaminants/index.cfm#Microorganisms> Accessed May 10, 2013.
141. S.C. Edberg , E.W. Rice , R.J. Karlin and M.J. Allen, *Escherichia coli: The best biological drinking water indicator for public health protection*, *Journal of applied microbiology*, (2000), vol. 88, 106S-116S.
142. http://en.wikipedia.org/wiki/Ultraviolet%20%93visible_spectroscopy Accessed December 1, 2012.
143. http://en.wikipedia.org/wiki/Scanning_electron_microscope Accessed December 1, 2012.
144. http://en.wikipedia.org/wiki/Transmission_electron_microscopy Accessed December 1, 2012.
145. http://en.wikipedia.org/wiki/Dynamic_light_scattering. Accessed February 12, 2013.
146. http://en.wikipedia.org/wiki/Inductively_coupled_plasma_atomic_emission_spectroscopy Accessed April 16, 2013.
147. Shateri Khalil-Abad M, Yazdanshenas ME, Nateghi MR (2009) Effect of cationization on adsorption of silver nanoparticles on cotton surfaces and its antibacterial activity. *Cellulose* 16(6):1147–115.
148. Rance GA, Khlobystov AN (2010) Nanoparticle-nanotube electrostatic interactions in solution: the effect of pH and ionic strength. *PCCP* 12(36):10775–10780

149. AshaRani PV, Mun GLK, Hande MP, Valiyaveetil S (2009) Cytotoxicity and genotoxicity of silver nanoparticles in human cells. *ACS Nano* 3(2):279–290
150. B. C. Reinsch, C. Levard, Z. Li, R. Ma, A Wise, K. B. Gregory, G. E. Brown, Jr., and G. V. Lowry, Sulfidation of silver nanoparticles decreases Escherichia coli growth inhibition, *Environ. Sci. Technol.* (2012), 46, 6992-7000.
151. Boufi, S.; ReiVilar, M.; Parra, V.; Ferraria, A. M.; Botelho do Rego, A. M. *Langmuir* 2008, 24, 7309–7315.
152. http://en.wikipedia.org/wiki/Fourier_transform_spectroscopy Accessed May 12, 2013.
153. http://en.wikipedia.org/wiki/X-ray_photoelectron_spectroscopy Accessed February 22, 2013.
154. R. G. Pearson, “Hard and soft acids and bases,” *J. Am. Chem.Soc.*, vol. 85, Nov. (1963), pp. 3533-3539.
155. T. L. Ho, “The Hard Soft Acids Bases (HSAB) principle and organic chemistry,” *Chem. Rev.*, vol. 75, Feb.(1975), pp. 1-20.
156. Sung Yong Park, Su-Yeol Ryu and Seung-Yeop Kwak, Antibacterial Metal Fiber Hybrid with Covalent Assembly of silver and Palladium Nanoparticles on Cellulose Fibres, International Conference on Biology, Environment and Chemistry, IPCBEE (2011) vol. 1.
157. E. Pretsch, P. Bühlmann, C. Affolter, A. Herrera and R. Martínez, *Determinació estructural de compostos orgánicos*, Elsevier Masson (2002).
158. Battocchio C, Meneghini C, Fratoddi I, Venditti I, Russo M V, Aquilanti G, Maurizio C, Bondino F, Matassa R, Rossi M, Mobilio S and Polzonetti G, Silver Nanoparticles Stabilized with Thiols: A Close Look at the Local Chemistry and Chemical Structure *Journal of Physical Chemistry C* (2012) 116 19571-8.
159. Rodriguez JA, Hrbek J (1999) Interaction of sulfur with well-defined metal and oxide surfaces: unraveling the mysteries behind catalyst poisoning and desulfurization. *Acc Chem Res* 32(9):719–728.
160. Lu, Q.; Gao, F.; Komarneni, S. *Chem. Mater.* (2006), 18, 159–163.
161. Huang, H.; Yang, X. *Carbohydr. Res.* (2004), 339, 2627–2631.
162. Ferraria A M, Boufi S, Battaglini N, Botelho do Rego A M and ReiVilar M (2010) Hybrid Systems of Silver Nanoparticles Generated on Cellulose Surfaces *Langmuir* 26 1996-2001.
163. Meagan S. Mauter, Yue Wang, Katetochi C. Okembo, Chinedum O. Osuji, Emanuel P. Giannelis and Menachem Elimelech, Antifouling Ultrafiltration Membranes via Post – Fabricaton Grafting of biocidal nanomaterials, *Applied Materials and interfaces*, vol. 3, (2011), 2861-2868.
164. www.sigmaaldrich.com. Accessed March 02, 2013.

APPENDIX A

Chapter 3 -Experimental and methods.

CHAPTER 3

EXPERIMENTAL AND METHODS

3.1 Materials selection

The purpose of imparting antimicrobial activity into water filters is to prevent transmission and spreading of pathogenic microorganisms, inhibit odour development resulting from microbial degradation, and creating a material or device which is able to act as a preventative and/or curative treatment. Ideal antimicrobial incorporation needs to fulfil a number of requirements in order to achieve the maximum benefit from the antimicrobially functionalized products. An antimicrobially treated material is defined as being hygienic and therefore, should have the following requirements [109,110,111].

- Effective inhibition against a broad spectrum of bacterial and fungal species,
- Non-toxicity to the consumer, manufacturer and the environment,
- Durability,
- Avert from irritations and allergies,
- Applicability with no adverse effects on quality of the product,
- Easy to use and affordable.

For this project we have decided to make cellulose grafted membranes with metallic nanoparticles for the high speed sterilization of water. The filters will be made from a cellulose backbone or support which is commercially available; it will be functionalized and covalently bonded to silver nanoparticles. The above mentioned factors were some of the major and contributing factors in the selection of the materials used in the fabrication of these membranes to be employed in the high speed sterilization of contaminated water. A number of chemicals have been employed to impart antimicrobial activity to textile materials. These chemicals include inorganic salts, organometallics, iodophors (substances which slowly release iodine), phenols and thio-phenols, antibiotics, hetero-cyclics with anionic groups, nitro compounds, ureas, formaldehyde derivatives, and amines [109]. There is always a continuous search to have an eco-friendly “green” process to substitute for toxic chemicals therefore, there has been an increasing interest in functionalization based environmentally friendly biodegradable (if possible) reagents.

From this point of view, amino polysaccharides such as chitosan have been excellent candidates for eco-friendly finishes.

For our research we opted to choose cellulose filters, from a commercial source as the backbone for our filters. Cellulose fibres have found a broad application in the medical textile field as it holds quite unique characteristics. These characteristics include high moisture and liquids' adsorption, low impurity content, antistatic behaviour, and good mechanical properties. However, cellulose fibres are not without fault, they also provide an excellent surface for microorganism's growth. The molecular structure and the large active surface area of the cellulose fibres make them an ideal matrix or in the case of this project support "back-bone" for the design of water filters, and other bioactive, biocompatible and intelligent materials [112,113,114]. From literature cellulose fibres are amongst if not the most interesting basic material for antimicrobial functionalization. The surface modification of the cellulose fibres is currently considered to be the best route for obtaining modern functionality on textiles for the use in medical applications [109]. Hence by using thiol or amine functional groups to functionalize the fibres in order to attach the antimicrobial agent (silver NPs) and impart antimicrobial properties, then develop water filters capable of inactivating various types of bacteria as it passes through. The filters used in this research are from Prat Dumas, France and have pore sizes ranging from 2-3 μm and its parameters can be found in Table 2 below.

Table 2 Parameter of commercial cellulose filters from Prat Dumas, France.

Qualitative Filter Paper	
Material	100% cellulose
Weight/Surface area	100 g/m ²
Thickness	200 μm
Pore size (micrometric retention)	2-3 μm
Equivalence	Whatman 5
Air permeability	650 mmH ₂ O
Resistance in the wet state	0.5 Kg/cm

This pore size is important as it needs to be large enough to allow the bacteria to pass through at a reasonable flux but still small enough to allow contact with the antimicrobial agents.

There are several antimicrobial agents that could have been used for the antimicrobial functionalization of the cellulose acetate filters; however, we choose to use silver nanoparticles in the form of spheres and wires in the assembly of our filters. Antimicrobial agents can either be applied in an after-treatment process or incorporated into a polymer solution prior to extrusion or into spinning bath [109,115]. For this research we have chosen an after-treatment process. As incorporation of antimicrobial substances within a fibre matrix is suitable only for synthetic fibres. After-treatment processes can be done to both natural and synthetic fibres thus a wider spectrum of materials which can be used with this method without limiting the possibilities of starting materials. Methods like padding, spraying, coating and foam finishing have been developed [109,115]. Many other methods have also been reported such as the one which will be used in this work, which uses nano-sized colloidal dispersion of nanoparticles, chemical modification for covalent bond formation with the fibre (Figure7), crosslinking of the active agent onto the fibre using cross-linker and even sol gel processes [109].

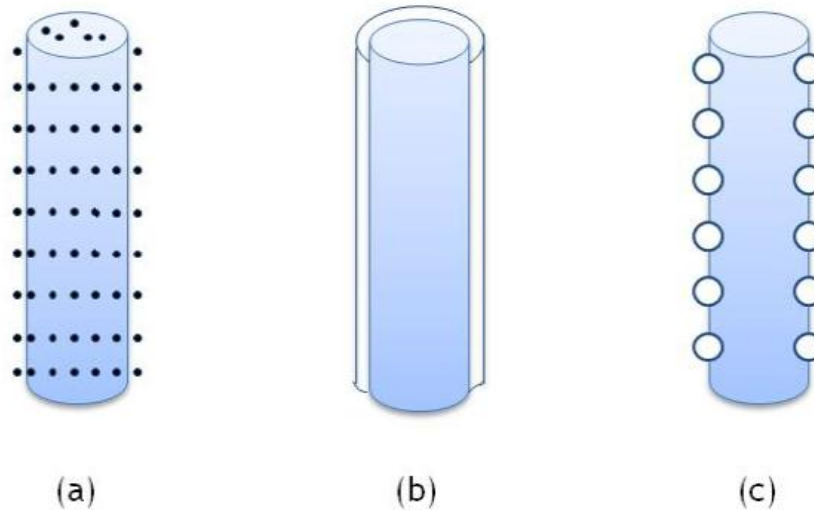


Figure 7 Antimicrobial agents are a) incorporated into the fibre; b) applied on the fibres surface; c) chemically bound onto the fibres [108].

Silver can be said to be one of the most widely used metals in industries for inhibiting microbes, although some other metals such as zinc, copper and cobalt amongst others have shown effective

inhibitions as well [109,114].Renewed interest in silver as an antimicrobial material has appeared recently as there has been an increase of multi-drug resistance of microbial strains to conventional antibiotics [116].As a broad spectrum antimicrobial agent, silver nanoparticles are well known for their cytotoxicity [117] and are currently the most widely commercialized nanomaterial [118]. Silver nanoparticles are increasingly being used in many medical and consumer products, including antiseptic sprays, antimicrobial coatings for medical devices that sterilize air and surfaces, water filters and a host of other applications [119].As early as 1000 B.C. silver was used to make water potable (120).It is believed that heavy metals react with proteins by combining with the thiol (-SH) groups, which leads to the inactivation of proteins [121]. In the presence of moisture (e.g. from air or water), metal ions are formed and in turn inhibit microbial replication. Ag NPs' antimicrobial mechanism can be briefly explained as follows: metal ions destroy or pass through the cell membrane, and bind to the -SH groups of the cellular enzymes thus resulting in a consequently critical destruction of the enzymatic activity which causes the microorganism's metabolism to undergo a change and thus their own growth to be inhibited, leading up to the death of the cell. The metal ions also catalyse the production of oxygen radicals that oxidize the molecular structure of bacteria. Silver ions can lead to denaturation of proteins, and cell death because of their reaction with nucleophilic amino acid residues in proteins, and their attachments to sulphhydryl, amino, imidazole, phosphate and carboxyl groups of membrane or enzyme proteins. Silver is also known to inhibit a number of oxidative enzymes such as yeast alcohol dehydrogenase, the uptake of succinate by membrane vesicles and the respiratory chain of *Escherichia coli*, causing metabolite efflux and interference with DNA replication [122]. It is also believed that polycationic antimicrobial compounds target the cytoplasmic membranes of microorganisms and thus the mechanism usually takes place in a six step process [115]:

Adsorption onto the microbial surface

1.1 Diffusion through the cell

1.2 Binding to the cytoplasmic membrane

1.3 Disruption of the cytoplasmic membrane

1.4 Release of cytoplasmic constituents such as K^+ ion, DNA and RNA

1.5 Death of the cell.

Antimicrobial agents such as silver nanoparticles can act in two distinct ways (Figure 8):

By contact; the antimicrobial agent inhibits microbes only on the fibre surface (substances are permanently attached to the fibre surface),

By diffusion; the antimicrobial agent is slowly released onto the fibre surface and/or from the surface (substances with controlled-release mechanism).

Silver nanoparticles have extremely large specific surface area, thus increasing their contact with bacteria or fungi, and vastly improving their bactericidal and fungicidal effectiveness [31].

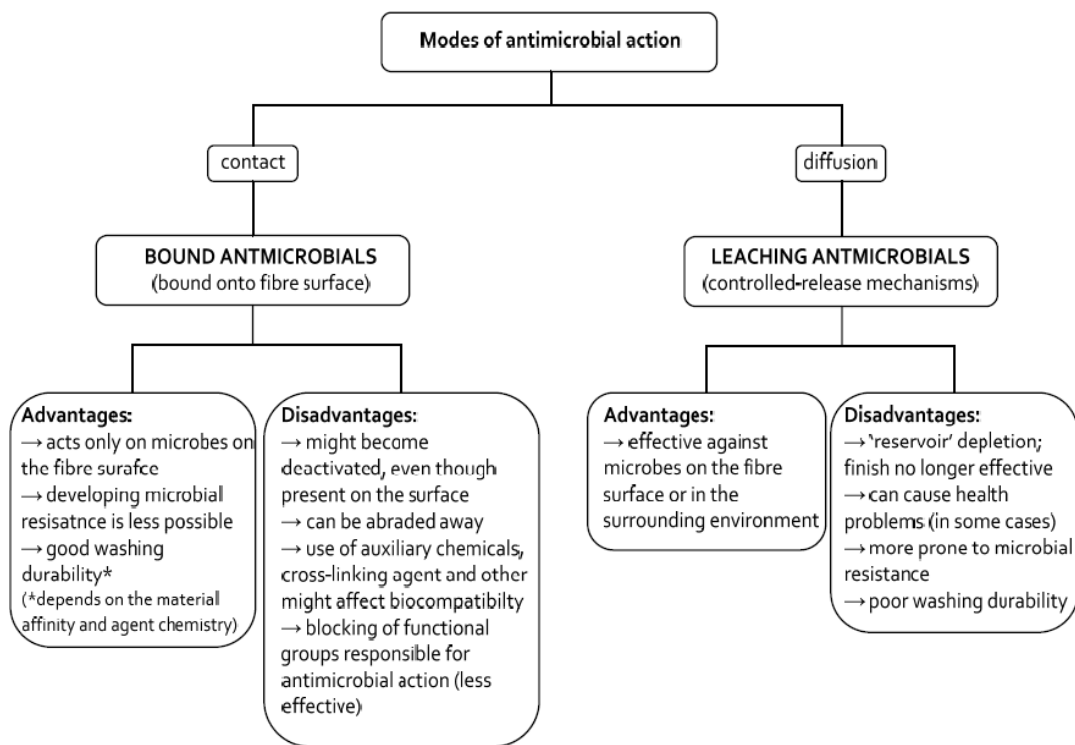


Figure 8 Modes of antimicrobial action [123]

Bound antimicrobials are chemically bound to the fibre's surface, where they form a barrier against microorganisms, and control the spread of those microorganisms that come into contact

with the fibre surface [124, 125]. The main advantage of these agents is that they do not leach-off the substrates into the surroundings, so the probability of microorganisms developing resistance to them is small. Because bound antimicrobials are firmly attached onto the fibre surface they are more durable to laundering than leaching antimicrobials. However, the washing durability of an agent cannot ensure its durability regarding the antimicrobial function [125]. Even though antimicrobial agent is present on the surface, it might lose its activity, i.e. become deactivated, or can be abraded away. Chemical bond formation, such as covalent binding, which is our goal in this work, is achieved under certain conditions and is strongly dependent upon proper anchoring groups (thiol and amine) available in the agent and in the fibre structure. The major drawback of this kind of process is that by attaching active agents to the fibres, chemical bonds are formed between the functional groups, which results in blocking of those functional groups responsible for antimicrobial effectiveness. Therefore, antimicrobial activity decreases, as the rate of dissolution can be impaired and hence there be less ions being released in the case of silver (the ions are said to be responsible for the antimicrobial activity of the silver and this will be discussed further in this section), however this is not always the case [124].

Silver nanoparticles are not without disadvantages however, despite the efficacy of antimicrobials based on silver, concerns about bacterial resistance have been reported in several papers [126]. However, the use of devices containing silver must be undertaken with caution; since a concentration-dependent toxicity has been demonstrated. There is no doubt that the release of silver ions from the crystalline core of silver nanoparticles contribute to the toxicity of these nano-materials. However, whether it is the nanoparticle itself that exerts a “particle-specific” toxicity still remains exclusive. If an answer were to be arrived at it would greatly help to both advance antimicrobial applications of Ag NPs and to clarify their potential behaviour and impact on the environment [127]. Many studies using different organisms have concluded that the toxicity of the Ag NPs is not solely due to the silver released from the nanoparticles (e.g., silver ions or dissolved silver). These cases saw the Ag NPs being at times more toxic than silver salts at equivalent concentration [128]. However, this observation may be perplexed by ligands in the exposure medium as they may bind to the dissolved silver. Ligands may be chloride, sulphide, phosphate or organic acids whose presence can decrease the bioavailability (and hence the toxicity) of the released silver ions to a greater extent than that of the Ag NPs [129,130] other

studies have concluded that the toxicity is directly related to the dissolved silver, perhaps because of the different chemical constituents in the exposure media [131]. It has also been demonstrated that the antimicrobial activity of Ag NPs is however, due solely to the release of silver ions and even relatively low concentration ($\mu\text{g/L}$) concentrations of silver ions (released or adsorbed to Ag NP coatings) can account for the biological responses. Particle properties that affect toxicity such as size [132], shape [133], surface coating [131], and surface charge [134] likely affect toxicity indirectly through mechanisms that influence the rate, extent, location and or timing of silver ions release. The size is inversely proportional to the toxicity due to the higher specific surface area and faster release of silver ions [135]. The full control of the toxicity of the silver nanoparticles requires deeper understanding of their release, specification and bioavailability of the silver ion [136, 137]. The advent of Ag NPs as promising antimicrobial nano-materials, therefore, requires clear and full elucidations of their potential toxicity.

The targeted bacterium in this study is *Escherichia coli* is a Gram-negative, facultative anaerobic, rod-shaped bacterium that is commonly found in the lower intestine of warm-blooded organisms (endotherms) [138]. We all know about *E. coli*, it lives in, on, and around faecal matter to put it in layman's terms. Most *E. coli* strains are harmless, but some serotypes can cause serious food poisoning in humans, and are occasionally responsible for product recalls due to food contamination. The bacterium has been well known for a long time, and it is difficult to avoid when it comes to food and water. Which is why it is sort of disconcerting to find out that all drinking water invariably has *E. coli* in it; it is just kept down to levels that are considered "safe." *E. coli* is Gram-negative and non-sporulating. Cells are typically rod-shaped, and are about 2.0 microns (μm) long and 0.5 μm in diameter, with a cell volume of 0.6–0.7 (μm)³ [138].



Figure 9 Images of *E. coli* bacteria found in water [139].

According to that data sheet below from the Environmental Protection agency of the United States of America (EPA), *E. coli* is acceptable as long as it does not appear in more than 5% of the water samples collected in a given month [140]. Hence it is almost always certain that there will be *E. coli* in drinking water. If the municipality tests their water 100 times in a month, 5 of those samples can be infected with *E. coli*, but the water will still be permitted to go out to the city's residents. And once you get down to decimal places of hundredths or thousandths of a per cent there will be some *E. coli* in the water.

Table 3 Data sheet of some microbial contaminants found in drinking water [140].

Microorganisms				
Contaminant	MCLG ¹ (mg/L) ²	MCL or TT ¹ (mg/L) ²	Potential Health Effects from Long-Term Exposure Above the MCL (unless specified as short-term)	Sources of Contaminant in Drinking Water
<i>Cryptosporidium</i>	zero	TT ³	Gastrointestinal illness (e.g., diarrhea, vomiting, cramps)	Human and animal fecal waste
<i>Giardia lamblia</i>	zero	TT ³	Gastrointestinal illness (e.g., diarrhea, vomiting, cramps)	Human and animal fecal waste
Heterotrophic plate count	n/a	TT ³	HPC has no health effects; it is an analytic method used to measure the variety of bacteria that are common in water. The lower the concentration of bacteria in drinking water, the better maintained the water system is.	HPC measures a range of bacteria that are naturally present in the environment
<i>Legionella</i>	zero	TT ³	Legionnaire's Disease, a type of pneumonia	Found naturally in water; multiplies in heating systems
Total Coliforms (including fecal coliform and <i>E. Coli</i>)	zero	5.0% ⁴	Not a health threat in itself; it is used to indicate whether other potentially harmful bacteria may be present ⁵	Coliforms are naturally present in the environment; as well as feces; fecal coliforms and <i>E. coli</i> only come from human and animal fecal waste.

Public health protection requires an indicator of faecal pollution or contamination to water. It is however, not necessary to analyse drinking water for all pathogens as this would be very tedious and time consuming. *Escherichia coli* are found in all mammal faeces at concentrations of 10^9 g⁻¹, but it does not multiply appreciably in the environment. In the 1890s, it was chosen as the biological indicator of water treatment safety. Because of method deficiencies, *E. coli* surrogates or carriers namely 'faecal coliform' and total coliforms tests were developed and became an integral part of drinking water regulations. *E. coli* survives in drinking water for between 4 and 12 weeks, depending on environmental conditions (temperature, microflora, etc.). Bacteria and viruses are approximately equally oxidant-sensitive, but parasites are less so. Under these

conditions in distribution systems, *E. coli* will be much more long-lived [141]. Hence this is the reason for choosing *E. coli* as the primary bacterium target in this work.

Based on the dimensions of the bacteria and the parameters of the filter we should be able to produce a gravity fed antifouling membrane filter capable of inactivating bacteria as it passes through with the hope of providing clean water to many depending on the various need of the consumer.

In order to carry out this task the following experiments were carried out.

3.2 Synthesis of Nanoparticles

3.2.1 Synthesis of Silver nano-wires

High-yield silver nanowires were synthesized according to a well-known procedure which is described below. All glassware were washed with soap, aqua regia, and rinsed thoroughly with de-ionized water and acetone before and after use.

Materials: Silver nitrate (AgNO_3), Ethylene glycol ($\text{C}_2\text{H}_6\text{O}_2$), Poly Vinyl Pyrrolidone (PVP with $M_w \sim 55000$ Da.)

Preparation of Solutions:

10 mL of ethylene glycol and 169.87 mg AgNO_3 (0.1M AgNO_3), 10 mL of ethylene glycol and 166.71 mg PVP.

AgNO_3 was dissolved in ethylene glycol at room temperature and under constant stirring. In a second vessel PVP was dissolved in ethylene glycol and stirred until totally dissolved and placed to ultra-sonic for approximately 3 minutes. The second solution now homogenous was added to the first in a drop wise manner and agitated for a further 2 minutes. The drop wise addition was done manually by means of a pipette. The new mixture was then placed in two (2) autoclaves each containing 10mL of solution and placed inside the oven for 2.5 hours at a temperature of 160°C . After 2.5 hours the autoclaves were removed from the oven and allowed to cool. Two methods of cooling were employed:

The autoclaves were placed on a dry surface and allowed to cool by air until temperature was stabilized to room temperature (usually 1.5 hours)

The autoclaves were placed inside a water bath and allowed to stabilize to room temperature (30 minutes).

The resulting silver nano wires (Ag NWs) were purified of any excess ethylene glycol or PVP by multiple centrifugations and re-dispersion in different solvents (acetone and ethanol). After cooling the liquid mixture obtained is mixed with 10-15mL of acetone in 2 centrifugation tubes and centrifuged for 20 minutes at 3000 rpms twice. After each centrifugation the supernatant was removed and fresh solvent added and the tubes were put to ultra-sonic for five (5) minutes. After the first 2 centrifugations with acetone the solvent was changed to ethanol and the process was repeated twice giving a total of 4 centrifugations each for 20 minutes at 3000 rpms. At the end of centrifugation the resulting Ag NW's were then stored in absence of light and labelled for characterization.

3.2.2 Synthesis of Silver nano spheres.

Materials: Silver nitrate (AgNO_3), Ethylene glycol ($\text{C}_2\text{H}_6\text{O}_2$), Poly Vinyl Pyrrolidone (PVP with $M_w \sim 10000$ Da.).

Preparation of Solutions:

0.158g AgNO_3 (0.1M $\text{AgNO}_3 \sim$ extra pure 99.9999%), 20 mL of ethylene glycol and 2.4g PVP.

PVP was gently added (step wise) to the ethylene glycol under constant stirring of 450-600 rpms for 2 hours. After the time elapsed AgNO_3 was added to the homogenous mixture of polymer and ethylene glycol and stirred for exactly 20 minutes.

The resulting mixture was then subjected to microwaves in order to synthesize the nano spheres of specific diameters. Using a CEM focused microwave synthesis method enabled with the program Synergy, SintNPsAG32s, SintNPsAG23s and SintNPsAG12s each exposing the mixture to 32,23 and 12 seconds respectively, 200 Watts of power and maximum temperature of 200°C , which intern synthesized spheres of diameters 5-30 nm in diameter. After the vessel is retrieved from the microwave the dispersion is mixed with deionized water. The new dispersion

is placed inside a basket of water and ice and allowed to cool to room temperature. The dispersion is then transferred to a centrifugation tube and a second tube is filled with water to balance the centrifuge. The tubes are subjected to centrifugation at 21000 rpms for 1 hour; this process is repeated 6 times. For the first 5 times with the aid of a pipette some of the supernatant was removed and replaced with fresh deionized water, on the 6th time as much of the supernatant as possible was removed and tubes filled partially with water. The nano spheres were stored in the absence of light and labelled for characterization.

3.3 Fabrication and Characterization Methods

3.3.1 Chemical Structure Characterization

Uv-VIS Spectroscopy-Uv-Vis absorption peaks that are characteristic for metallic nanostructures and conjugated molecules were measured using a Hellmanex JASCO V-670 spectrophotometer ($200 < \lambda < 800$ nm). Uv- Vis refers to absorption spectroscopy or reflectance spectroscopy in the ultraviolet-visible spectral region. This means it uses light in the visible and adjacent (near-UV and near-infrared (NIR)) ranges. The absorption or reflectance in the visible range directly affects the perceived colour of the chemicals involved [142].

3.3.2 Materials Characterization

Scanning Electron microscopy (SEM) - Scanning electron microscopy images were obtained with a Quanta FEG 250 Scanning Electron Microscope. A type of electron microscope that produces images of a sample by scanning it with a focused beam of electrons. The electrons interact with atoms in the sample, producing various signals that can be detected and that contain information about the sample's surface topography and composition. The electron beam is generally scanned in a raster scan pattern, and the beam's position is combined with the detected signal to produce an image. SEM can achieve resolution better than 1nm. Specimens can be observed in high vacuum, low vacuum and in environmental SEM specimens can be observed in wet conditions [143].

Transmission Electron Microscopy (TEM) - Transmission Electron Microscopy images were obtained with a FEI Technai T20 (LTEM) transmission electron microscope. A microscopy technique whereby a beam of electrons is transmitted through an ultra-thin specimen, interacting

with the specimen as it passes through. An image is formed from the interaction of the electrons transmitted through the specimen; and the image is magnified and focused onto an imaging device [144].

Dynamic light Scattering (DLS) - Particle size distribution was attained by the Brookhaven 90 plus photo correlation spectroscopy. Also known as photon correlation spectroscopy or quasi-elastic light scattering is a technique in physics that can be used to determine the size distribution profile of small particles in suspension or polymers in solution [145].

Inductively coupled plasma atomic emission spectroscopy (ICP-AES) should be used to distinguish quantitatively the amount of PVP and silver in the final product. Also referred to as inductively coupled plasma optical emission spectrometry (ICP-OES), and is an analytical technique used for the detection of trace metals. It is a type of emission spectroscopy that uses the inductively coupled plasma to produce excited atoms and ions that emit electromagnetic radiation at wavelengths characteristic of a particular element. The intensity of this emission is indicative of the concentration of the element within the sample [146].

3.4 Modification of Cellulose filters

3.4.1. Functionalization of cellulose fibres and attachment of metallic particles.

Metal cellulose filters may be formed by electrostatic-assembly using direct impregnation or by in situ reduction techniques [147]. Electrostatic interactions lead to highly- efficient depositions of metal nanoparticles onto cellulose fibres [7]. Nanoparticles however, may still be released when the fibres are subjected to different pH environments; this is due to the ionic charge which is stabilizing the metal nanoparticles and the bond strength of the electrostatic interactions which are easily influenced by pH values [148]. Low durability between cellulose fibres and metallic nanoparticles lead to deterioration in the desired properties, in our case the antimicrobial activity. Recent studies in, 2009 revealed that the unwanted release of nanoparticles may be harmful to human health as nanoparticles can easily penetrate into the human body resulting in cell damage[149]. Thus it is important to have a strong and stable linkage between the nanoparticle and the cellulose fibres. This is important in order to ensure efficient deposition and durability of the metal nanoparticle for an eco-friendly and of course human friendly device such as our filters

to be produced. Suppression of the release of metal nanoparticles from substrates by covalent attachment using thiol chemistry have been demonstrated and had low nanoparticle release due to their metal- sulphur interactions [7]. This was our reason for choosing thiol groups as our primary mode of functionalization for our cellulose substrate, using esterified mercaptoacetic acid. However, it has been reported that sulphidation of silver nanoparticles has decreased their ability to inhibit bacteria such as *E. coli* [150], which is our target bacterium. Hence an alternative was examined as NPs structured on cellulosic material can be the potential basis of “smart paper” or other devices which could lead to new prospective in different domains with large numbers of applications. From reported studies, films have been chemically modified by grafting different molecular groups such as amines, which leads to high levels of substitutions [151]. Given the aptitude of the amine groups to act as complexing centres 3-Aminopropyltriethoxysilane (APTES) and Polyethylenimine (PEI) were chosen as medication agents as an alternative to mercaptoacetic acid.

3.4.1.1 Thiol modification of cellulose filter

In order to attach the metallic nanoparticles to the cellulose fibres covalently the fibres need to first be modified by the addition of different functional groups, firstly by thiolation. The nanoparticles will be immobilized in the fibres by a strong and stable covalent bond with the thiol functional group.

100mL of Mercaptoacetic acid was mixed with 60 mL acetic anhydride, 40 mL acetic acid (36 %) and 0.3 mL concentrated sulphuric acid, and stirred thoroughly and allowed to cool to room temperature.

Discs 2.15 cm in diameter of cellulose filter paper were then immersed in the acidic mixture, and placed in a pre-heated oven at 40⁰C for 2 days. After completion of the thiolated reaction, the thiolated cellulose discs were washed several times with deionized water and dried in an oven.

3.4.1.2 Amine modification of cellulose filters.

The second functional group selected were amines using a) 3-Aminopropyl triethoxysilane (APTES) and b) Polyethylenimine (PEI).

Modification of cellulose: Amination by APTES:

40mL anhydrous toluene at 100°C was put under reflux for 3 hours and 1mL of 3-Aminopropyl triethoxysilane (APTES) was added for coating the total surface of the cellulose discs (2.15cm in diameter and having a circumference of approximately 6.8 cm and Area of 3.63 cm²).

The discs were placed in a three neck flask and toluene added under argon for about 20 minutes. After the oxygen is evacuated APTES is added under constant low stirring.

After the 3 hours allow mixture to cool to room temperature and remove the excess by washing with toluene and allow discs to dry.

Modification of cellulose: Amination by PEI:

A 1.3 wt. % solution of PEI was prepared using Polyethylenimine branched with molecular weight, $M_w \sim 25,000$ Da.

Filters were immersed in 20mL of the above solution and left on the roller and tilt mixer for 12 hours. After the designated time wash filters several times with deionized water and dry in an oven at 40°C or air dry.

3.5 Characterization of thiolated and aminated cellulose filters

Fourier transform spectroscopy is a measurement technique whereby spectra are collected based on measurements of the coherence of a radiative source, using time-domain or space-domain measurements of the electromagnetic radiation or other type of radiation [152]. An attenuated total reflection Fourier-transform infrared spectroscopy (ATR FT-IR) with a scan range from 4000 to 400 cm⁻¹ (Bruker Vortex 70 ATR-FTIR) was used to monitor the thiol and amine (from APTES and PEI) modifications of the cellulose filters.

The degree of the thiol or amine-modification should be evaluated by determining the sulphur and nitrogen element contents using X-ray photoelectron spectroscopy (XPS).

3.6 Assembly modified-cellulose and metallic nanoparticles filter

3.6.1 Assembly of thiol and amine modified cellulose filters.

The metal nanoparticles will be covalently introduced to the thiol-modified or amine-modified cellulose fibres by means of immersion of the discs in the as-prepared colloidal metal nanoparticle aqueous dispersions. The schematic representation below in Figure 10 depicts the procedure for the thiol functional group attachment and is similar to that of the amine modification.

500 μ L of each silver nanoparticle colloidal dispersions (wires and spheres) was added to the thiol-modified or amine-modified cellulose specimens (Diameter = 2.15 cm, Circumference = 6.8 cm, Area = 3.63 cm²), respectively. It was then stored in a pre-heated oven at 40 °C until dry (usually 1-1.5 days).

After drying, the specimens were rinsed several times with deionized water to remove loosely bound metal nanoparticles and then dried in an oven at 40 °C.

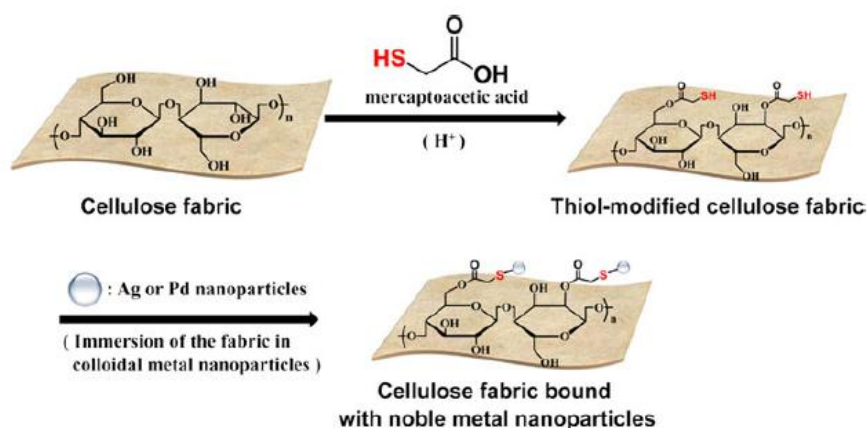


Figure 10 Schematic illustration of the preparation procedure for thiolated cellulose bound with nanoparticles [7].

3.6.2 *In situ* preparation of metal-cellulose filter

Discs were immersed into 1 mM AgNO₃ aqueous solution for 1 minute, followed by rinsing with ethanol for 5 minutes.

The precursors in the fabric were reduced in 200 mM sodium borohydride, (NaBH₄) aqueous solution for 10 minutes and then rinsed with deionized water.

The resulting filters were then wiped and dried in the oven at 40⁰C in the same manner as above.

3.7 Release Testing of metal-cellulose membrane filter.

In order to investigate the durability and robustness of the metal-cellulose filters, a release test of metal nanoparticles from the fibres was carried out by washing of the fibres specimens under various pH conditions.

Three types of dispersion (neutral, acidic, and basic) were prepared by adding an acid (Hydrochloric acid, HCL), or a base (sodium hydroxide, NaOH) into 100mL deionized water, giving a range of pH values 0-6, and 8-12 respectively and also using deionized water with a pH of approximately 7.

The solutions were stored in an oven at 40 ⁰C before use. Approximately 10mL of the solution was used per cellulose filter disc.

The tube containing the specimen was agitated for 5, 10, 15 and 20 minutes in an ultrasonic bath. After washing the specimens were removed from the tube and rinsed with deionized water, wiped with soft tissue and dried in an oven for the next washing.

The process was repeated twice.

3.8 Characterization of metal- cellulose membrane filter

HR(S)-TEM using Tecnai F30 High resolution microscope, and FE-SEM were used to observe whether or not the cellulose membranes were loaded with nanoparticles and to see how dispersed the nanoparticles was. Samples for HR-TEM imaging were prepared by embedding the yarns of metal-cellulose in a spurr resin and hardening the resin at 70 ⁰C for 24 h. The embedded

specimens were then cross-sectioned using an ultramicrotome equipped with glass knife. Cross sections of the embedding block with thicknesses of ~80 nm were collected on TEM copper grids and dried before imaging.

Inductively coupled plasma atomic emission spectroscopy (ICP-AES). From the ICP-AES the loading amounts of metals in the metal-celluloses were determined.

X-ray photoelectron spectroscopy (XPS) is a quantitative spectroscopic technique that measures the elemental composition, empirical formula, chemical state and electronic state of the elements that exist within a material. The binding property of metal nanoparticle with the thiol-modified or amine-modified cellulose filters were investigated using XPS analysis [153].

Bacterial Testing

Bactericidal tests were done after the synthesis of silver nanoparticles and the assembly of the metal-cellulose membrane filters. The effect of silver nanoparticles on bacterial was considered as two aspects: The first, the possible effect was the inhibition of bacterial growth, via the retardation of bacterial cell duplication; the other effect of the nanoparticles was the direct killing of bacterial cells, which may be the result of one or more mechanisms.

Therefore, bacterial growth inhibition and cell killing must be distinguished from each other in order to direct the path of the research as we look for the bactericidal mechanism of silver nanoparticles on bacterial cells. However, these two effects were always found to be coupled as from a biological stands they were naturally linked together. In addition of the medium growth tests, bacterial viability tests were also applied to decouple these processes. Based on counting the live cells on agar surface, we were able to measure the percentage of dead cells. A comparison of this data with the data derived from medium growth test may allow the actual effects of silver nanoparticles on bacterial cells recognized.

Materials

Phosphate Buffered Saline (PBS), Tryptic Soy Broth (TSB), Agar plates (Agar powder and distilled water), *Escherichia coli* bacteria.

Bacteria Growth Test.

In general, bactericidal effects could be divided into two types: 1) direct killing of the bacterial cells and 2) bacterial growth retardation. There is no indication of path is better than the other. It is quite reasonable for antibiotics to kill one kind of bacterium while they work to retard the growth of bacteria on another kind of bacterium. In this regard, experiments were setup to distinguish which of these two mechanisms were initiated when silver nanoparticles were incubated with the Gram-negative bacterium *Escherichia coli*. Bacterial growth tests show the overall effects of silver nanoparticles on the bacteria.

The methodology is as follows:

A 10ml culture of *E. coli* was grown overnight, to the late log phase, in a nutrient broth of TBS. As mentioned previously in chapter 2 in the population growth of bacteria, the bacteria are alive in the log phase, and the population was relatively large for study. As the relative number of bacteria influenced the bactericidal effects, it was required to determine the cell numbers at the very beginning of the test and hold it constant for the beginning of each test.

The nutrient medium was then mixed with silver nanoparticles (spheres and wires respectively). The concentrations of silver nanoparticles used were chosen from a range from 0 mg/mL to 120 mg/mL. The bacteria containing mixture was then cultured at 37⁰C over night; the mixture was violently stirred to keep the suspension's uniformity. The turbidity data was taken every 35 minutes based on the generation time of the bacteria (*E. coli* ~ 30 minutes) using a turbidimetre. From the turbidity density data, one could easily correlate the turbidity into the number of bacterial cells. By studying the bacterial growth curve, we can identify whether or not the silver nanoparticles possessed strong effects on bacterial cells. Further tests were also conducted in order to clarify the specific effect (agar plate test – counting of colonies).

Bacteria Viability Test (Agar plate Test)

To determine whether silver nanoparticles could kill the bacteria or cause the growth retardation, agar plate test was executed on the metallic-cellulose fibres.

The filter specimens (0.04 g each) were placed in a sterilized container (20 mL tube) and then 10 mL of the microorganism aqueous suspensions were dropped onto the surface of the specimens. The inoculated microorganisms in the filter specimens were cultured at 37 ± 1 °C for 18 h or overnight.

After cultivation of microorganisms, the filter specimens were shaken vigorously using ultra sonic bath for 30 minutes. A microorganism suspension was drawn, diluted (1: 10) in PBS and 25µL drops transferred to a nutrient agar plate and then it was cultured at 37 ± 1 °C for 24 h. The number of survival microorganism was determined by counting the colonies as a colony-forming unit (CFU)/mL, and bacteriostatic reduction rate of microorganisms was calculated as follows,

$$R (\%) = 100(B-A)/B$$

where R is the bacteriostatic reduction rate, A and B are the number of surviving microorganisms after 18 h for the agar plate containing test sample (metal-cellulose specimen) and the blank sample (unmodified cellulose filter), respectively.

For high speed test the solution was passed through the filters, the suspension drawn, diluted and transferred to agar plates directly followed by colony counting as above.

APPENDIX B

Supplementary information, graphs, data, figures and all miscellaneous items omitted from the main report.

Marketability and Feasibility: Sample Calculations of approximate cost to produce Ag-cellulose filters.

Table a. Cost Estimations for chemicals needed for synthesis of silver nanoparticles.

Name	Brand	Price(€)	Amount
Silver nitrate	Sigma Aldrich	67.40	25g
Ethylene glycol	Sigma Aldrich	34.90	100 ml
Polyvinyl pyrrolidone	Sigma Aldrich	25.46	100g
Total		127.76	

The Table below shows the cost of one synthesis for silver nanospheres. The calculations were based on the amount of reagents needed for one synthesis. For example, in the case of silver nitrate one synthesis requires 0.158g of AgNO₃ and according to the amount of AgNO₃ in containers of 25g; hence from one container 158 syntheses are possible. Taking into account the price of the container is €67.40 it is easy to calculate the cost per synthesis.

Table b. Cost estimation of one synthesis.

Reagent	Number of possible synthesis/reagent	Price for one synthesis (€)
Silver nitrate	$25/0.158=158$	$67.40/158=0.43$
Ethylene glycol	$100/20=5$	$34.9/5=6.98$
PVP	$100/2.4=41$	$25.46/41=0.62$
Total price		8.03

According to Sigma Aldrich for 25 mL and a concentration equal to 0.02 mg/mL, the price of 10 nm size silver nanoparticles is 63.15\$ [165]. For five times less the amount being charged by this commercial producer, the nanoparticles used in these filters has the same morphology and concentration. The cost of one synthesis of nano wires is approximately \$7.48. From one synthesis of wires and one synthesis of spheres (each 20mL) it is possible make several filters but it is dependent on the size of the filter desired. Papers from Prat Dumas, France with slow velocity filtration and having a pore size of 2-3 μ m and sold by lab box on average costs at most €11/100 (0.11 for each) and depending on the functionality the chemicals needed in total will cost approximately €200. All of these cost estimations are dependent on the size of the final

product but it is optimistic that one regular size filter paper similar to those used in the lab (125mm) could cost less than €1 to produce. Thus making the filters competitive in the market.

Synthesis of silver nanoparticles: Sample calculation

Silver nano wires:

$$10\text{ml EG} * \frac{1.113\text{ g}}{1\text{ ml Eg}} = 11.13\text{ g EG}$$

Amount of AgNO₃;

$$11.13\text{g EG} * \frac{1\text{ mol EG}}{62.07\text{gEG}} * \frac{1\text{ mol AgNO}_3}{178\text{ mol EG}} * \frac{169.87\text{g}}{1\text{ mol AgNO}_3} = 171\text{ mg}$$

Amount of PVP;

$$11.13\text{g EG} * \frac{1\text{ mol EG}}{62.07\text{gEG}} * \frac{1\text{ mol PVP}}{119\text{ mol EG}} * \frac{111\text{g PVP}}{1\text{ mol PVP}} = 167\text{ mg}$$

Silver nano spheres:

$$20\text{ml EG} * \frac{1.113\text{ g}}{1\text{ ml Eg}} = 22.26\text{ g EG}$$

Amount of AgNO₃;

$$22.26\text{g EG} * \frac{1\text{ mol EG}}{62.07\text{gEG}} * \frac{1\text{ mol AgNO}_3}{384\text{ mol EG}} * \frac{169,87\text{g}}{1\text{ mol AgNO}_3} = 158\text{ mg}$$

Amount of PVP;

$$22.26\text{g EG} * \frac{1\text{ mol EG}}{62.07\text{gEG}} * \frac{1\text{ mol PVP}}{16.5\text{mol EG}} * \frac{111\text{g PVP}}{1\text{ mol PVP}} = 2.412\text{ mg}$$

DLS Analysis: Graphs from different samples of silver nano spheres showing the reproducibility of the synthesis each time having 60% or greater nanoparticles less than 10 nm.

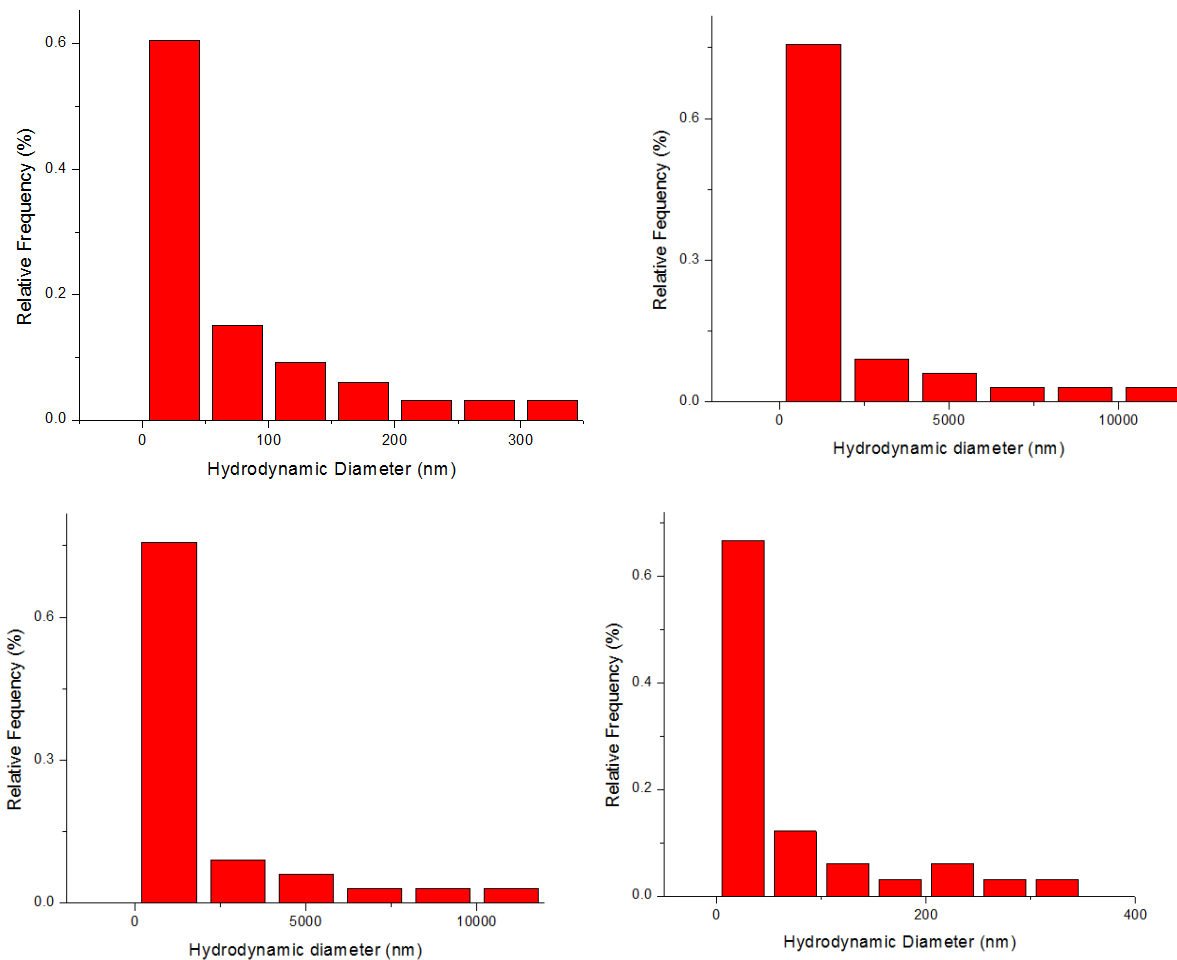


Figure a. 23s nano spheres produced a) February 8, 2013 b) February 13, 2013 c) March 10, 2013 and d) May 7, 2013

Rhodamine Experiments: To demonstrate the wettability of the modified cellulose papers.

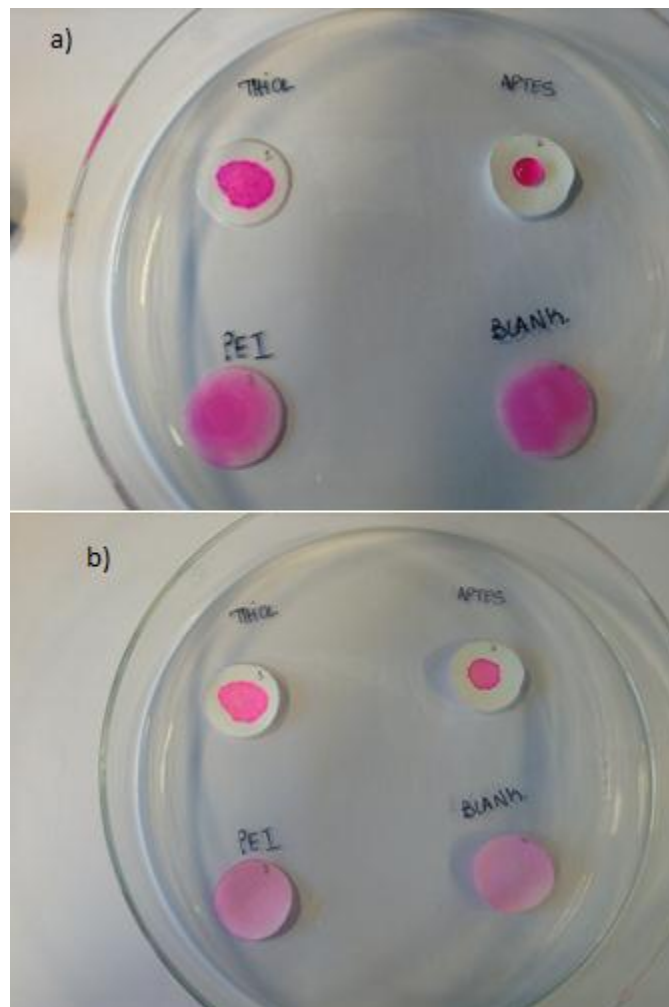


Figure b. Rhodamine wetted membranes a) Initial wetting b) After 24 hrs.

SEM Analysis: SEM analysis was used to confirm that the integrity of the filters was not tarnished after functionalization. The following images confirmed that there were no pin holes or defects.

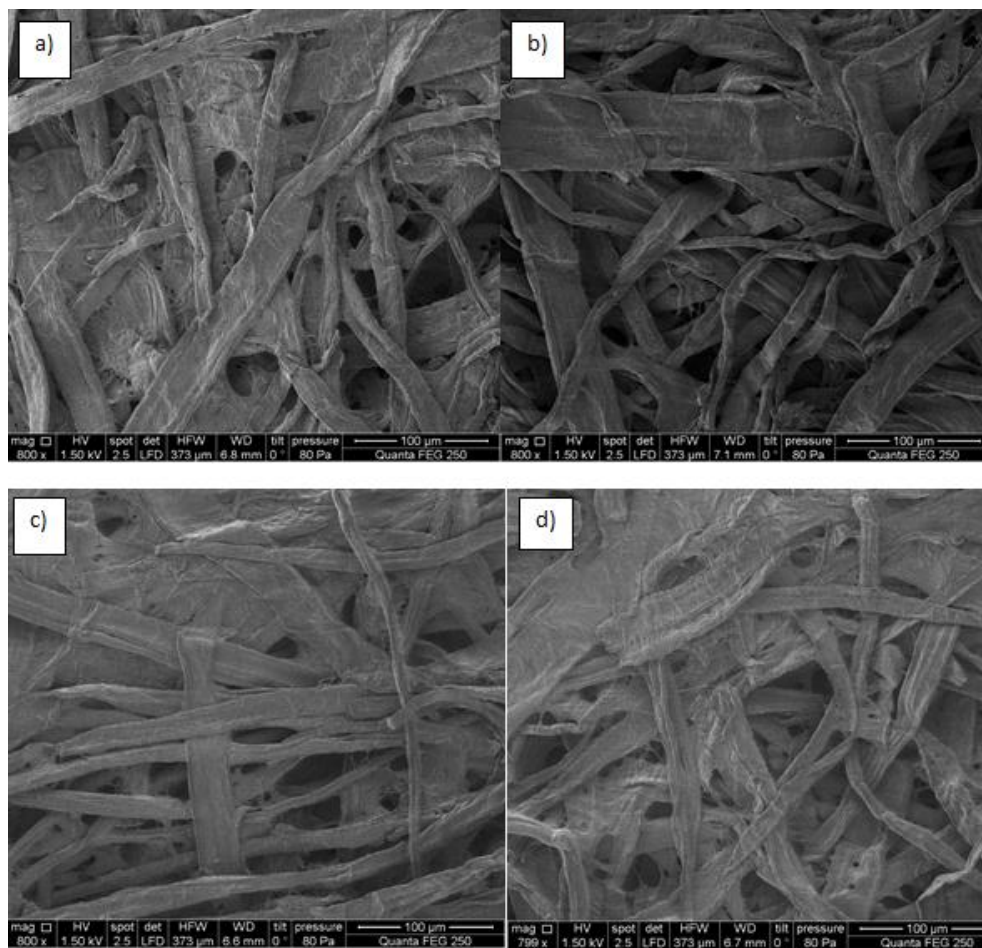
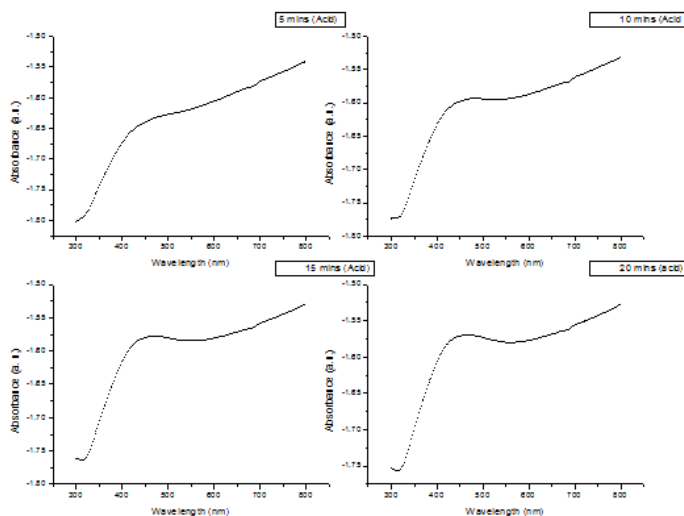


Figure 1 SEM images of cellulose fibres with different functionalities, a) PEI b) Thiol c) APTES and d) Un-modified cellulose.

Release Testing: Uv-vis graphs of APTES, PEI and Thiol-modified filters following release testing in different pH environments.

APTES- Acid



APTES-Base

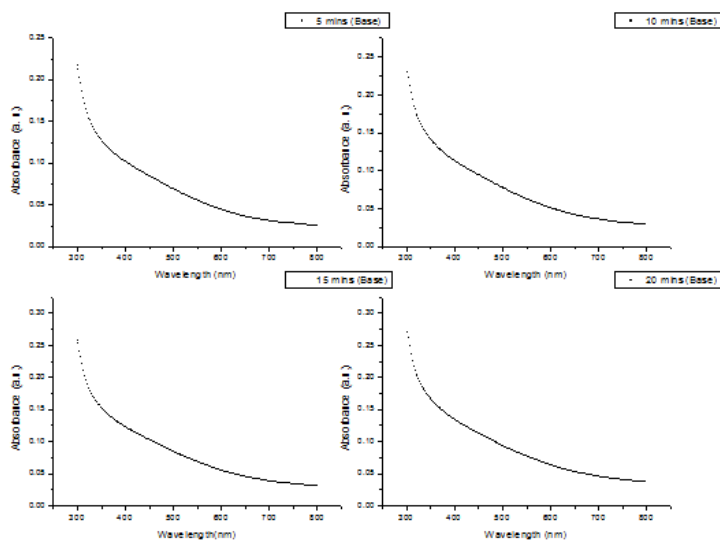
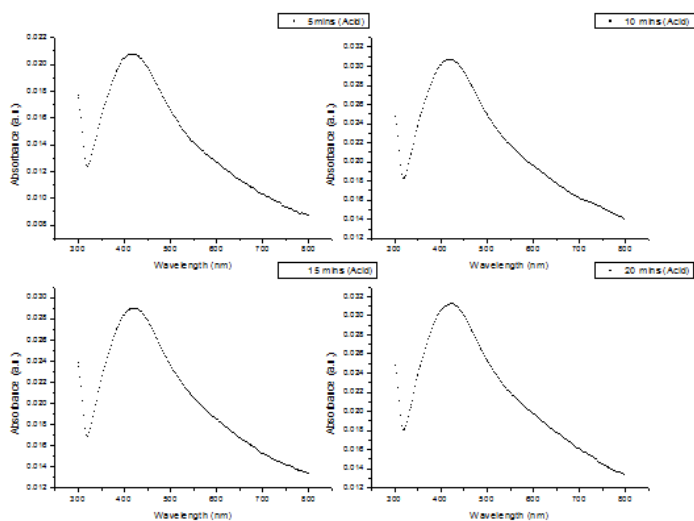


Figure c. a) Uv-vis spectra following release testing of a) APTE- modified cellulose filters in acidic condition and b)APTES-modified cellulose filters in basic conditions.

PEI- Acid



PEI-Base

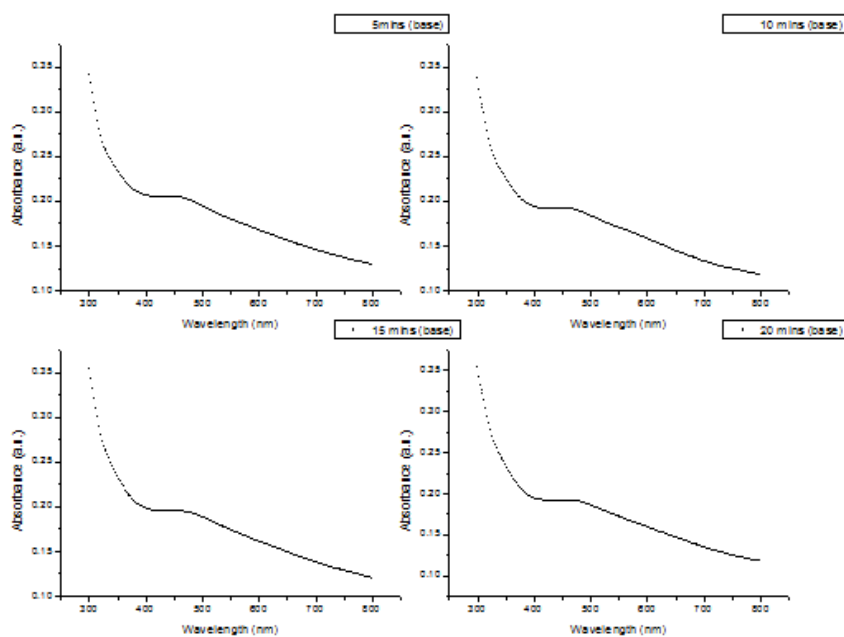
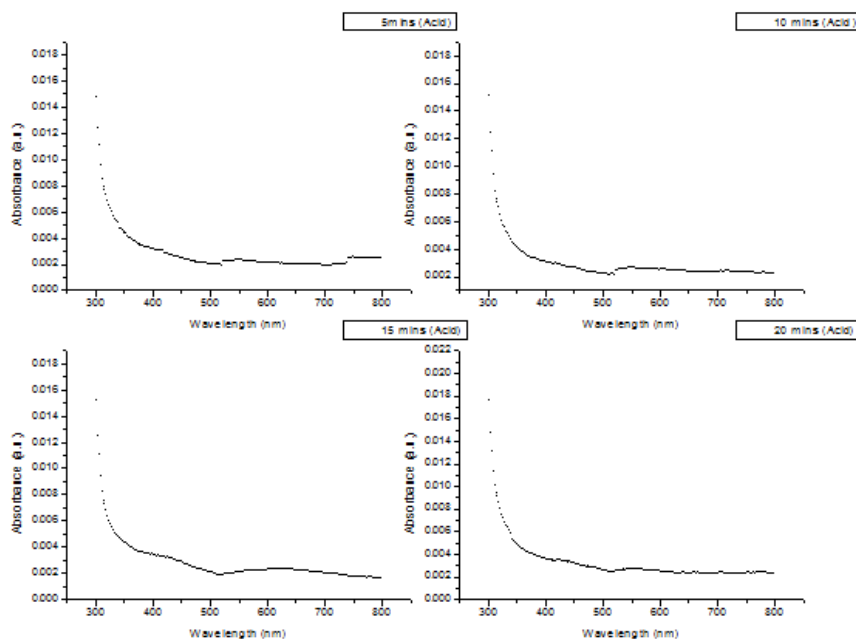


Figure d. UV-vis spectra following release testing of a) PEI- modified cellulose filters in acidic condition and b) PEI- modified cellulose filters in basic conditions.

Thiol- Acid



Thiol- Base

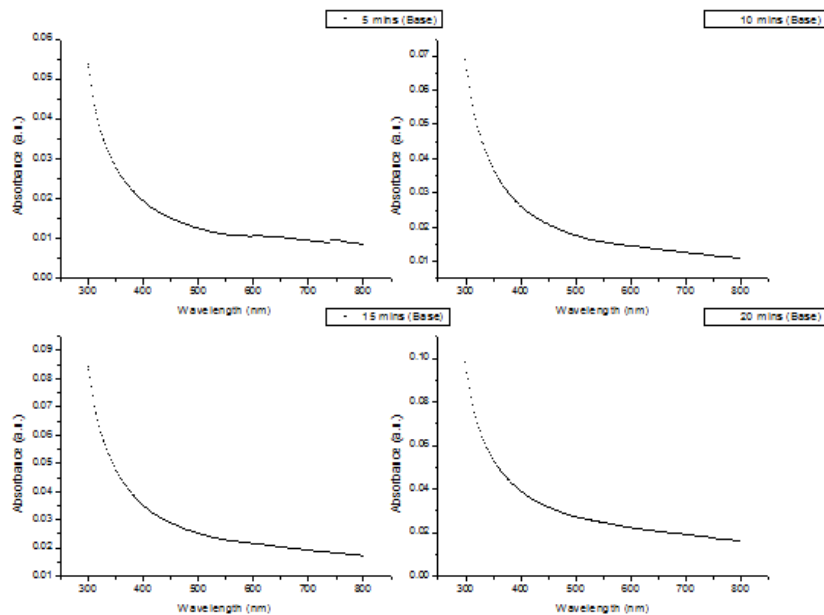


Figure e. UV-vis spectra following release testing of a) Thiol- modified cellulose filters in acidic condition and b) Thiol- modified cellulose filters in basic conditions.

ICP-OES analysis of silver nanoparticles: Helps to demonstrate or corroborate the toxicity of the nano spheres

Table c. Shows total mass of silver and PVP content for different nanoparticles.

Nanoparticle	Total mass of nanoparticle (mg/L)	Total mass of silver (mg/L)	Total mass of PVP (mg/L)
Wires	90.909	4.746 (5.22%)	86.137
Spheres (23s)	860.75	2.609 (0.3%)	858.186

APPENDIX C

Pictures of some equipment used for characterization and experimental procedures.



European Master
ERASMUS MUNDUS MASTER IN
MEMBRANE ENGINEERING

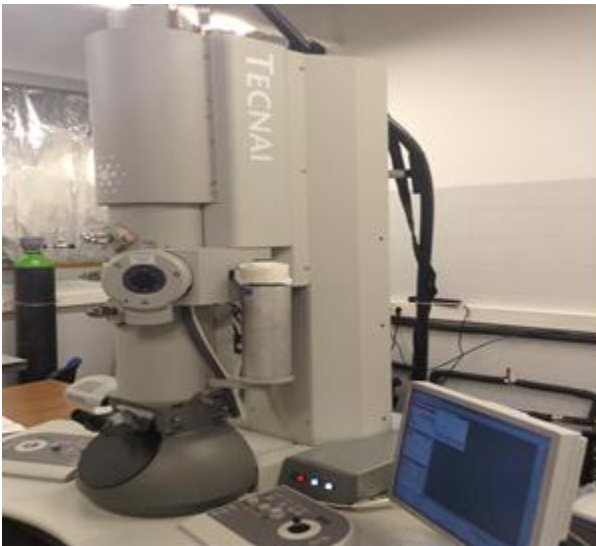


Universidad
Zaragoza

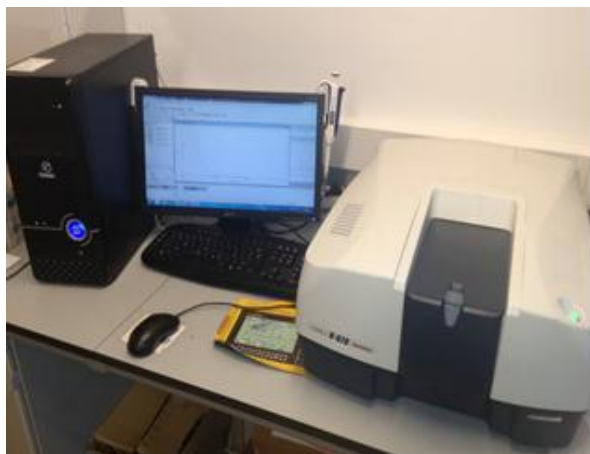




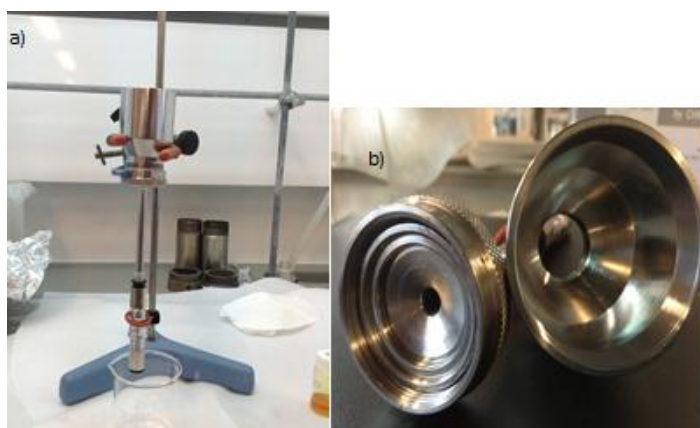
CEM microwave system used to synthesize silver nano spheres.



FEI Technai T20 (LTEM) transmission electron microscope used for TEM characterization.

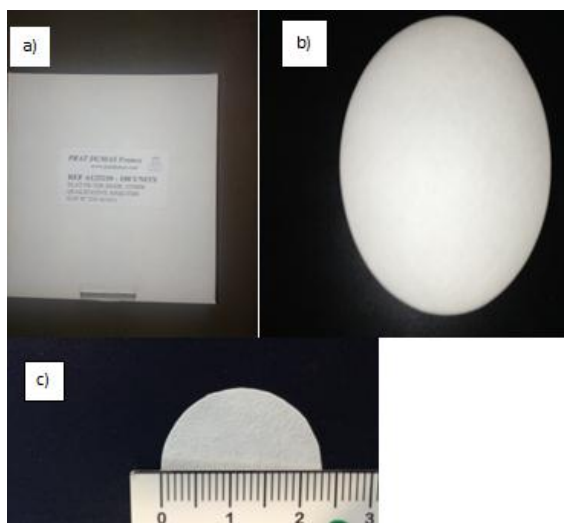


Hellmanex JASCO V-670 spectrophotometer used for Uv-Vis characterization.



The device used for passing liquid medium (PBS) containing bacteria through filter. Picture a) Shows the assembled device during operation and b) open device.

Prat Dumas filter papers used to make Ag-cellulose filters. a) Shows the packaged filters, b) Shows a single filter paper and c) Shows a typical filter used in the assembly of the Ag-cellulose filters (diameter-2.3cm).





Brookhaven 90 plus photo correlation spectroscopy used for particle size analysis (DLS)

Bruker Vortex 70 ATR-FTIR used for analysing thiolation and amination of the cellulose.

